FORECASTING COMPRESSIVE STRENGTH OF FLY-ASH-BASED GEOPOLYMER CONCRETE USING GENE EXPRESSION PROGRAMMING (GEP)

By

Mohsin Ali Khan

MCE-NUST-2021-274059

A thesis submitted in partial fulfillment of the requirements for the degree of

Master of Science

in

Structural Engineering

MILITARY COLLEGE OF ENGINEERING (MCE), NATIONAL UNIVERSITY OF SCIENCES AND TECHNOLOGY (NUST) ISLAMABAD, PAKISTAN (2021)

Certified that the contents and form of thesis titled **"FORECASTING COMPRESSIVE STRENGTH OF FLY-ASH-BASED GEOPOLYMER CONCRETE USING GENE EXPRESSION PROGRAMMING (GEP)"** submitted by Mohsin Ali Khan have been found satisfactory for the requirement of the degree.

Supervisor: _____

Associate Professor Lt. Col. Dr. Adeel Zafar

Department of Structural Engineering

Military College of Engineering (MCE)

National University of Science and Technology (NUST), Islamabad, Pakistan

Co-supervisor: _____

Assistant Professor Dr. Muhammad Faisal Javed

Department of Civil Engineering

COMSATS University Islamabad (CUI), Abbottabad Campus, Pakistan

Committee Member 1: _____

Associate Professor Col. Dr. Syed Hassan Farooq

Department of Structural Engineering

Military College of Engineering (MCE)

National University of Science and Technology (NUST), Islamabad, Pakistan

Committee Member 2: _____

Assistant Professor Dr. Muhammad Shahid Siddique

Department of Structural Engineering

Military College of Engineering (MCE)

National University of Science and Technology (NUST), Islamabad, Pakistan

DEDICATION

Dedicated to my beloved mother, father, brothers, sisters and the rest of the family and friends who have stood behind me till the accomplishment of this research.

ACKNOWLEDGEMENTS

I am thankful to ALMIGHTY ALLAH, who gave the opportunity and enabled me to complete my Master's Degree. Firstly, I would like to express my profound gratitude to my supervisor, Associate Professor, Lt. Col. Dr. Adeel Zafar and co-supervisor, Assistant Professor, Dr. Muhammad Faisal Javed for their guidance, unceasing support and motivation during all phases of conducting this research work. It has been an absolute privilege for me to work under their kind supervision. They were always open to discussions, encouraged innovative ideas and accomplishments and steered me in the right direction whenever he deemed necessary.

Furthermore, I am indebted to Lecturer Furqan Farooq, for his expertise, sincere and valuable recommendations and advices extended to me.

I would also like to express my deepest appreciation to all my colleagues and friends, particularly Javad Ahmad, Sangeen Khan, Yasar Khan, Nasar Khan, Anees Khan and Ahsan Mehmood for their moral support and companionship during this endeavor.

I am also thankful for the partial financial support from Lecturer Khizar Khan, my friend Ubaid Zaman and uncle Naveed Ali during my study period and the research support from Military College of Engineering (MCE), National University of Science and Technology (NUST), Islamabad and COMSATS University Islamabad (CUI), Abbottabad Campus.

Finally, and most importantly, I would like to extend my heartiest gratitude to my father, mother, and siblings for their prayers, encouragement, endless love and unfailing support throughout my years of study and research which made my struggle period smooth and gratifying.

LIST OF PUBLICATIONS

Article Related to Thesis	Status
Khan, M.A., Zafar, A., Akbar, A., Javed, M.F., & Mosavi, A., "Application of Gene Expression Programming (GEP) for the Prediction of Compressive Strength of Geopolymer Concrete." ***Materials 2021***, *14*, 1106. https://doi.org/10.3390/ma14051106 **(Q2, IF=3.057)**	**Published** (From thesis)
Khan, M. A., Memon, S. A., Farooq, F., Javed, M. F., Aslam, F., & Alyousef, R. "Compressive Strength of Fly-Ash-Based Geopolymer Concrete by Gene Expression Programming and Random Forest." Advances in Civil Engineering, **2021**. https://doi.org/10.1155/2021/6618407 **(Q2, IF=1.176)**	**Published** (From extended research)
Khan, M. A., Zafar, A., Farooq, F., Javed, M. F., Alyousef, R., Alabduljabbar, H., & Khan, M. I. "Geopolymer Concrete Compressive Strength Via Artificial Neural Network, Adaptive Fuzzy Interface system and Gene Expression Programming with K-Fold Cross-Validation." ***Frontiers in Materials 2021***, *8*, 66. https://doi:10.3389/fmats.2021.621163 **(Q2, IF=2.705)**	**Published** (From extended research)
Khan, M.A., Javed, M.F., Zafar, A., Alabduljabbar, H., Chu, Y.M & Khan, M.I. "Sustainable Use of Fly-ash: Use of Gene-Expression Programming (GEP) and Multi-Expression Programming (MEP) for Forecasting the Compressive Strength Geopolymer Concrete." ***Ain Shams Engineering Journal 2021*** **(Q2, IF=1.984)**	**Published** (From extended research)

Other Article	Status
Javed, M.F.; Farooq, F.; Memon, S.A.; Akbar, A.; **Khan, M.A**.; Aslam, F.; Alyousef, R.; Alabduljabbar, H.; Rehman, S.K.U. "New Prediction Model for the Ultimate Axial Capacity of Concrete-Filled Steel Tubes: An Evolutionary Approach." ***Crystals 2020***, 10, 741. https://doi.org/10.3390/cryst10090741 **(Q2, IF=2.404)**	**Published**

ABSTRACT

To produce geopolymer concrete (GPC), fly-ash (FA) like waste material has been effectively utilized by various researchers. The laboratory methods to find the compressive strength (f_c') of fly-ash based geopolymer concrete (FGPC) are expensive, time-consuming, and require skilled personnel. In this research, the soft computing techniques known as gene expression programming (GEP) were executed to deliver an empirical equation to estimate the f_c' of FGPC. To build a model, a consistent, extensive and reliable data base is compiled through a detailed review of the published research. The compiled data set is comprised of 298 f_c' experimental results. The 10 utmost dominant parameters are counted as explanatory variables, in other words, the extra water added as percent FA ($\%E_W$), the percentage of plasticizer ($\%P$), the initial curing temperature (T), the age of the specimen (A), the curing duration (t), the fine aggregate to total aggregate ratio (F/A_G), the percentage of total aggregate by volume ($\%A_G$), the percent SiO_2 solids to water ratio ($\%\, S/W$) in sodium silicate (Na_2SiO_3) solution, the NaOH solution molarity (M), the activator or alkali to FA ratio (A_L/F_A), and the Na_2SiO_3 to NaOH ratio (N_s/N_o). A GEP empirical equation is proposed to estimate the f_c' of FGPC. The accuracy, generalization, and prediction capability of the proposed model was evaluated by performing parametric and sensitivity analysis, applying statistical checks, and then compared with non-linear and linear regression equations. The performance index (ρ) for training set and validation set approaches to zero, witnesses the better GEP model. In the validation stage, the ρ reveals that GEP model is 53% and 46% better than linear and non-linear regression models respectively. The model correctly meets the appropriate requirements for external validation considered. The validation of the proposed GEP model via experimental results shows that it possesses higher generalization and predictive capability and is appropriate to practice in the preliminary design of FGPC according to the Pakistani environment.

Keywords: waste material; fly-ash; gene expression programming (GEP); geopolymer concrete (GPC); compressive strength; regression analysis

TABLE OF CONTENTS

TITLE **PAGE**

LIST OF TABLES

TABLE DESCRIPTION **PAGE**

LIST OF FIGURES

FIGURE DESCRIPTION **PAGE**

LIST OF SYMBOLS AND ABBREVIATIONS

Symbol	Description
FA	Fly Ash
GPC	Geopolymer concrete
FGPC	Fly Ash Based Geopolymer Concrete
OPC	Ordinary Portland Cement
ANNP	Alkali Activated Natural Pozzolan
AI	Artificial Intelligence
ANN	Artificial Neural Network
GA	Genetic Algorithm
GP	Genetic Programming
GEP	Gene Expression Programming
ET	Expression Tree
f_c'	Compressive Strength
E_c	Elastic Modulus
f_{st}	Split Tensile Strength
T^0C	Temperature for Curing of Specimen
A	Age of Specimen
F/A_G	Fine Aggregate to Total Aggregate Ratio

N_S/N_O	Sodium Silicate to Sodium Hydroxide Ratio
M	Molarity of NaOH Solution
A_L/F_A	Alkali to Fly-Ash Ratio
$\% P$	Percentage of Superplasticizer
$\% E_W$	Percentage of Extra Water Added
$\% S/W$	Percentage of SiO_2 Solids to Water Ratio
MAE	Mean Absolute Error
RSE	Root Squared Error
RMSE	Root Mean Squared Error
R	Coefficient of Correlation
RRMSE	Relative Root Mean Squared Error
ρ	Performance Index
SA	Sensitivity Analysis
k	Slope of the Regression Line

CHAPTER 1

INTRODUCTION

1.1. Background

Fly ash has gained an increasing attention recently as their use improves the physical and mechanical properties of concrete. Therefore, it has been the subject of interest for many researchers since a decade. As a result, numerous theoretical and empirical methods have been proposed to determine the slump, compressive strength, tensile strength, elastic modulus and flexural strength of different fly ash based geopolymer concretes (FGPC). Compressive strength is considered to be the principal factor in the mix design of geopolymer concrete production.

The most reliable method for determining the stated properties of FGPC is from results of laboratory tests, however, such tests are expensive, time consuming and require the availability of skilled personnel to conduct them. In addition, concrete in test cylinder specimens may differ from that in the actual structure due to different curing techniques and environment. Therefore, the properties of FGPC are very often predicted and used for design. Different researchers used various artificial intelligence techniques (AI) to predict the properties of FGPC. The gene expression programming (GEP) is one of the latest AI technique that has been employed for the to predict the compressive strength of FGPC considering the most sensitive parameters.

1.2. Problem Statement/Justification for the Selection of Topic

Globally the concrete is the second material used universally next to the water, as construction is growing vastly throughout the globe. Each year, through the globe 25 billion tons of concrete are manufactured. The Ordinary Portland Cement (OPC) is an important ingredient used in the production of concrete. As per the present world statistics, every year around 2.6 billion Tons of OPC are required. This quantity will be increased by 25% within a span of another 10 years. But the manufacture of OPC is carried with an adverse effect. To manufacture one ton of OPC, one ton of

carbon dioxide is emitted to the atmosphere, creates an alarming situation to the environment. Since the Limestone is the main source material for the OPC an acute shortage of limestone may come after 25 to 50 years.

Moreover, in the production of OPC not only a huge amount of energy is released, but it also consumes natural resources significantly. One ton of OPC production consumes 4GJ of energy. For sustainable development, we need to develop an alternative binder to produce concrete. At the same time, the large quantity of fly ash generated around the globe is not used effectively and mostly disposed into landfills. As geopolymer concrete doesn't require cement utilization, thus the manufacturing of cement will be decreased which leads to the minimization of environmental pollution caused by the emission of carbon dioxide. We can address these issues through the production of geopolymer concrete by arranging them.

Geopolymer binder = fly ash from thermal industries + chemical supplements

Extensive research is carried out on the production of FGPC. Though there no effective and proper mix design procedure developed till now. The mechanical properties of FA-based GPC critically depends on several parameters like the extra water added as percent FA ($\%E_W$), the percentage of plasticizer ($\%P$), the initial curing temperature (T), the age of the specimen (A), the curing duration (t), the fine aggregate to total aggregate ratio (F/A_G), the percentage of total aggregate by volume ($\%A_G$), the percent SiO_2 solids to water ratio ($\%\, S/W$) in sodium silicate (Na_2SiO_3) solution, the NaOH solution molarity (M), the activator or alkali to FA ratio (A_L/F_A), the sodium oxide (Na_2O) to water ratio (N/W) for preparing Na_2SiO_3 solution, and the Na_2SiO_3 to NaOH ratio (N_s/N_o) [13,28–35]. We need to formalize the properties of GPC. In this research, one of the artificial intelligences (AI) techniques, gene expression programming (GEP) will be used to construct a mathematical model for the slump, compressive strength, tensile strength, flexural strength, elastic modulus FGPC.

1.3. Objectives

The utilization of geopolymer concrete made of fly-ash like waste, is on rise since last two decades but its application in the construction industry is still limited due to the anomalous behavior of the mix proportion variables. Also, extensive literature is available on the experimental determination of the compressive strength of FGPC but yet no method is available to estimate the compressive strength of FGPC based on mix proportion with maximum variables. However, this study utilizes AI techniques as alternate to predict compressive strength using expensive experimental regime. The objectives of this research can be summarized as follow:

I. To construct a widespread data base having compressive strength as response parameter and employ the GEP technique for determining a model that can accurately predict the compressive strength FGPC.

II. To validate the model using the experimental data in the validation set via different statistical metrics, external validation criterion suggested in literature, sensitivity analysis, and parametric analysis.

III. To verify the accuracy of the GEP model by performing experiments on FGPC casted under Pakistani environment.

1.4. Fly Ash Production in Pakistan

The production of fly ash in Pakistan is increasing day by day. If we are associated with the construction manufacturing material then the addition of the fly ash is the right option. we can buy it in various kinds of by-products in Pakistan. Many thermal power stations are producing a large amount of fly ash. We can easily find the suppliers of fly ash in Islamabad, Karachi, and Lahore situated in Pakistan. Also, it is found in some parts of Sindh and Baluchistan province. 5 Star Mining

fly ash available in Pakistan is of high-quality. Table 1.1 shows the province wise coal production in Pakistan. Around 185 billion tons of coal can be produced throughout Pakistan.

Table 1.1. Coal production in Pakistan

Province	**Coal production per year (Billion tons)**
Sindh	184.623
Balouchistan	0.235
Punjab	0.217
Khyber Pukhtoon-khwa	0.092
Azad Kashmir	0.009
Total	**185.175**

FGPC offers several economic benefits over OPC. The cost of one ton of fly ash is only a small fraction (if not free in some parts of the world) of the cost of one ton of OPC. FGPC production is carried out along with the use of different chemicals supplements. The most effective chemicals being used in the production of FGPC are sodium hydroxide solid (NaOH) and sodium silicate solution (Na_2SiO_3). In Pakistan, based on the current bulk cost of Na_2SiO_3 and NaOH, we can estimate that the cost of chemicals supplements needed to react one ton of fly ash is approximately PKR 6000. This is significantly smaller than the current price of OPC.

Besides, the appropriate usage of one ton of fly ash earns one carbon-credit that currently has a redemption value of about PKR 3500. Based on the previous researches, one-ton fly ash can be utilized to manufacture approximately 2.5 cubic meters of good quality FGPC, and hence earn monetary benefits through carbon-credit trade. This carbon credit significantly adds to the economy of Pakistan offered by the production of FGPC. And the bulk cost of chemicals needed to manufacture this concrete is cheaper than the bulk cost of one ton of OPC.

Given the fact that fly ash is considered as a waste material, the FGPC is, therefore, cheaper than the OPC. The special properties of FGPC can further enhance economic benefits. In all, there is so much to be gained by using geopolymer concrete.

1.5. Advantages

The superior properties of FGPC lead to vast advantages set at room temperature;

I. The compressive strength of FGPC is high compared to the OPC. The compressive strength of geopolymer concrete is about 1.5 times more than that of the compressive strength with the OPC concrete, for the same mix.

II. The geopolymer Concrete showed good workability as of the OPC Concrete.

III. In high-performance concrete, it can improve both the strength and durability properties of the concrete.

IV. The FGPC has a higher resistance to all inorganic solvents, as geopolymer materials do not generate any dangerous alkali-aggregate reaction, even in the presence of high alkali content. Eventually saves the repair cost of the builder.

V. It Keeps house, building or other industrial areas warm in winter and cool in summer because it is heat resistant.

VI. It contains water resistance, dampness and seepage keep the buildings and homes walls presentable.

VII. It is lightweight thus decreasing the cost in steel structure because it allows good compressive strength.

VIII. The drying shrinkage and creep of FGPC are small, hence reduces the tensile stresses in concrete. Eventually leads to economic benefit.

IX. The overall cost of FGPC is significantly lower than OPC concrete if it is produced in bulk.

X. The performance of geopolymers is better than the organic polymers in terms of fire resistance, durability under ultraviolet light, and did not involve any toxic substances.

1.6. Areas of Application

In the short term, there is a large potential for FGPC applications for bridges, such as precast structural elements and decks as well as structural retrofits using geopolymer-fiber composites. Geopolymer technology is most advanced in precast applications due to the relative ease in handling sensitive materials (e.g., high-alkali activating solutions).

FGPC can be used in the construction of pavement, sand replacement, cement alternatives, and tuff tiles. Moreover, we also use it in lightweight bricks and blocks. Furthermore, its use in making concrete slabs, road embankments, soil stabilization, and land files is also worthy.

The FGPC can also be used in the manufacture of railway sleepers, as its engineering performances are excellent, and the drying shrinkage was small. FGPC are used to strengthened concrete structures as well as geopolymer coating to protect the transportation infrastructures. The geopolymer composites have been successfully applied to strengthen reinforced concrete beams.

1.7. Outline of Thesis

The present research study is an effort to predict the mechanical properties of fly-ash based geopolymer concrete by use of gene expression programming. The study includes five chapters; Introduction, Literature Review, Research Methodology, Results, Analysis and Discussion, in the end the main findings of the study are presented along with suggestions for future research.

Chapter 1 identifies the studied problem in relevance to the national needs. It includes the scope and objectives of the research. A brief description of what will be covered in each chapter is included.

Chapter 2 covers the detailed literature review of the production of fly-ash, its utilization in the construction industry, and the use of artificial intelligence technique namely gene expression programming (GEP) to develop an effective and accurate GEP based model for the estimation of compressive strength of FGPC.

Chapter 3 covers the methodology followed in this research. Which includes the collection of experimental data from the peer reviewed published articles, the division of data, and the initial statistics of data. This chapter also explain the steps that are carried out to develop the GEP model. This includes the selection of input and output variables and pre-processing and determination of GEP model's parameters. It also includes the details of experimental setup.

Chapter 4 covers the overall results and discussion of the research. Which includes the translation of the expression tree into a mathematical expression for the development of a GEP model for the compressive strength of FGPC, performance evaluation of the developed model via statistical criteria and the selected external validation criteria, and the analysis of model through sensitivity and parametric study. In the end the performance of the model is also evaluated against linear and non-linear regression models.

Chapter 5 summarizes the main conclusions of this work and some suggestions for further research and development.

CHAPTER 2

LITERATURE REVIEW

2.1. Utilization of Fly Ash in Concrete Production

According to a report published by United Nations, the population of world is increasing at a rapid rate and is expected to reach 9.7 billion by year 2050 [1]. The increase in population is proportional to spike in the construction activities [1]. The construction industry is the largest consumer of world's energy (approximately one third of the total energy consumption) and responsible for 30% of global carbon dioxide (CO_2) emission [1]. The production of 1 ton of OPC and concrete, which are the most consumed man-made material releases 0.73-0.85 and 0.05-0.13 tons of CO_2 to the environment, respectively [1].

Therefore, the application of green concrete is considered as a prominent factor to reduce global CO_2 emissions and negative environmental impacts [1]. Green concrete utilizes supplementary cementitious materials (fly ash, calcined clay or ground granulated blast furnace slag) as low carbon alternatives to OPC [1]. The pozzolanic material from agricultural and industrial by-products, for example, silica fume, fly ash, metakaolin and rice husk ash (RHA) has received increasing attention recently, as their utilization improves the physical and mechanical properties of the mixed concrete cement, the expense and the decrease of negative ecological impacts [2, 3].

Fly ash (FA) is the unburned leftover residue from thermal coal plants [1]. Which is transported by gases emitted from the burning zone in the boiler. FA is collected through mechanical or electrostatic separator [2]. Annually around 375 million tons of FA is produced throughout the globe, with a disposal cost as high as $20–$40 per ton [3]. It is dumped into landfills in sub-urban areas [4]. However, dumping tons of FA exclusive of treatment sets off a malignant impact on the green environment [5]. The hazardous materials in FA like silica, alumina, and oxides such as a ferric

oxide (Fe_2O_3) are intervening factors in water, soil, and air pollution. This ultimately leads to health issues and different geo-environmental problems [6,7]. A good waste management employment is desirable for the sustainability of a safe environment [8]. FA, if not properly disposed of, will affect the whole ecological cycle. Ultra-fine particles of FA act in the same way as poison when they reach the respiratory system. Consequently, causing physiological disorders and other related health issues like cancer, hepatic disorder, anemia, dermatitis, and gastroenteritis. FA pollutes surface and underground water which stresses aquatic life and causes skin diseases and diarrhea [7].

For every human about three tons of concrete is produced [11]. Around 25 billion tons of concrete is manufactured every year globally [12]. According to current world stats, approximately 2.6 billion tons of cement is produced per year. This will rise by 25 percent in the next 10 years [13]. However, the manufacturing of cement has an adverse effect on the environment. One ton of CO_2 is emitted into the air to produce one ton of cement. This creates an alarming situation for the environment. Limestone is the major resource of ordinary Portland cement. Severe limestone unavailability could occur in 25–50 years [14,15]. The worldwide construction industry consumes one-third of the entire resources and is liable for 30 percent CO_2 release globally. Thus, production of green concrete is important to reduce adverse environmental effects [16,17]. FA can be used as supplementary material in the cementitious matrix. It has been utilized by researchers to make green concrete [18–21]. FA utilization in the construction industry is a smart choice as it will reduce the usage of cement and the harmful effect of its disposal into landfills.

The plentiful availability of fly ash around the world creates the opportunity to use this burning coal product, as a substitute for OPC to produce concrete. When used as a replacement for partial OPC, in the existence of water and room temperature, calcium silicate hydrate (C-S-H) gel is formed after the reaction of fly ash and calcium hydroxide. The advancement in the application of

high-volume fly ash concrete, empowered the substitution of OPC up to 60% by mass. Which is considered as a noteworthy improvement. However, 20% is the optimum amount reported [3, 4].

Geopolymer is a binder that can be generated via polymeric reaction of alkaline liquids with the aluminum and the silicon in source materials of the geological origin or by-product materials like rice husk ash and fly ash [3]. The authors recommended that pozzolans like fly-ash may be activated via alkaline liquids to form a binder and thus completely replace the use of OPC in concrete [3]. For now, the main contents to be activated are silicon and calcium in the fly-ash [3]. The fundamental binder produced is a C-S-H gel, as the result of the hydration process [3].

Extensive research is available regarding the use of geopolymer technology to make fly-ash based geopolymer concrete (FGPC). Fly-ash geopolymer binder shows excellent short and long-term mechanical properties [3]. Different researchers reported that compressive strength, split tensile strength, flexural strength and elastic modulus of geopolymer concrete depends on different parameters [3]. Like the type of alkaline activator, the temperature of the curing regime, the time required for curing etc. [3].

Researchers have reported that for an acceptable polymerization, the critical parameters that need to be controlled are the extra water added as percent FA ($\%E_W$), the percentage of plasticizer ($\%P$), the initial curing temperature (T), the age of the specimen (A), the curing duration (t), the fine aggregate to total aggregate ratio (F/A_G), the percentage of total aggregate by volume ($\%A_G$), the percent SiO_2 solids to water ratio ($\%\ S/W$) in sodium silicate (Na_2SiO_3) solution, the NaOH solution molarity (M), the activator or alkali to FA ratio (A_L/F_A), the sodium oxide (Na_2O) to water ratio (N/W) for preparing Na_2SiO_3 solution, and the Na_2SiO_3 to NaOH ratio (N_s/N_o) [13,28–35]. However, Van Jaarsveld et al. [102] studied that elevated temperature curing for a long time may deteriorate the structure of hardened material, that reveals that high temperatures for extended periods may debilitate the structure of solidified material.

The researchers narrated that the in comparison with other parameters, the curing temperature greatly affect the compressive strength of geopolymer concrete. The compressive strength is increased with the increase curing temperature. There is a significant increase in compressive strength to 60 ^{0}C temperature and 48 hours curing time. The compressive strength cured at 60 ^{0}C for 24 hours did not alter with the age and stayed steady at roughly 60 MPa, because of the quick pace of polymerization reaction [63].

The author's investigated that the compressive strength of fly-ash based geopolymer concrete increases significantly with the increase of H_2O-to-Na_2O molar ratio, while the effect of Na_2O-to-SiO_2 molar ratio is insignificant. Additionally, the compressive strength gets decreased with the increase of water to geopolymer solid ratio [63].

Modulus of elasticity is one of the important parameters to access structural performance. The authors described that due to heat curing elastic modulus and long-term compressive strength of fly-ash based FGPC was indicated as 82% and 66% of that OPC concrete respectively [67]. They observed that elastic modulus and compressive strength increases with the increase of curing temperature up to 75 ^{0}C for 24 hours. Furthermore, the authors also indicated that the elastic modulus of heat-cured FGPC was increased due to the presence of silicate ions in the activator solution, while the bond and shrinkage properties are adversely affected [67].

The authors observed that, although alkali-activated natural pozzolan (AANP) mixes gained lower values of static modulus of elasticity than OPC mixtures during first 14 days, the values were about 5–20% higher than OPC mixes in long-term tests [24]. Thus, a wide variation in the modulus of elasticity of geopolymer concrete was observed in the previous studies [24].

The utilization geopolymer concrete made of FA-like waste, is on the rise for the last two decades as lesser amounts of cement are used in geopolymer concrete (GPC) [22–26]. FA has been used effectively in the construction industry but its application is still limited due to the anomalous

behavior of FA [27]. FGPC is adopted extensively by builders. No method is available to estimate the mechanical properties of FGPC based on a mix ratio with maximum variables considered in this research. The mechanical properties of FGPC critically depends on several parameters like the extra water added as percent FA ($\%E_W$), the percentage of plasticizer ($\%P$), the initial curing temperature (T), the age of the specimen (A), the curing duration (t), the fine aggregate to total aggregate ratio (F/A_G), the percentage of total aggregate by volume ($\%A_G$), the percent SiO_2 solids to water ratio ($\%\ S/W$) in sodium silicate (Na_2SiO_3) solution, the NaOH solution molarity (M), the activator or alkali to FA ratio (A_L/F_A), the sodium oxide (Na_2O) to water ratio (N/W) for preparing Na_2SiO_3 solution, and the Na_2SiO_3 to NaOH ratio (N_s/N_o) [13,28–35]. This creates ambiguity in the prediction properties of GPC.

Moreover, a rapid spike in the use of soft computing techniques to build an empirical model has been observed recently [36,37]. Gene expression programming (GEP) is one of the popular soft computing methods utilized by various researchers in several engineering perspectives. Actual GEP is inspired by the reproduction of DNA molecules at gene level [38]. Tanyildizi et al. [39] predicted different mechanical properties of lightweight concrete subjected to elevated temperature. The author projected two different GEP models with chromosome levels equal to 30, head size 8, and number of genes equal to 4. Multiplication and addition are the two different linking functions used. The execution time of the GEP depends on the chromosome level, which dictates the size of the population. Genetic operators help in the genetic variation of the chromosomes. The chromosome that delivers the best results is forwarded to subsequent generations and the process is repeated until the achievement of an acceptable fitness.

Recently, different researchers use the GEP for the estimation of various mechanical characteristics of different types of concrete. The researchers use experimental and literature-based data for the prediction of compressive strength of sugar cane bagasse ash (SCBA) concrete via GEP

[36]. Furthermore, the authors proposed a formula using GEP for estimating the axial capacity of concrete filled steel tube (CFST) with just 277 instances [37]. Furthermore, Nour et al. [40] worked with GEP algorithms for the estimation of compressive strength of CFST containing recycled aggregates.

2.2. Application of Artificial Intelligence Technique in Civil Engineering

The latest research in the extent of Artificial Intelligence (AI) methods contributed to the formulation of consistent, reliable and accurate models to the problems in structural engineering [79].Artificial neural networks (ANN), fuzzy logic, genetic algorithms (GA), and genetic programming (GP) use AI techniques built on natural tools [80-101]. In these methods, training of the available data resolves the problem. The configuration detection capabilities of the AI methods (support vector regression or ANN) can lead to the generalization of complicated patterns, therefore can be applied in the vast field of engineering. Though, several of these methods involve a prebuilt base type (best model architecture) and thus need an enormous memory. By employing such approaches, the presence of an enormous sum of hidden neurons often allows it impossible to establish a realistic relation between the outcome and the inputs. By means of ANN, the strength of rice husk ash (RHA) based concrete were predicted [100]. The strength predictive model is highly correlated with the 66 experimental datasets. ANN was used for the establishment of mix proportion of self-compacting concrete (SCC) [23]. In these models, however, there is a realistic correlation, yet no empirical expression was projected for practicable use. That is because of the complexity of the ANN model structure, and is considered as the main obstruction in the wide-scale adoption of ANN approach [92]. From the comparative study of ANN and GP approach to predict concrete slabs punching shear strength, the author finds that the ANN models become overfitted when evaluated by comparison with values of the design code. This is attributable to their complex structure [25]. Also, the multicollinearity makes an issue in these methods. Updated ANN technique likewise extended to assess silica fume concrete compressive strength (f_{cc}) and elastic modulus (E_c) of concrete

incorporates recycled aggregate [101]. Because of the complexities of the relationship proposed, a devoted graphical interface was created for the model functional usage [101].

A strong soft computing technique, Genetic programming (GP), is valuable as it ignores previous form of established relation for the development of the model [102, 103]. An extension of GP, Gene expression programming (GEP), to encode a small program, uses easy, fixed length linear chromosomes [104]. GEP has an advantage that simple mathematical expression can represent outcome that is appropriate for practicable usage of better predictive accurateness. It has currently used as an alternate to the common techniques of prediction especially in the civil engineering field [105-114]. The establishment of these models was utilized for the prediction of the influence of the class of cement strength on f_c' of cement mortar, concrete split tensile strength (f_{st}), self-compacting concrete hardened and fresh properties, design of lightweight concrete, f_c' of concrete including rice husk ash and mechanical properties of lightweight concrete incorporating silica fumes.

As the compressive strength is considered as the primary factor in the analysis and design of concrete structure. So, the Researchers focused on the experimental route to find out the fly-ash based GPC's compressive strength [36-78]. In order to save time, cost and to sustain the use of fly-ash in the building construction industry, the development of accurate and reliable expression is needed in order to relate the mix proportion and compressive strength of GPC made with fly-ash. A comprehensive and thorough revision of the literature discloses that there are few empirical models to predict the compressive strength of fly-ash based GPC [47, 53, 115]. Though, the predictions of such empirical models are confined to a specific data base i.e., to the corresponding study experimental results. So, the prediction from such models is not viable and accurate outside the corresponding database file. So far, no empirical model exists to effectively predict the compressive strength of fly-ash based GPC built on GEP. In order to fill this research gap, the GEP approach is employed to establish generalized empirical equation for the prediction of the f_c' of fly-ash based GPC with a tolerable error. A detailed database has been developed on the basis of worldwide

published research. The comprehensive database accomplishment guarantees that the models are consistent and accessible for the data that is not exercised in the model's establishment. The model's performance is also verified by observation of the statistical error, parametric analysis, sensitivity checks and linear and non-linear regression analysis.

2.2.1. Overview of Genetic Programming (GP)

Koza proposed GP, in order to provide an alternate for fixed length binary strings (used in GA) [116]. It is based on the realistic usage of the genetic and natural selection idea [79, 104]. The induction of nonlinear parse tree structure makes it an adaptable programming technique. It is indeed an exact technique independent of the domain, where a computer code is structured to address an issue dependent on the Darwinian reproductive principle and equivalent to the existing genetic operations like reproduction, mutation and crossover [114, 116]. A mechanism is formulated in the reproduction phase to decide which programs will diminish. At the execution phase, a particular proportion of trees, displaying the unpleasant fitness, are put down, while the remaining trees filled up the population as per the chosen procedure [105, 114]. In the mutation process the model is secured from premature convergence [114]. Figure 2.1 illustrates the method to develop a computer program through GP approach to solve a problem.

Five main parameters to be defined throughout the GP methodology are the collection of the terminals (the constants and the input variables), the set of primitive functions (domain-explicit functions), the fitness evaluation, the control variables (cross-over and population size etc.) and the termination criteria followed by result designation method [114, 116]. Three genetic operators were identified in GP, but just tree crossover is used practically, thus creates an enormous parse trees population [116]. One more limitation of GP is ignorance of the independent genome. The GP uses non-linear structures that acts as both the genotype and the phenotype make it unlikely to produce basic and simplistic expressions [104].

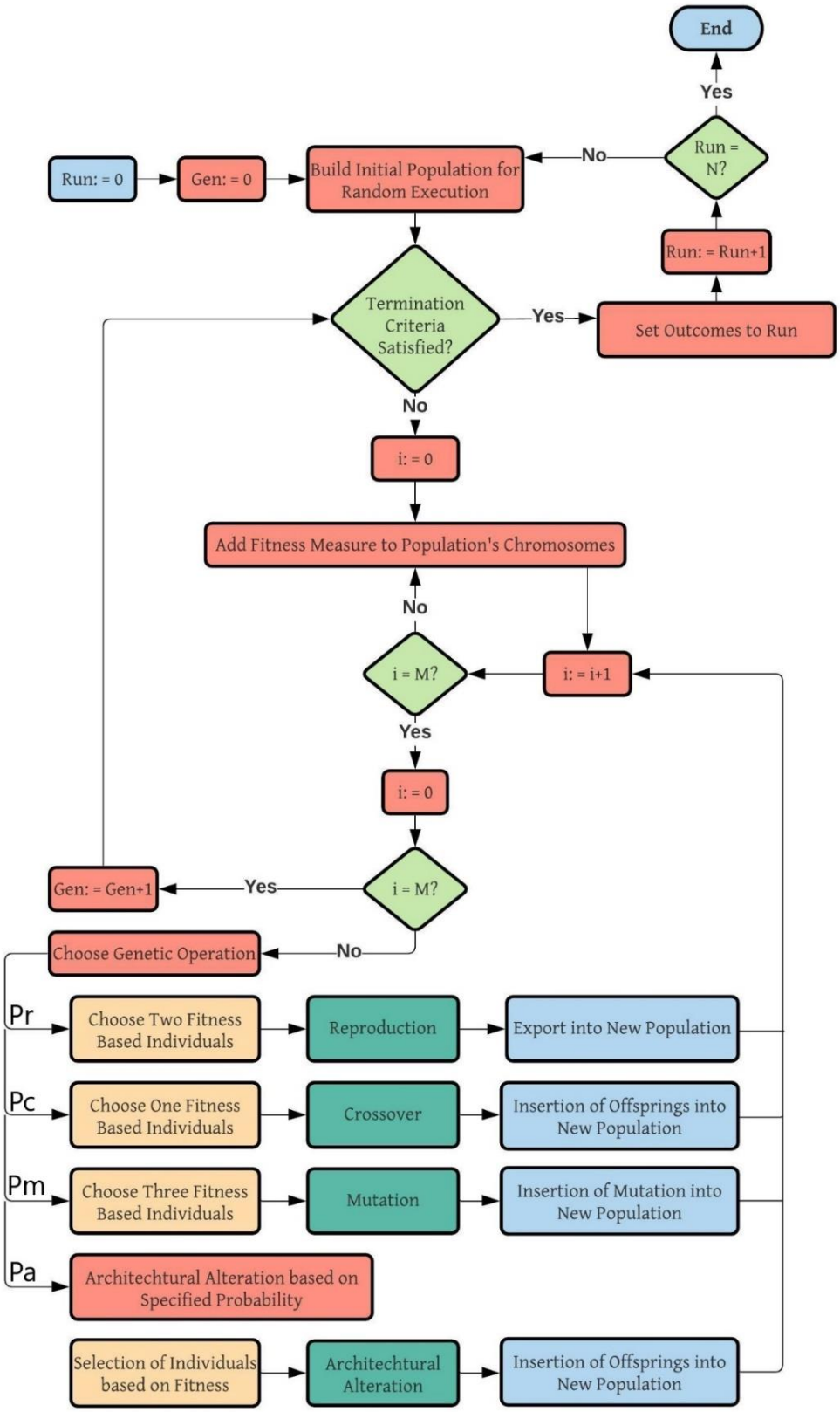

Figure 2.1. Flow chart of the genetic programming (GP) algorithm [37].

2.2.2. Overview of Gene Expression Programming (GEP)

Ferreira proposed GEP that is a modified version of GP. It is built on evolutionary theorem of population [104]. It combines together the parse trees (GP) and the rudimentary fixed-length linear chromosomes (GA). The parameters necessary are identical to those used in the GP i.e., function set terminal set, fitness parameter, terminal constraints, and control parameters. Within that algorithm, while processing in the computer program, a character string of a specific size is assumed and contrasted with the parse tree of various size in the GP. Entities coded as linear sequence of fixed size strings (genome) are afterward displayed by means of nonlinear entities of various shape and sizes identified as trees of expression or expression trees (ETs), which are evolved chromosomes-specific structures [114]. It's indeed analogous to case that the genotype and phenotype are kept separate in GEP and the code will advantage completely from the evolutionary approach [104]. A significant alteration throughout GEP is that just the genome is transmitted towards the subsequent generation and thus it isn't needed to repeat the whole structure as the entire changes actually occur in a simple linear way. One other noteworthy characteristic is the establishment of entities by a single chromosome composed of various genes then categorized as tail and head [114]. Every gene with in GEP comes in the form of fitted lengths parameter, terminal sets of constants, and the functions used are the arithmetic operations. Also, in genetic code operator, there is a stabilized interaction amongst both the associated function or terminal and the chromosome symbol. The chromosome-level genetic mechanism makes the development of genetic variance within the simple process of GEP [79]. The necessary information for the development of an empirical model is registered into the chromosomes and to infer this information a novel language i.e., karva has been established. If the sequence of gene is provided, then it is viable to deduce the particular phenotype and vice versa called a karva or K-expression [104]. Karva 's transformation towards the ETs usually begins on or after the leading position in the ETs, and proceeds throughout the string. By take of the record in the nodes through root layer to a deepest layer, ETs can indeed be converted into K-expression [102]. The size of the

K-expression and GEP gene may or may not be identical, because the size of the ET changes in the GEP algorithm that results in the presence of a variety of redundant elements. Exactly the same aren't really required for mapping the genome.

In Figure 2.2 the phases covered in the algorithm of GEP are shown. The method starts with arbitrary formation of fixed size chromosomes for all that individuals. These are afterwards identical to the ET's and for each individual the fitness strength is estimated. In support of the appliance of reproduction process, the best fitted individuals are selected. For a number of generations, the reiteration lasts with new individuals till the accomplishment of a finest result. Genetic functions like cross-over, reproduction and mutation are implemented for population alteration.

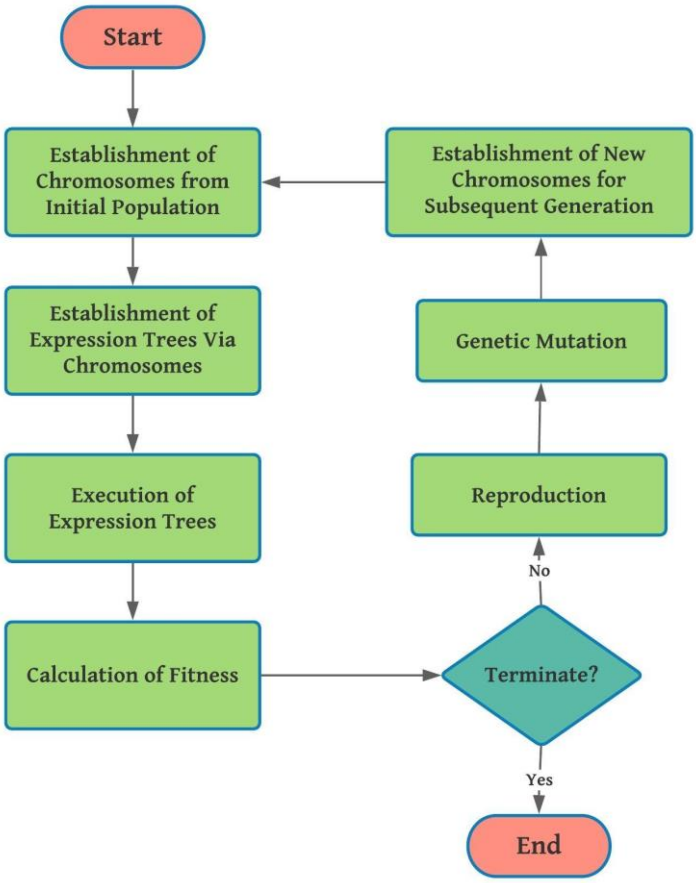

Figure 2.2. Gene expression programming (GEP) algorithm flow chart [37].

2.3. Summary

This chapter presents detailed literature review on the utilization of fly-ash as replacement of OPC in the concrete. The impact of the utilization of such hazardous materials on the sustainability problems occurring due to usage of conventional materials in the concrete has also been discussed briefly. Moreover, the background of artificial intelligence techniques has been elaborated and the recent application in the field of civil engineering has been highlighted.

CHAPTER 3

RESEARCH METHODOLOGY

In this chapter the methodology adopted for the for the empirical study of the collected data will be elaborated. Compressive strength (f_c') is the main factor in analysis and design of concrete structure. To save time, cost, and to sustain the use of FA in the construction industry, the development of accurate and reliable expression is needed that can relate the mix proportion and f_c' of FGPC. The detailed methodology implemented for the experimental investigation of FGPC would be discussed.

3.1. Data Collection

A detailed database for the f_c' of FGPC, was compiled from previously published, experimental researches (see APPENDIX A1) [60,61,63,67–99]. The database comprises of total 298 samples which include 101 cylindrical specimens of size 200 mm × 100 mm, height × diameter, 166, and 31 cube specimens of size 150 mm and 100 mm, respectively. f_c' of cube and cylindrical specimens depends on the length to diameter (L/D) ratio [100,101]. The f_c' of 100 mm cubes are 5% greater than 150 mm cubes. While f_c' of 150 mm cubes are 20% greater than cylindrical specimens of size 100 mm × 200 mm. With the increase of the volume of the specimen, the number of voids also increases, so, the specimen with smaller dimension will have lesser f_c' than the larger dimension specimen. Furthermore, the stress is inversely related to the cross-sectional area of the specimen. The one with smaller cross-sectional area will have higher stresses, which means high internal resistance to failure. Table 3.1 displays the normalization of the compressive strength of various types of specimens considered in this study. The comprehensive database guarantees the model reliability and accessibility for the data that is not exercised in the development of the empirical model.

Table 3.1. Type of specimens and compressive strength normalization factor.

Type of sample	Number of data points	Normalization factor
Cylindrical $(200 \times 100)\ mm$	101	1
Cube $(100\ mm)$	166	1×0.8
Cube $(150\ mm)$	31	0.95×0.8

The composed database covers data about the explanatory parameters, namely, the extra water added as percent FA ($\%E_W$), the percentage of plasticizer ($\%P$), the age of the specimen (A), the curing duration (t), the fine aggregate to the total aggregate ratio (F/A_G), the percentage of total aggregate by volume ($\%A_G$), the percent SiO_2 solids to water ratio ($\%\ S/W$) in sodium silicate (Na_2SiO_3) solution, the NaOH solution molarity (M), the activator or alkali to FA ratio (A_L/F_A), and the Na_2SiO_3 to NaOH ratio (N_s/N_o) for the response of compressive strength. All the samples collected for the mentioned parameters are heat cured initially for 24 h at different temperatures. The f_c' increases with curing time but researchers reported that the rate of increment in the f_c' of FGPC is rapid until 24 hours [63]. The early strength of GPC is higher due to the geo-polymerization process and limited literature is available for longer curing duration. Van Jaarsveld et al. [102] described that for longer than 24 h curing time, the f_c' is not increased. Every model performance depends on the distribution of explanatory parameters [103]. The marginal histograms of all ten input parameters used in this study are shown in Figure 3.1, which dictates that all 10 explanatory parameters selected are distributed through its range for the compressive strength. The bar charts added above and to the right of the main plot add more information to the data. Along with the distribution of the input variables, it also shows the distribution of the compressive strength. Every explanatory variable has a strong impact on the variation of the compressive strength of FGPC.

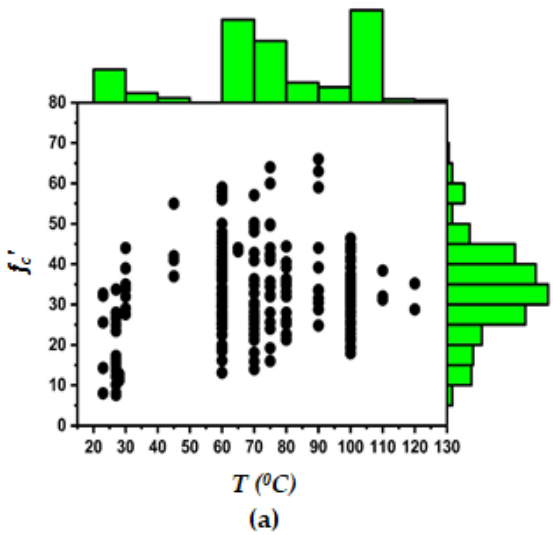

(a)

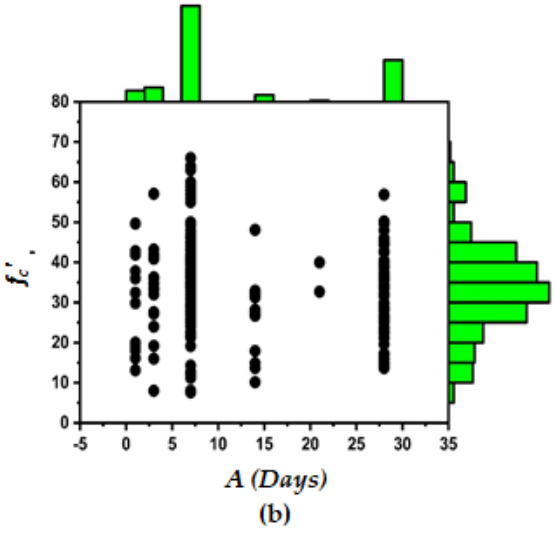

(b)

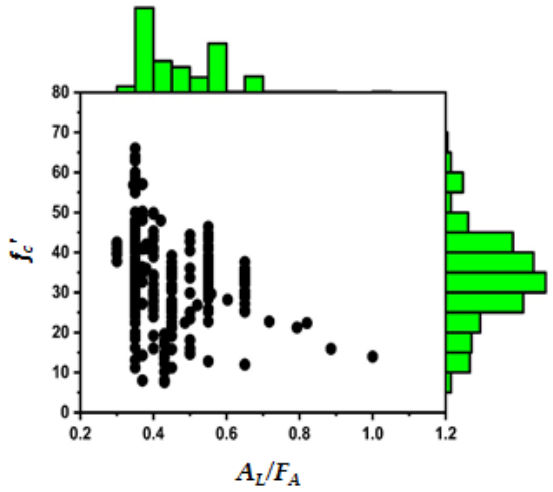

(c)

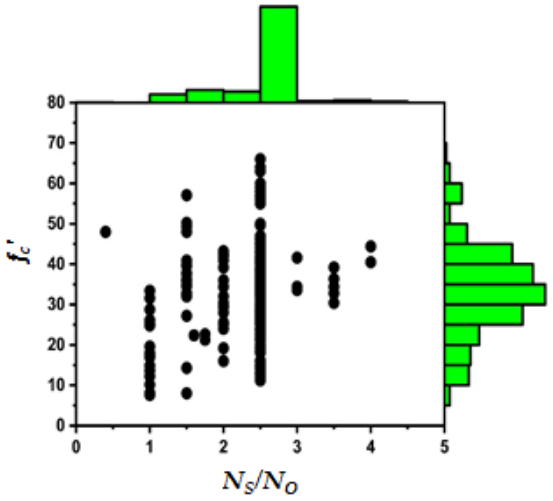

(d)

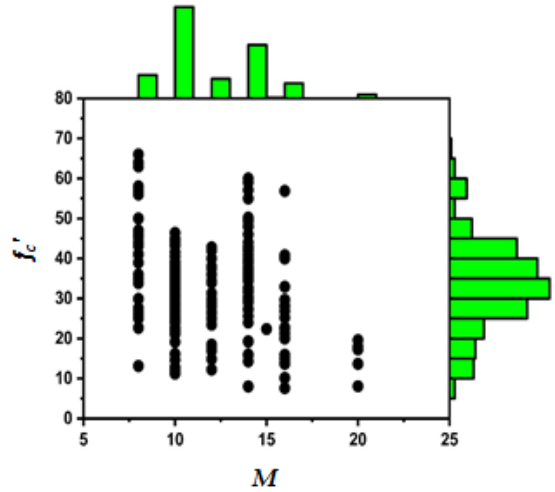

(e)

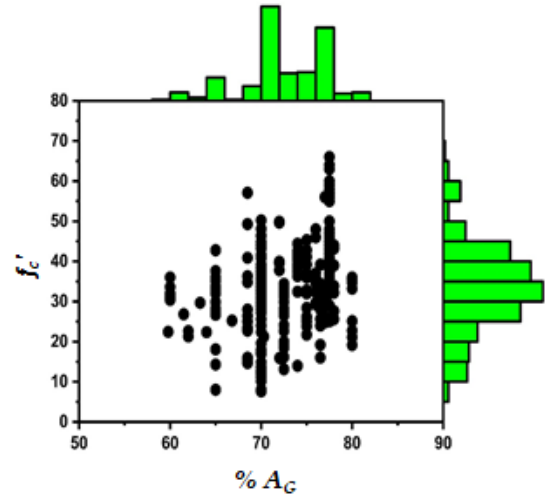

(f)

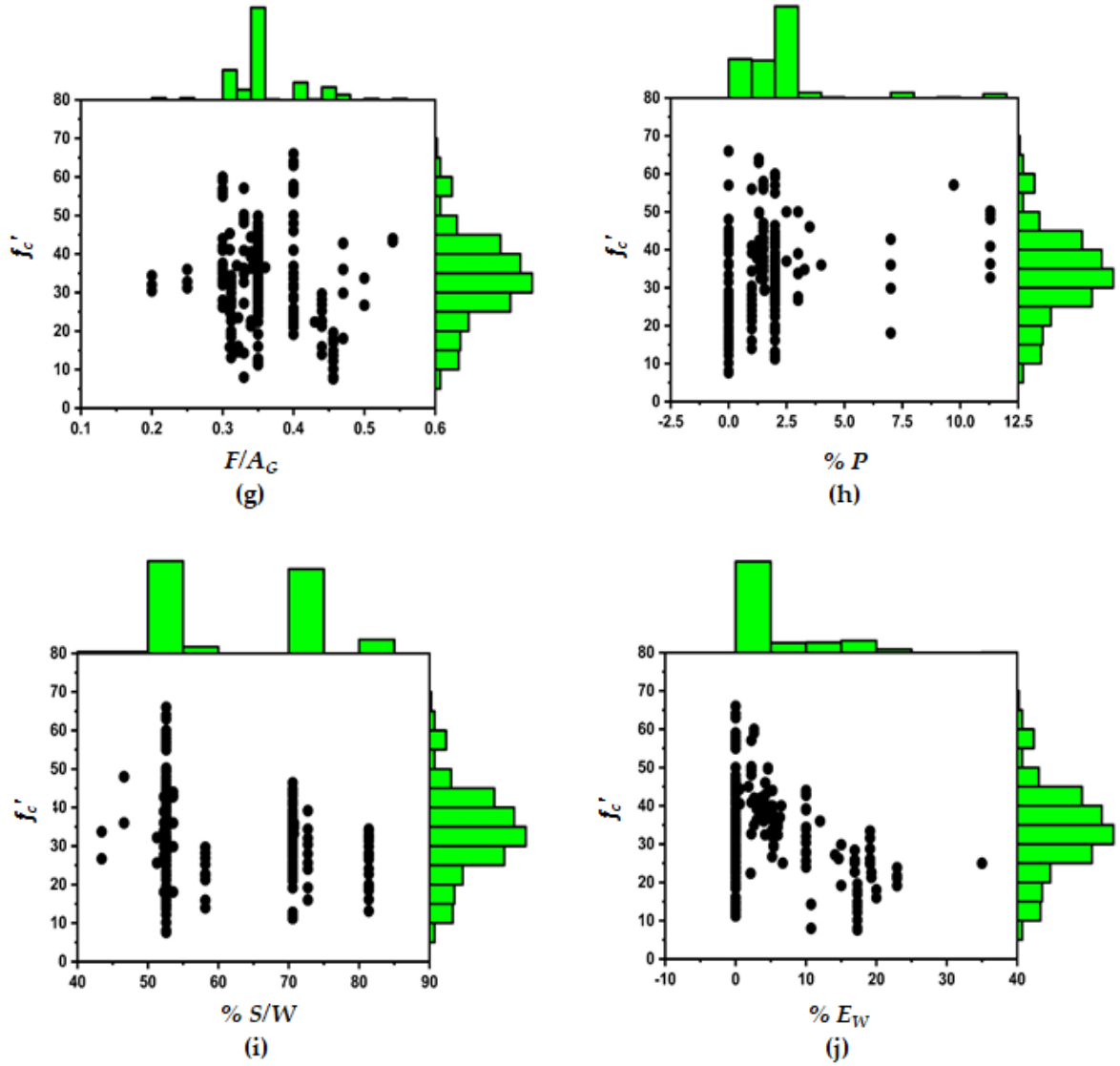

Figure 3.1. Marginal histogram of explanatory parameters against output variables. **(a)** Temperature for curing of specimen *(T^0C)*, **(b)** Age of specimen *(A)*, **(c)** Alkali to fly-ash ratio *(A_L/F_A)*, **(d)** Sodium silicate to sodium hydroxide ratio *(N_S/N_O)*, **(e)** Molarity of NaOH solution *(M)*, **(f)** Percentage of total aggregate by volume *(A_G)*, **(g)** Fine aggregate to total aggregate ratio *(F/A_G)*, **(h)** Percentage of superplasticizer *(% P)*, **(i)** Percentage of SiO_2 solids to water ratio *(% S/W)*, **(j)** Percentage of extra water added *(% E_W)*.

To conduct the generalized study, both cubes and cylindrical specimens are counted to construct a database. The output and input variables' ranges, along with their mean values are

presented in Table 3.2 For the achievement of reliable and consistent predictions of the compressive strength, it is endorsed to utilize the suggested model with the ranges provided.

Table 3.2. Range, mean and standard deviation of explanatory and response parameter.

Parameters	Minimum value	Maximum value	Mean value	Standard deviation
Explanatory parameters				
T (°C)	23	120	71.57	24.61
A (days)	1	540	20.87	45.73
A/F	0.3	1	0.4545	0.1187
N_S/N_O	0.4	4	2.275	0.5168
M	8	20	11.68	2.6415
A_G (%)	60	80	72	4.753
F/A_G	0.2	0.5	0.3568	0.0493
P (%)	0	11.3	1.998	2.326
S/W (%)	43.4	81.4	61.68	10.167
E_W (%)	0	35	3.889	6.341
Response				
$f_c^{'}$ (MPa)	8.2	63	37	11.154

It should be noted that, for the evaluation of the validity, reliability, and consistency of the database, multiple trials were conducted. Datasets that diverged considerably from the global norm (about 20%) were not included in the model's creation and performance evaluation. To establish an

empirical model, 298 datasets for the prediction of compressive strength were used. In this research, the data points were arbitrarily divided into two statistically consistent sets known as the training and validation sets [37]. Furthermore, 70% (208 data points) of the total data are assigned to the training set and 30% (90 data points) to the validation set [37]. The training set was employed for training the empirical model known as gene progression, whereas validation data points were utilized for the justification and calibration of the established model's generalization capability as suggested in the literature [57].

3.2. Model Development and Evaluation Criteria

For the development of the model, the first step is the selection of input parameters that can influence the FA-based GPC's properties. Influential parameters that effect the compressive strength (f_c') of GPC made with FA were selected for the generalized model development. The detailed study is carried out and the performance of several initial runs is computed. Hence, the FA-based GPC's compressive strength is taken into account as the function of Equation (1).

$$f_c' = f\left(T, A, M, \%\frac{S}{W}, \frac{A_L}{F_A}, \frac{N_S}{N_O}A_G, \frac{F}{A_G}, \%P, \%E_W\right) \quad (1)$$

Chromosomes, genes, and expression trees (ETs) perform a central role in the development of the GEP model. The program's running duration is regulated through the size of the population (chromosome number). The chromosome is comprised of genes that are used for encoding of the subexpression trees (sub-ETs). Considering the predictive model complexity, the stages counted as population size were 150. The model's architectural structures rest on the gene number and head-size with the latter dictating the difficulty of every term and the latter deciding the sum of the model's sub-ETs. Thus, population size 150, genes 3, and head size 10 is considered for the development of the model. The chromosomes are subjected to genetic variation through genetic operators. In mutation, the component of the gene's tail or head is randomly selected and replaced with a randomly

selected component of the terminal or function set. The transposition function involves the transposition of the sequences inside the chromosomes, in other words, root insertion sequence (RIS) and insertion sequence (IS). After all, the recombination combines and splits up 2 chromosomes in order to substitute their elements. For creating the fair empirical model, the adjusted settings recommended in earlier literature were used [41]. To execute the GEP algorithm, GeneXproTool was used. Table 3.3 illustrates the adjusted setting of the hyperparameters utilized in the formation of the GEP empirical equation.

Table 3.3. Adjusted Setting of parameters for the GEP model.

Parameters	**Adjusted setting for f'_c**
General	
Population chromosomes	150
Genes	4
Head size	10
Linking function	Multiplication
Function Set	$-, +, /, \times, \sqrt[3]{}$
Arithmetical constants	
Constant per gene	10
Data type	Floating data
Upper Bound	10
Lower bound	–10

Genetic operators	
Mutation rate	0.00138
Inversion rate	0.00546
IS transportation rate	0.00546
RIS transportation rate	0.00546
One-point recommendation rate	0.00277
Two-point recommendation rate	0.00277
Gene recombination rate	0.00755
Gene transportation rate	0.00277

A correlation coefficient (R) is mostly applied to measure model performance. However, it cannot be merely studied as the sign of model predictive accuracy as it is insensitive towards division and multiplication of outcomes to a constant [104]. For that reason, in this research the mean absolute error (MAE), the root means square error (RMSE), the relative root mean squared error (RRMSE), and the relative squared error (RSE) are also considered. Moreover, the model performance evaluation performance index (ρ) is recommended, as it covered the function of both the R and RRMSE [103]. The equations of error functions used in this study are provided as Equations (2)–(7):

$$RMSE = \sqrt{\frac{\sum_{i=1}^{n}(e_i - m_i)^2}{n}} \quad (2)$$

$$MAE = \frac{\sum_{i=1}^{n}|e_i - m_i|}{n} \quad (3)$$

$$RSE = \frac{\sum_{i=1}^{n}(m_i - e_i)^2}{\sum_{i=1}^{n}(\bar{e} - e_i)^2} \quad (4)$$

$$RRMSE = \frac{1}{|\bar{e}|}\sqrt{\frac{\sum_{i=1}^{n}(e_i - m_i)^2}{n}} \quad (5)$$

$$R = \frac{\sum_{i=1}^{n}(e_i - \bar{e}_i)(m_i - \bar{m}_i)}{\sqrt{\sum_{i=1}^{n}(e_i - \bar{e}_i)^2 \sum_{i=1}^{n}(m_i - \bar{m}_i)^2}} \quad (6)$$

$$\rho = \frac{RMSE}{1 + R} \quad (7)$$

where m_i and e_i are the i^{th} model outcome value and experimental value, respectively. While $\bar{m}_i$ and $\bar{e}_i$ are the model's outcome average value and experimental average value, respectively. Additionally, *n* denotes the overall data points. High R-value and low RMSE, MAE, RSE, and RRMSE shows a best-calibrated model. It is suggested that for a deep correlation between measured and predicted values, the R-value should be greater than 0.8 (as for ideal model R = 1) [105]. The (ρ) value near to zero replicates better model performance.

3.3. Experimental Program for Validation of GEP Model According to Pakistani Environment

The geopolymer concrete can be prepared from different source material like ground granulated blast furnace slag (GGBS), metakaolin, waste foundry and fly-ash etc. The objective of this particular section is to encourage the use of fly ash in the construction industry.

3.3.1 Fly-Ash

The fly-ash was obtained from the local supplier at Lahore, Pakistan. The chemical composition of fly-ash was assessed via X-ray Florescence (XRF) as presented in Table. The cumulative composition of silica (SiO_2), iron oxide (Fe_2O_3) and alumina (Al_2O_3) are 90.71% that is greater than 70%, Which satisfy the condition for pozzolan as per ASTM C618-05. As indicated through loss of ignition (LOI), a very less percentage of carbon was noted. Figure 3.2. represent the black color of fly-ash.

Table 3.4. Detail Analysis of fly-ash via X-ray Florescence (XRF)

Oxides	Percentage by mass
Silica (SiO_2)	53.49
Aluminum oxide (Al_2O_3)	26.86
Iron oxide (Fe_2O_3)	10.36
Calcium oxide (CaO)	3.31
Magnesium oxide (MgO)	1.13
Phosphorous oxide (P_2O_5)	1.52
Potassium oxide (K_2O)	0.55
Sodium oxide (Na_2O)	0.33
Titanium oxide (TiO_2)	0.12
Manganese oxide (MnO)	0.44
Loss on ignition (LOI)	1.13

Figure 3.2. Pictorial representation of fly-ash

3.3.2. Alkaline Solution

In the current study, the combination of sodium hydroxide (NaOH) solution and sodium silicate (Na_2SiO_3) solution were selected as alkaline medium. The sodium-based solution was selected instead of potassium, as they were easily available and cheaper. Both the chemical supplements were obtained from HDE trading Ltd Sheikhupura, Punjab, Pakistan. The NaOH were in pellets form with 98% purity.

The concentration of NaOH solution were represented by molarity (M). For instance, the 8 M NaOH solution was prepared by dissolution of 8*40=320 gram of pellets in water. Where 40 represents the molecular weight of sodium hydroxide. The Na_2SiO_3 solution had 14.7% sodium oxide (Na_2O), 29.4% silicon oxide (SiO_2) and 55.9% water (H_2O) by mass.

Figure 3.3. Sodium hydroxide and sodium silicate solution

3.3.3. Aggregates

Both fine and coarse aggregates were obtained from locally available query site. As shown in Table 3.5, three different sizes of coarse aggregate and fine were used. The fineness modulus (FM) was 5.0. In all mixes a consistent 30% fine and 70% coarse aggregate (15%-20mm, 20%-14mm, and 35%-7mm) were utilized. The fine and coarse aggregate portion in the entire concrete mix were kept at 75% by mass.

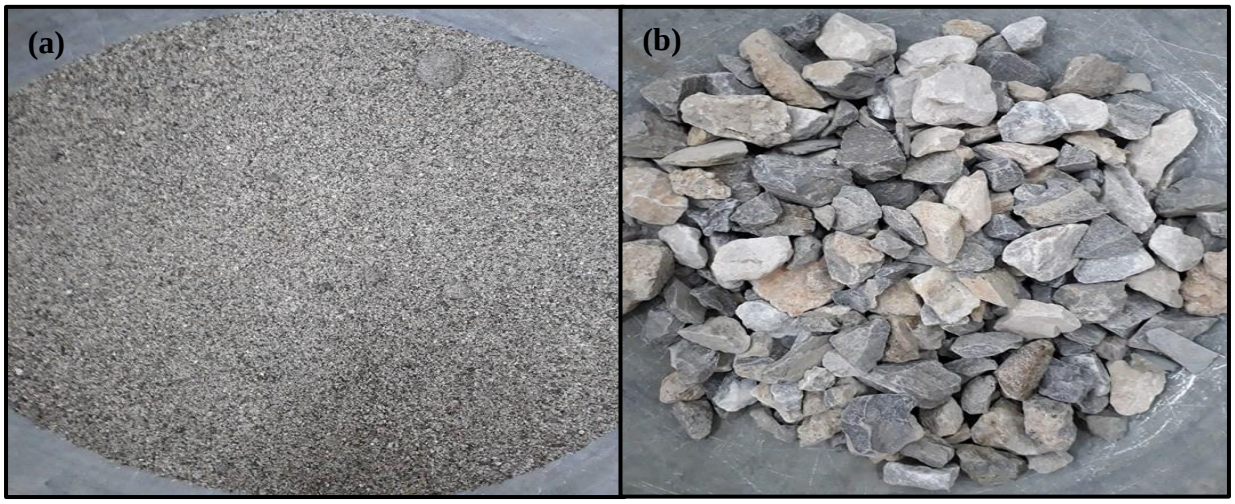

Figure 3.4. Aggregates collected from query site **(a)** Fine aggregate **(b)** Coarse aggregate

Table 3.5. Gradation of aggregates

Size of sieve (mm)	Coarse Aggregate (mm)			Fine Aggregate	Mixture	BS 882:92
	20	14	7			
19	93.44	100	100	100	99.016	95-100
9.5	3.98	18.40	98.9	100	68.89	
4.75	0.89	1.09	21.1	100	37.73	35-55
2.36	0.88	1.0	3.76	100	31.65	
1.18	0.85	0.81	2.04	98.89	30.67	
0.6	0.78	0.7	1.53	78.87	24.45	10-35
0.3	0.75	0.6	1.06	17.53	5.86	
0.15	0.54	0.43	0.68	1.3	0.77	0-8

3.3.4. Mixing

In 2002, Davidovits recommended to prepare the mixture of NaOH and Na_2SiO_3 solution at least a day prior to its addition into a solid element (fly-ash and aggregates). The solid constituents were dry mixed three minutes and after the addition of solution the mixing process was continued for another four minutes.

3.3.5. Mixture Proportion

For validating the robustness of GEP model, six different FGPC mixes were prepared on trial-and-error method (See Table 3.6). The specimen was designated as GC-x. Where "x" ranges from 1 to 6. In GC1 to GC3, keeping all other variables at constant, the molarity of NaOH solution is varied from 8M to 12M with an increment of 2M. While in GC4 to GC6, the ratio between Na_2SiO_3 solution to NaOH solution is varied from 1.5 to 2.5 with an increment of 0.5. For each mix proportion three

cubes of size 150 mm were casted. The cubes were demolded after 24 hours and were subjected to curing at 60^0C for next 24 hours.

Figure 3.5. Geopolymer concrete **(a)** Green concrete **(b)** Casting of cubes **(c)** Temperature curing

Table 3.6. Experimental mixture proportion for validation of GEP model

Mix Designation	T (°C)	A (days)	A/F	N_S/N_O	M	A_G (%)	F/A_G	P (%)	S/W (%)	E_W (%)
GC1	60	7	0.35	1	8	75	0.4	0	52.59	0
GC2	60	7	0.35	1	10	75	0.4	0	52.59	0
GC3	60	7	0.35	1	12	75	0.4	0	52.59	0
GC4	60	7	0.35	1.5	8	75	0.4	0	52.59	0
GC5	60	7	0.35	2	8	75	0.4	0	52.59	0
GC6	60	7	0.35	2.5	8	75	0.4	0	52.59	0

3.3.6. Testing Setup

The hardened cubes specimens were subjected to compression testing machine having maximum capacity of 2000 kN. And the compressive strength of each geopolymer mix were determined in reference to BS 1881: Part 116: 1983 Standard.

Figure 3.6. Compressive strength testing machine

3.4. Summary

In this chapter the methodology adopted has been explained in detail. The type of data collected for modelling the compressive strength of FGPC has been elaborated and the performance measures have also been discussed. The criteria adopted for the model development has been explained.

CHAPTER 4

GEP MODELLING RESULTS AND DISCUSSION

4.1. Expression Trees for GEP Model

The GEP algorithm's output for the compressive strength (f_c') model as an expression tree is shown in Figure 4.1. The empirical relationship was obtained by decoding these expression trees (ETs) that encompass five arithmetical operations, namely, $+, -, \times, /$ and $\sqrt[3]{}$.

GEP ETs use the indicators to express the explanatory variables. The corresponding symbols and description of each indicator are provided in Table 4.1.

Table 4.1. Indicators of GEP expression tree.

Indicator in expression tree	description	symbol
d_o	The temperature for curing in degrees Celsius	T
d_1	The age of the sample	A
d_2	Ratio of alkali or activator to the fly-ash	A_L/F_A
d_3	Ratio of Na_2SiO_3 to NaOH	N_s/N_o
d_4	NaOH solution molarity	M
d_5	Percentage of total aggregate by volume	$\% A_G$
d_6	Ratio of fine aggregate to total aggregate	F/A_G
d_7	Plasticizer as percent fly-ash	$\% P$
d_8	Percentage of SiO_2 solids to water ratio	$\% S/W$

d_9	Extra water addition as percent fly ash	% E_W

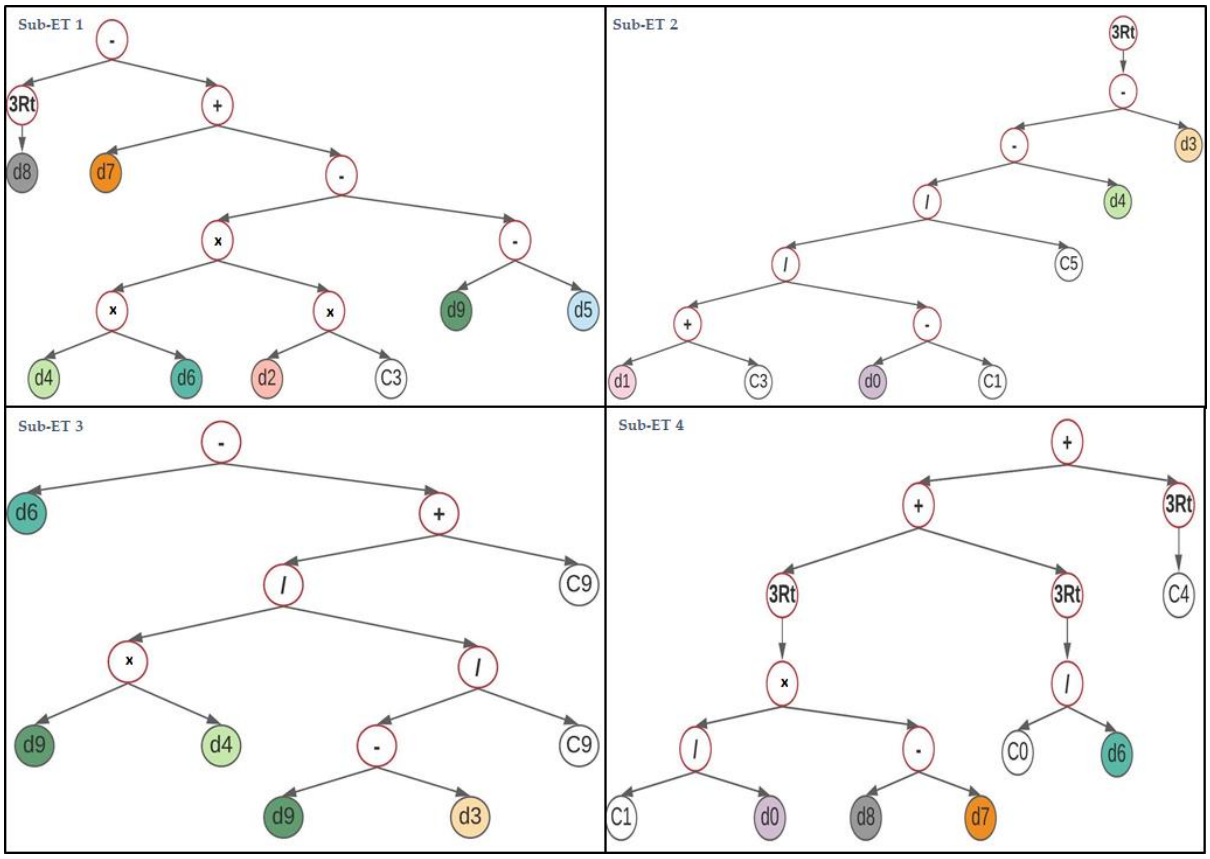

Figure 4.1. GEP model expression trees (ETs) for compressive strength $f_c^{'}$.

4.2. Formulation of Compressive Strength for FGPC

Equation (8) is the simplified equation that is presented to estimate the compressive strength, f_c', for GPC made with FA in MPa. It is comprised of four variables namely A, B, C, and D represented as Equations (9)–(12) and have been translated from the sub-ETs 1, 2, 3, and 4, respectively, as illustrated in Figure 4.1.

$$f_c'(MPa) = A \times B \times C \times D \qquad (8)$$

Where;

$$A = \sqrt[3]{\frac{S}{W}\%} - P\% + \left(M \times \frac{F}{A_G} \times \frac{A_L}{F_A} \times 6.61\right) + E_W\% - A_G\% \qquad (9)$$

$$B = -\sqrt[3]{\frac{A+80}{0.083(T-17.87)} + M + \frac{N_S}{N_O}} \quad (10)$$

$$C = \frac{F}{A_G} - \left(E_W\% \times M - \frac{0.0003}{\frac{N_S}{N_O} - E_W\%} \right) - 0.0003 \quad (11)$$

$$D = \sqrt[3]{\frac{\left(P\% - \frac{S}{W}\%\right) 1.16}{T}} + \sqrt[3]{\frac{0.17}{\frac{F}{A_G}}} + 0.77 \quad (12)$$

Figure 4.2 represents the comparison of regression lines between experimental and model outcomes for both the training samples and validation samples. A strong correlation can clearly be seen which is represented via slopes of the regression lines, namely, 1.000 and 0.9892, for the train and validation samples, respectively.

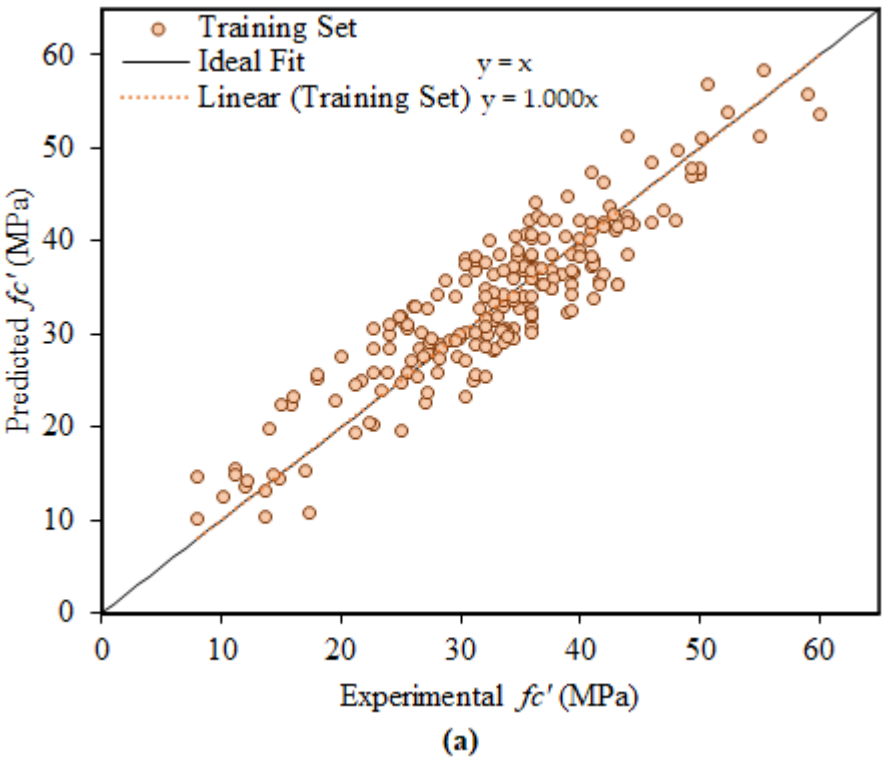

(a)

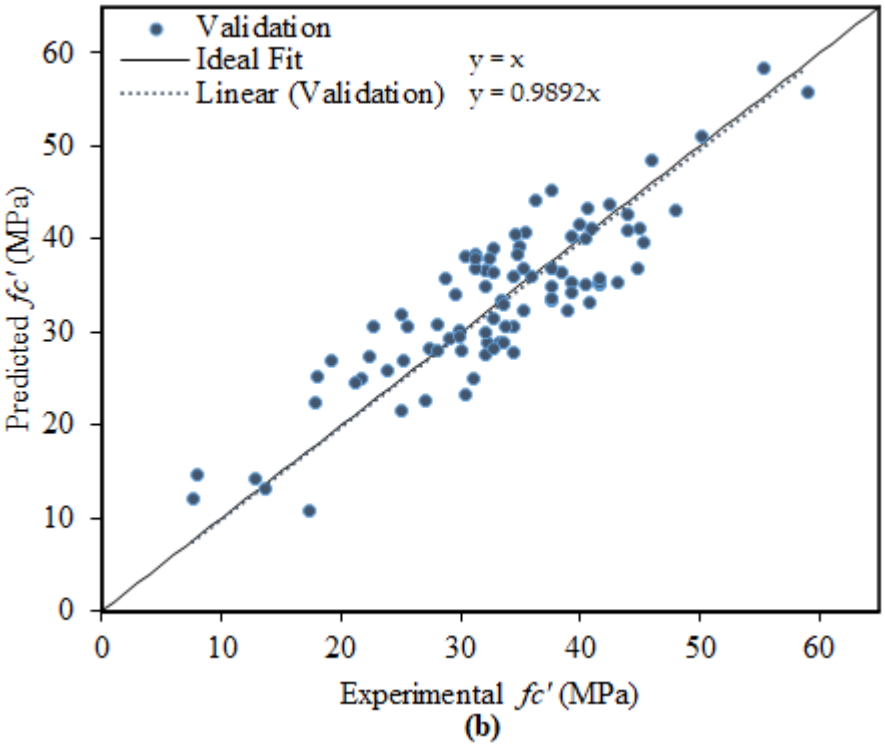

Figure 4.2. Experimental and predicted compressive strength values comparison: (**a**) training set values and (**b**) validation set values.

4.3. Sensitivity and Parametric Analysis

Sensitivity analysis (SA) is performed to investigate the relative contribution of input variables that are exercised to estimate the compressive strength f_c' of GPC made with FA, using Equations (13) and (14). SA defines the dependency of the outcome on the input variable.

$$N_i = f_{max}(x_i) - f_{min}(x_i) \tag{13}$$

$$SA = \frac{N_i}{\sum_n^{j=1} N_j} \tag{14}$$

Where x_i represents the i^{th} input variable. $f_{max}(x_i)$ and $f_{min}(x_i)$ represent the maximum and minimum values of outcome, respectively, that depends on its i^{th} input dominion, where other input

variables are maintained at a constant average value. The difference between $f_{max}(x_i)$ and $f_{min}(x_i)$ gives the range N_i of the i^{th} input variable. The sensitivity and parametric study were both conducted for the training data set, as both the training and validation data sets are consistent [41,105]. Results of sensitivity analysis are presented in Figure 4.3. The figure clarifies that, from a material engineering perspective, the involvement of the explanatory parameters to the f_c' of GPC made with FA are similar.

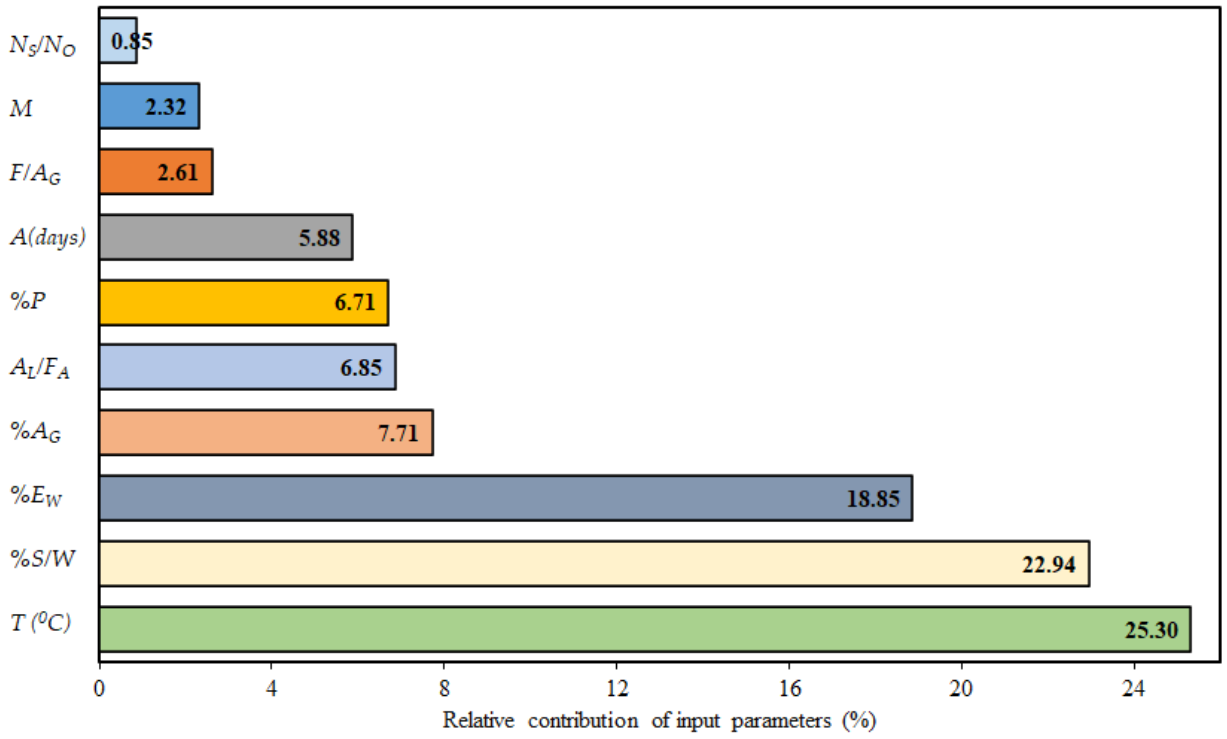

Figure 4.3. Percent relative contribution of input parameter.

Besides, the effectiveness of most influential input variables in the projection of the compressive strength of FA-dependent GPC is obtained by performing parametric analysis. Changes in compressive strength were recorded only by changing the value of one variable from maximum to minimum and other inputs were maintained at average values. Figure 4.4 illustrates the GEP model's parametric analysis results.

It is known that the temperature for curing of the samples is the prompting parameter in controlling the compressive strength (f_c') of GPC made with FA. Its relative contribution is 25.3% as depicted in Figure 4.3. Figure 4.4 shows that the f_c' increases at various rates with the increase of T, A, $\%A_G$, (F/A_G), (N_s/N_o), and $\%P$, but decreases with $\%E_W$, (A_L/F_A), M, and $(\%\,S/W)$.

Hydrates and silicates are released by the alkali-activating solution that helps in the formation of the polymeric structure of alumina silicates. Extra heat is needed for speeding up the reaction process and to improve the mechanical characteristics of GPC. Figure 4.4 shows that the f_c' increases with the increase in the curing temperature up to 100 °C. At higher curing temperature the moisture from the concrete is lost, even if sealed properly. Analogous results have also been witnessed in earlier literature [64]. The decrease in the rate of increment of f_c' of GPC after 240 days, is due to the decrease in the number of unreacted particles. Wardhono et al. [73] presented scanning electron microscopy (SEM) images, which show that gel fills up the voids after 240 days leading to the formation of compacted and semi-homogenous microstructure. Furthermore, it can be depicted from Figure 4.4 that the f_c' increases with an increase in the amount of total aggregate, however, the total aggregate relates to the ratio between fine aggregate to total aggregate content.

Alkali to FA ratio is linked to the ratio between sodium silicate to sodium hydroxide, and the molarity of NaOH. The increase in the f_c' is greatly altered with the amount of sodium silicate that transforms the microstructure of GPC. In the development of the sodium silicate solution, the ratio between percentage silica to water needs to be higher. The higher the sodium silicate content, the greater the compressive strength will be. The lower ratio of alkali to fly ash in combination with higher sodium silicate to sodium hydroxide ratio, and lower molarity of NaOH solution results in higher compressive strength. However, the amount of NaOH solution must remain enough to complete the process of dissolution of the geopolymer. Similar findings have also been observed in a previous study [74].

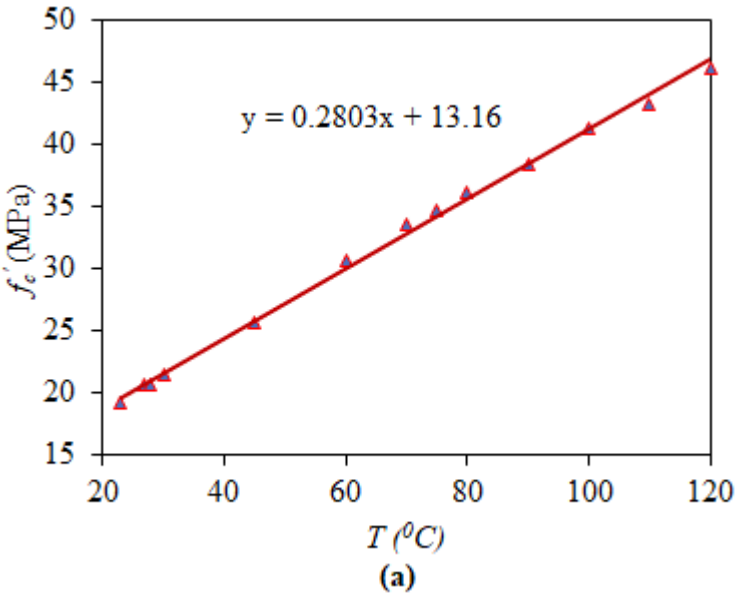
y = 0.2803x + 13.16
f_c' (MPa)
T (^{0}C)

(a)

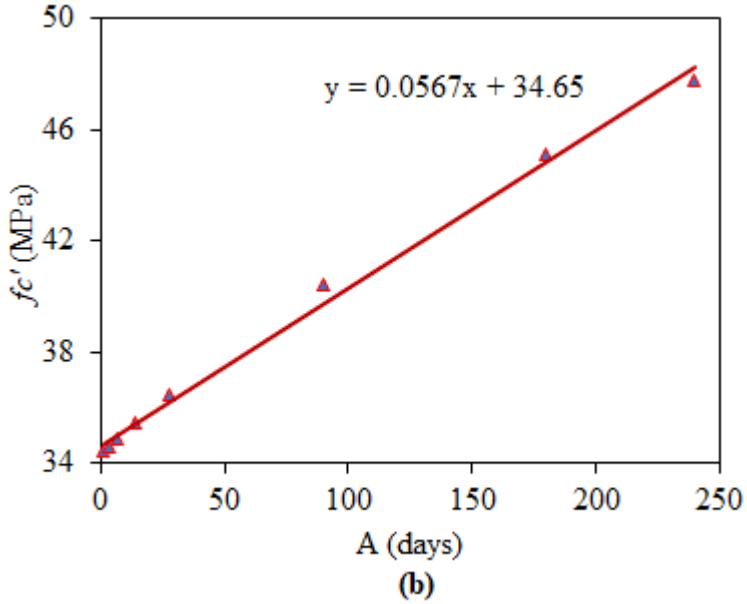
y = 0.0567x + 34.65
fc' (MPa)
A (days)

(b)

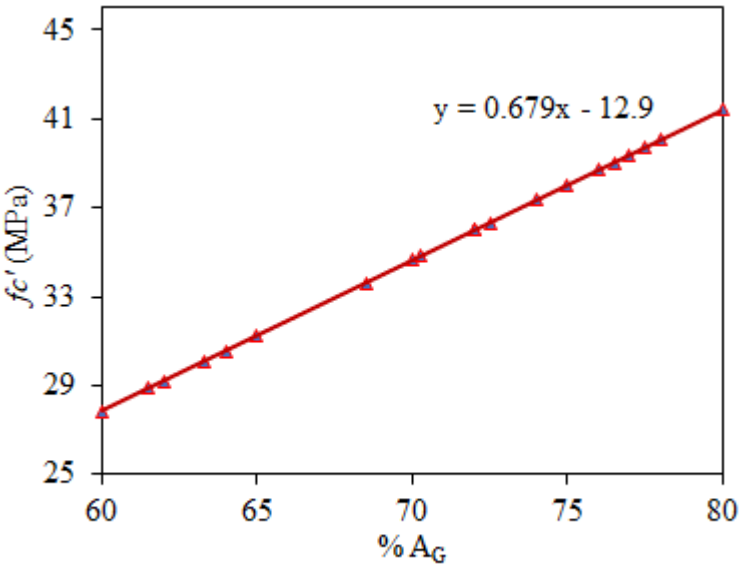
y = 0.679x - 12.9
fc' (MPa)
% A_G

(c)

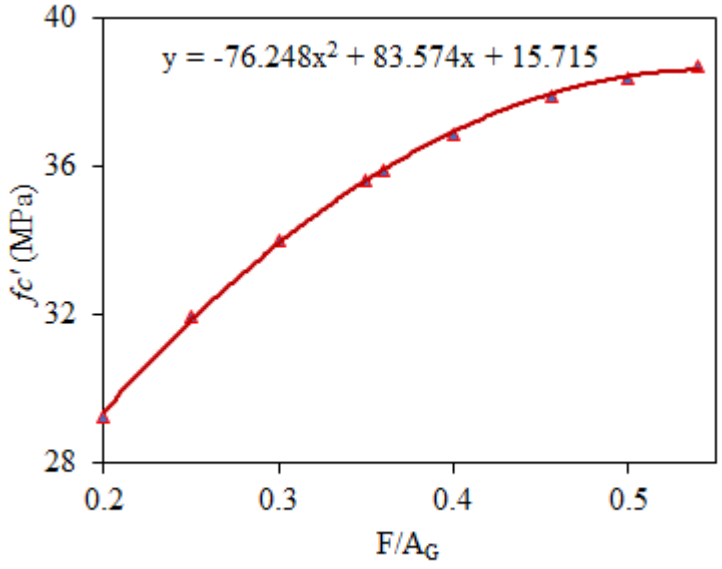
y = -76.248x^2 + 83.574x + 15.715
fc' (MPa)
F/A_G

(d)

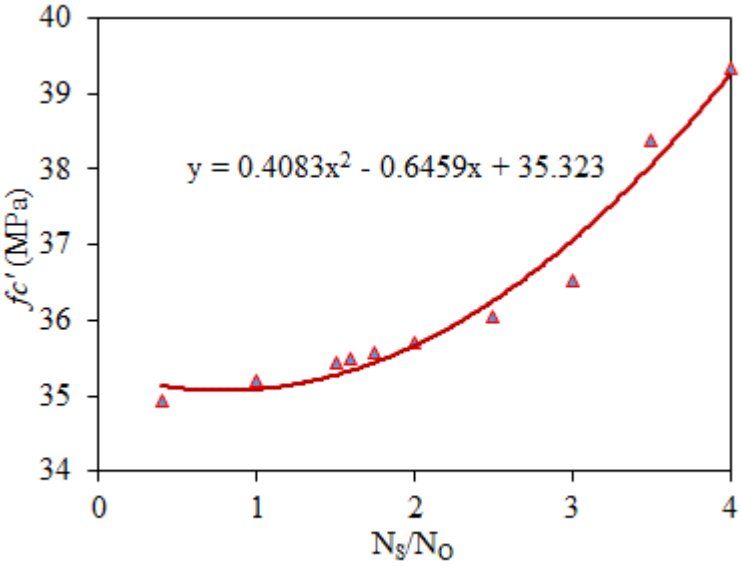
y = 0.4083x² - 0.6459x + 35.323
fc' (MPa)
40
39
38
37
36
35
34
0
1
2
3
4
Ns/No

(e)

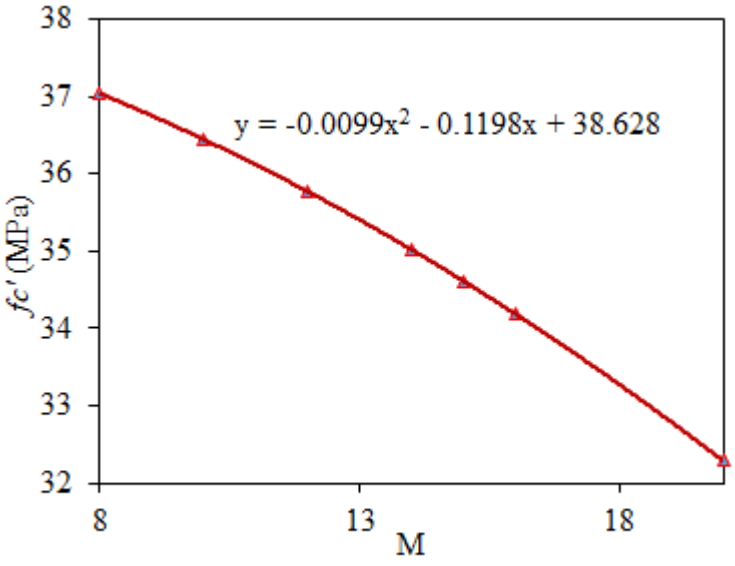
y = -0.0099x² - 0.1198x + 38.628
fc' (MPa)
38
37
36
35
34
33
32
8
13
18
M

(f)

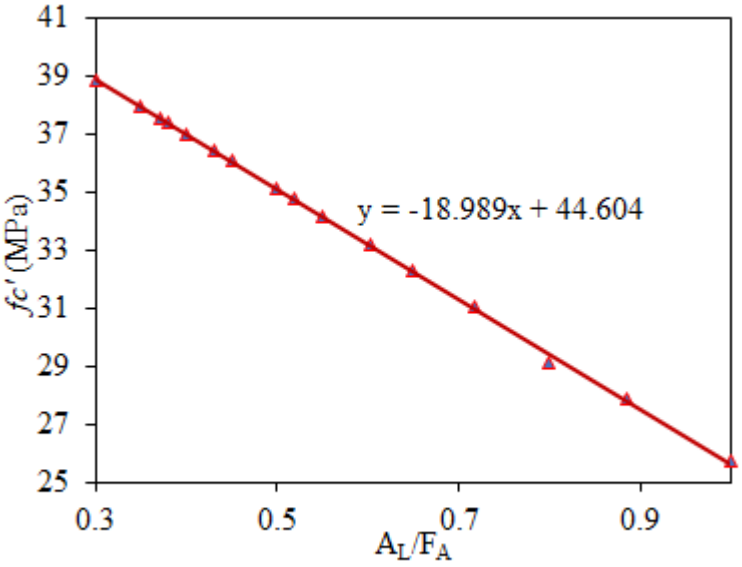
y = -18.989x + 44.604
fc' (MPa)
41
39
37
35
33
31
29
27
25
0.3
0.5
0.7
0.9
AL/FA

(g)

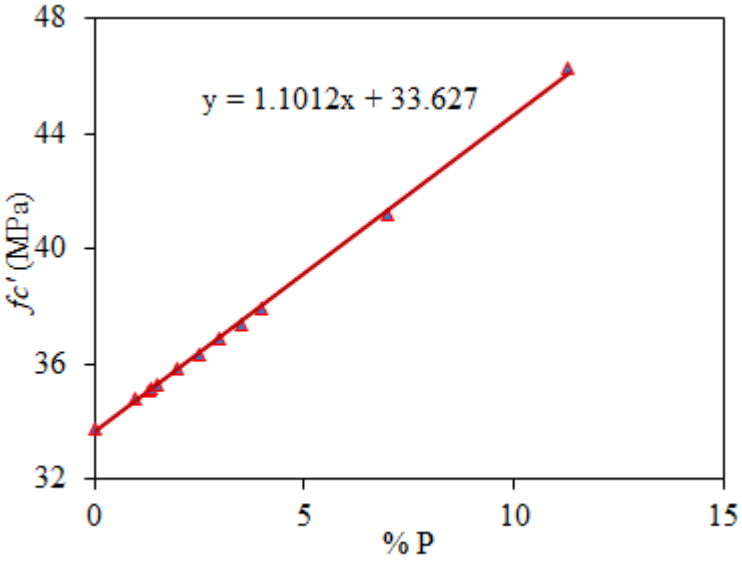
y = 1.1012x + 33.627
fc' (MPa)
48
44
40
36
32
0
5
10
15
% P

(h)

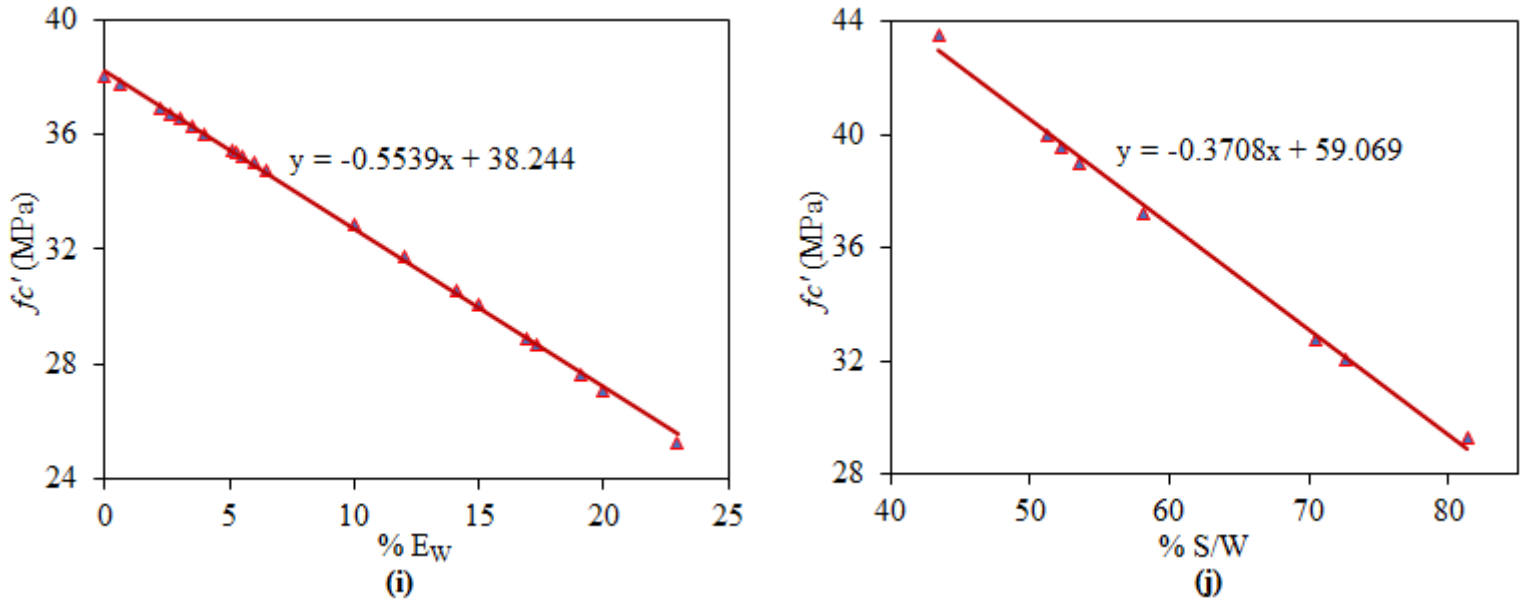

Figure 4.4. Influence of input parameters variation on the compressive strength. **(a)** Temperature for curing of specimen *(T^0C)*, **(b)** Age of specimen *(A)*, **(c)** Percentage of total aggregate by volume *(A_G)*, **(d)** Fine aggregate to total aggregate ratio *(F/A_G)*, **(e)** Sodium silicate to sodium hydroxide ratio *(N_S/N_O)*, **(f)** Molarity of NaOH solution *(M)*, **(g)** Alkali to fly-ash ratio *(A_L/F_A)*, **(h)** Percentage of superplasticizer *(% P)*, **(i)** Percentage of extra water added *(% E_W)*, **(j)** Percentage of SiO_2 solids to water ratio *(% S/W)*.

In GPC, the total water content is the addition of the water content required in preparing the solution of sodium silicate and sodium hydroxide and the addition of extra water needed. To prevent cracking and to achieve a practical GPC, it is necessary to consider the addition of extra water and plasticizer [90]. The addition of extra water or plasticizer as a percent FA contributes 18.85% and 6.71% respectively to the f_c' in comparison with other input factors. f_c' of GPC increases with the increase in plasticizer and decreases with the addition of extra water as evident from Figure 4.4, as the addition of extra water beyond certain limits leads to bleeding and segregation in fresh concrete mix.

Figure 4.4 is in line with the previous studies of other researchers [74,90]. The results of parametric analytics for the proposed GEP model correctly encompasses the influence of input variables to estimate the f_c' of FA-based GPC.

4.4. Performance Evaluation of GEP Model

According to the previous study, to achieve a reliable GEP equation, the ratio between the number of data points in the database to the number of input parameters should be at least equal to three [103]. While in this study a higher value of 30 has been used. Table 4.2 represents the statistical analysis for validation sets and training sets of the GEP model. These results illustrate the effectiveness of training models and the strong correlation between experimental and predicted outcomes with minimal error. The RMSE, MAE, and RSE for the training set of the GEP model are 5.971, 5.832, and 0.325, respectively, and are calculated as 2.643, 2.057, and 0.0675 from the validation samples. The statistical measure of the training and validation set are similar, which indicates the higher generalization capability of the model. Thus, the developed model can predict accurate and reliable outcomes for the new data. Table 4.2 witnesses ρ approach zero (as ideal cases equal zero).

Figure 4.5 illustrates the absolute error of both the experimental and predicted model outcomes, which gives an overall idea of the maximum percentage of error. The average percent error and maximum percent error were calculated as 6.47% and 8.32% respectively, which confirms that the experimental and model outcomes are similar. Furthermore, the occurrence frequency for the maximum error is comparatively smaller. Almost 90% of model predictive outcomes for validation set have the error below 10%, while the average percent error is less than 5.56%. This verifies the accuracy and generalization of the developed GEP equation.

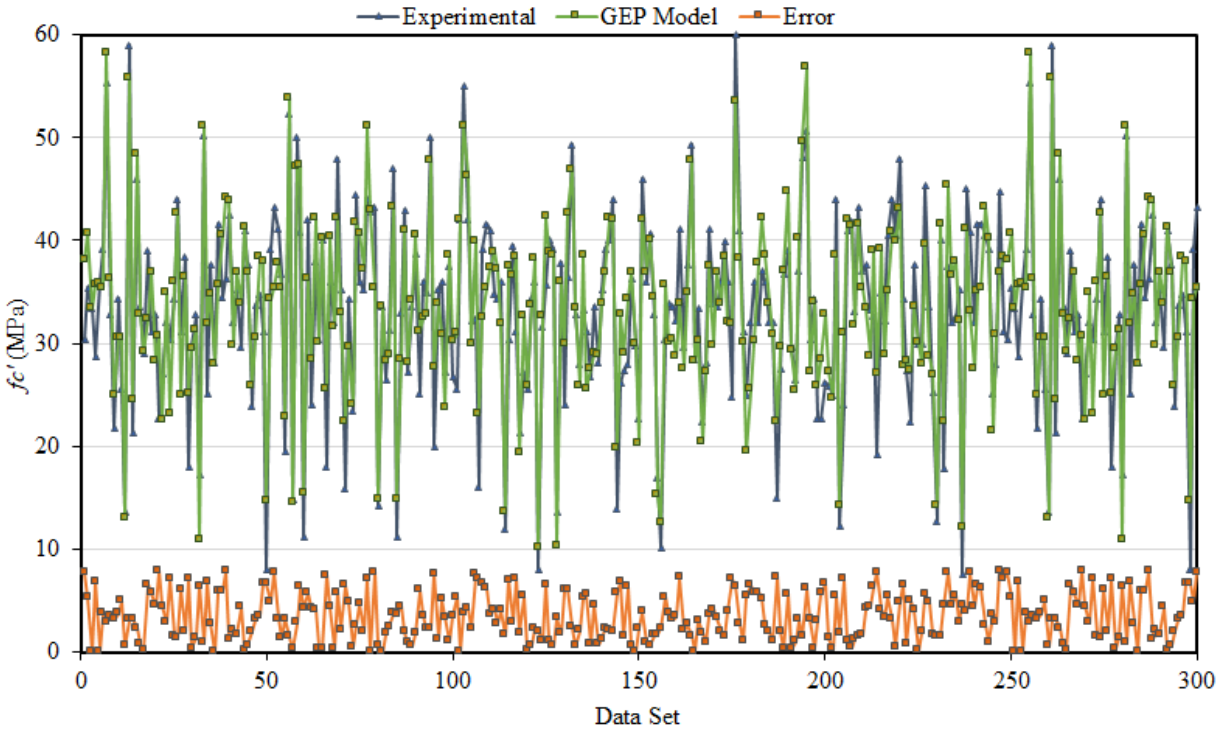

Figure 4.5. Absolute error representation of experimental and predicted outcomes.

For external validation and testing of the proposed GEP model, various statistical error tests were also employed. The literature discloses a suggested criterion that the slope (inclination) of any of the regression lines (k *or* k') traversing the origin should be approximately equal to 1 [106]. The slope of regression lines is 1.001 and 0.995 as shown in Table 4.3. It shows greater accurateness and correlation. Moreover, the researchers proposed that the squared correlation coefficient (passing by origin) among the predicted outcome and experimental results (R_o^2) or among the experimental and predicted outcome ($R_o'^2$) should approach 1 [107]. Table 4.3 summarizes these checks and was applied to the developed GEP equation. The results of these external validations replicate that the proposed GEP model is valid. Thus, the proposed model is not only a correlation but also has predictive capacity.

Table 4.2. Statistical analysis of GEP, linear, and non-linear regression models.

Model	RMSE		MAE		RSE		RRMSE (%)		R		ρ	
	T_R [1]	V_{DN} [2]	T_R	V_{DN}	T_R	V_{DN}	T_R	V_{DN}	T_R	V_{DN}	T_R	V_{DN}
GEP	5.971	2.643	5.823	2.057	0.325	0.0675	16.949	4.949	0.8586	0.9643	0.0911	0.02519
Linear	6.986	5.546	6.543	4.967	0.589	0.304	19.20	10.21	0.8074	0.8976	0.1062	0.05382
Non-Linear	6.593	5.054	6.053	4.875	0.497	0.298	18.53	9.021	0.8357	0.9247	0.1009	0.04687

[1] T_R symbolizes training sample; [2] V_{DN} symbolizes validation samples.

Table 4.3. External validation of the GEP model using arithmetical parameter.

Expression	Requirement	GEP model, f'_c
$k = \frac{\sum_{i=1}^{n}(e_i \times m_i)}{\sum_{i=1}^{n}(e_i^2)}$	$0.85 < k < 1.15$	1.001
$k' = \frac{\sum_{i=1}^{n}(e_i \times m_i)}{\sum_{i=1}^{n}(m_i^2)}$	$0.85 < k' < 1.15$	0.995
$R_o^2 = 1 - \frac{\sum_{i=1}^{n}(m_i - e_i^o)^2}{\sum_{i=1}^{n}(m_i - \bar{m}_i^o)^2}, e_i^o = k \times m_i$	$R_o^2 \cong 1$	0.9998
$R_o'^2 = 1 - \frac{\sum_{i=1}^{n}(e_i - m_i^o)^2}{\sum_{i=1}^{n}(e_i - \bar{e}_i^o)^2}, m_i^o = k' \times e_i$	$R_o'^2 \cong 1$	0.9849

4.5. Comparison of GEP and Regression Models

No GEP model has been identified from the literature that would estimate the compressive strength (f'_c) of GPC made with FA and that considers the influencing input variables used in this research. So, it is necessary to establish linear and non-linear regression models, on the same data

points, for the prediction of the f_c' of FA-based GPC, the results are then judged against GEP Equation (8).

Equations (15) and (16) show the empirical expressions for the prediction of f_c' founded on linear and nonlinear regression study respectively.

$$f_c' = 12.81 + 0.226T + 0.0376A - 26.86\frac{A_L}{F_A} + 1.1296\frac{N_S}{N_o} - 0.3935M + 0.6412A_G\% \\ -0.4075\frac{F}{A_G} + 1.256P\% - 0.452\frac{S}{W}\% - 0.7125E_W\% \quad (15)$$

$$f_c' = -7.636 + 1.182T^{0.6809} + 0.3446A^{0.634} - 25.80\left(\frac{A_L}{F_A}\right)^{2.91} + 1.779\left(\frac{N_S}{N_o}\right)^{0.438} \\ -0.00895M^{2.24} + 0.7605(A_G\%)^{0.932} - 0.37099\left(\frac{F}{A_G}\right)^{1.064} + 2.259(P\%)^{0.7203} \quad (16) \\ -0.0804\left(\frac{S}{W}\%\right)^{1.345} - 0.2654(E_W\%)^{1.316}$$

The predicted results by all three equations are compared in Figure 4.6. The statistical indicators like RMSE, MAE, RSE, RRMSE%, R, and ρ for GEP model, linear and no-linear regression model are listed in Table 4.2. The ρ and RMSE of the established GEP equation are calculated as the least of all three models, for both the training and validation data points. The values of $RMSE_{training}$ and $\rho_{training}$ are 14.5% and 14% lower than the linear regression model, respectively. In the test stage, the proposed GEP model gives better performance than the non-linear regression model. $\rho_{testing}$ of the two models varies by 44%. Furthermore, Figure 4.6 shows that linear and non-linear regression equations failed in efficiently capturing a high f_c', which limits the application of the regression models.

These observations shows that the GEP model performed better than the linear and non-linear regression equations, for the same input variables. The regression methods have certain disadvantages as in they use some predefined expressions and pre-assume the residual's normality [105]. Whereas

modeling based on GEP implies that the model efficiently picks up the non-linear relationship between the dependent and independent parameters, with a higher generalization capacity and considerably decreases the error values in comparison with the regression models.

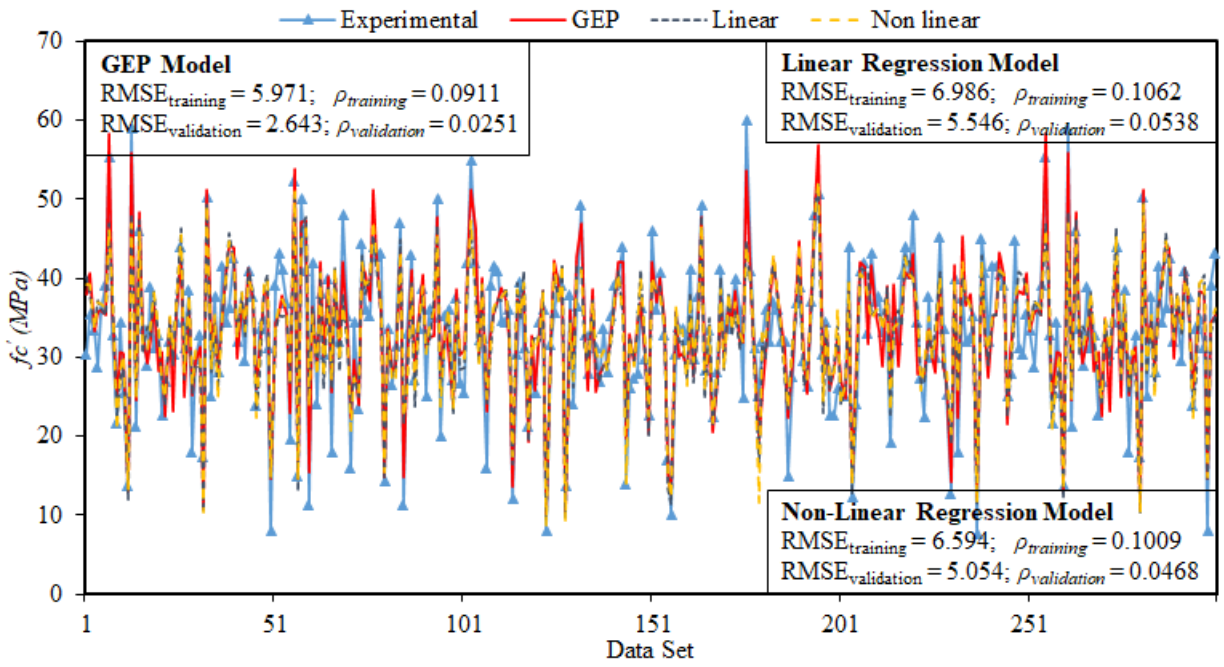

Figure 4.6. Comparison of $f_c^{'}$ of proposed GEP, linear regression, and non-linear regression models.

4.6. Experimental Test Results

The results for compressive strength of all six geopolymer concrete mixes were accomplished. The Table 4.4. shows the compressive strength from experimental results and GEP equation results along with the absolute error. The average absolute error for mixes (GC1-GC3), with variation in molarity of NaOH, is 2.49 MPa. While for GC3-GC4 (having variation in the ration between sodium silicate solution to sodium hydroxide solution) the average absolute error is 0.274 MPa. For both type of variation, the error is less than 10 %, which validates the outburst performance of GEP equation. Figure 4.7 (a) and 4.7 (b) shows the trend in experimental results for variation in molarity of NaOH solution and ratio between Na_2SiO_3 to NaOH solution respectively. The similar trend was also noted

for GEP equation in Figure 4.4 (f) and 4.4 (e). Which was in strong agreement with the previous study. Thus, the accuracy of GEP model is experimentally validated and can be confidently used in the pre-design of fly-ash based geopolymer concrete.

Table 4.4. Comparison between experimental and GEP results.

Mix Designation	Experimental Results (MPa)	GEP Equation (MPa)	Absolute Error (MPa)	Average (MPa)
GC1	46.23	42.70	2.52	
GC2	45.86	42.26	2.59	2.49
GC3	45.12	41.75	2.37	
GC4	43.25	42.91	0.340	
GC5	43.36	43.12	0.243	0.274
GC6	43.56	43.32	0.238	

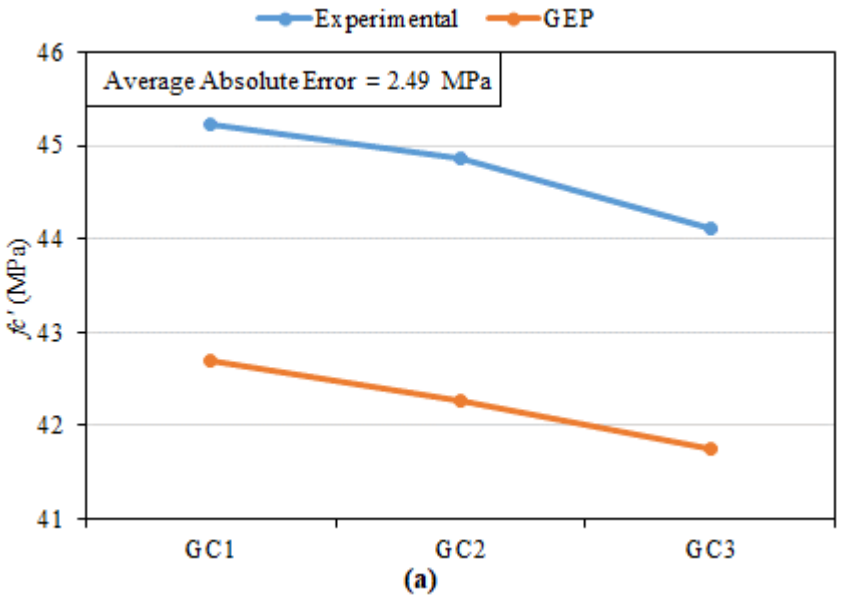

(a)

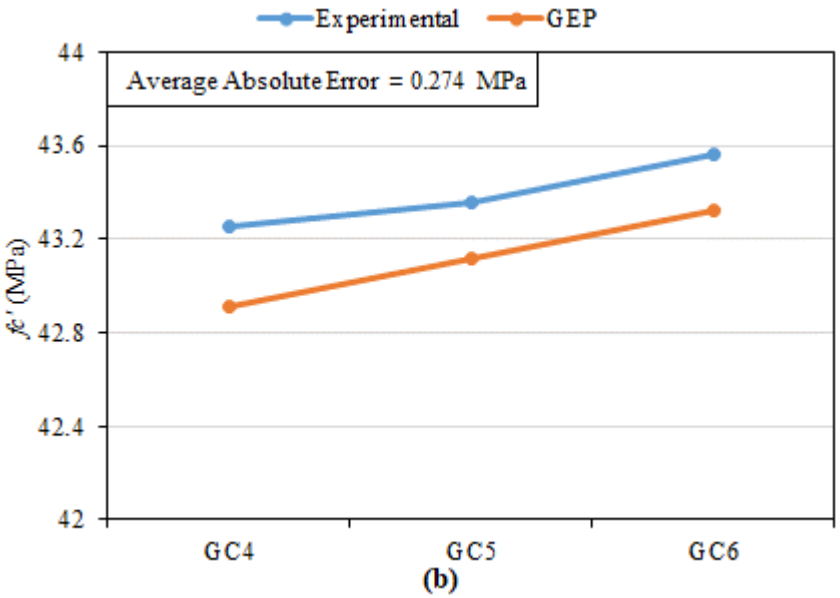

Figure 4.7. Comparison between experimental and GEP results **(a)** Variation in molarity of NaOH solution **(b)** Variation in ratio between Na_2SiO_3 to NaOH solution.

4.7. Summary

In this chapter the results obtained by the GEP modelling are explained in detail. Simplified models are developed which can be utilized for the prediction mechanical properties of concrete containing fly-ash for pre-design of concrete structures. The statistical parameters and objective functions satisfy the pre-defined criteria and are an indicator that the model performs well on all three datasets and possess higher capability to predict the accurate results on unseen data. Almost 90% of model predictive outcomes for validation set have the MAE below 10%, while the average percentage of MAE is less than 5.56%. Other error metrics considered in this study like MSE, RMSE, RRMSE also verifies the accuracy and generalization of the developed GEP equation. Sensitivity analysis was conducted by considering the classical stochastic method to understand the contribution of the input variables on the output. It was observed that the input variables considered in the current study had similar contribution to the output and thereby validating the hypothesis of selecting the most influential parameters on the output as variables for the modelling purpose. Parametric analysis results show that the models accurately captured the influence of actual physical phenomena. The ten

input variables considered in this study predicted the accurate results when one of the input variables was varied while keeping all the other variables at their mean value. A comparison of regression analysis techniques shows that GEP models possess high generalization and robustness. The models obtained from the regression technique are empirical and can be termed as a mere correlation between the input and output variables. The range of applicability of the regression models is quite limited. The GEP equation was also validated via experimental results that shows that the accurateness of the GEP model.

CHAPTER 5

CONCLUSION AND RECOMMENDATION

5.1. Conclusion

This research utilizes the gene expression programming technique (GEP) to establish an expression for the estimation of the compressive strength, f_c', of fly-ash based geopolymer concrete (FGPC). The projected GEP model is empirical and is built on the broadly distributed database, consisting of ten different highly prominent and influential explanatory variables, that comes from the published literature. Based on the results and discussion the following conclusions are formulated;

- The sensitivity and parametric study were conducted to study the effect of explanatory variables on the compressive strength of FGPC. The sensitivity analysis reveals that the increasing trend of the relative importance of explanatory variables used in GEP equation followed the order: T (25.30%) > %S/W (22.94%) > %E_W (7.71%) > %A_G (7.71%) > A_L/F_A (6.85%) > %P (6.71%) > A (5.88%) > F/A_G (2.61%) > M (2.32%) > N_S/N_O (0.85%). While in parametric study, it was deduced that the f_c' increases at different rates with the increase of T, A, $\%\mathrm{A_G}$, $(\mathrm{F}/\mathrm{A_G})$, $(\mathrm{N_s}/\mathrm{N_o})$, and %P, but decreases with $\%\mathrm{E_W}$, $(\mathrm{A_L}/\mathrm{F_A})$, M, and $(\%\,\mathrm{S}/\mathrm{W})$. The resulting trends were inline with the previous literature. Thus, the projected model successfully encompasses the impact of the explanatory variables to predict the exact pattern of FGPC compressive strength.
- The accurateness of the projected models is verified by the examination and assessment of statistical checks that are R, MAE, RSE, and RMSE, RRMSE, and performance index (ρ) for training and validation samples. The R-value for validation stage equaling 0.9643 confirms the stronger correlation between explanatory variables and response parameter. Almost 90% of model predictive outcomes for validation set have the MAE below 10%, while the average

percentage of MAE is less than 5.56%. The performance index (ρ) for training set and validation set approaches to zero, witnesses the better GEP model. The GEP model also meets the appropriate requirements considered for external validation that are $k, k', R_o^2, and\ R_o'^2$.

- The proposed GEP model perform better than the traditional linear and non-linear regression models with higher accuracy and without any prior assumptions. It shows the diverse nature of GEP model since it considers the linear and non-linear data as well. In the validation stage, the ρ reveals that GEP model is 53% and 46% better than linear and non-linear regression models respectively. Thus, the proposed GEP model is suitable to practice in the preliminary design of FGPC.
- The accuracy of proposed GEP model was validated via experimental study conducted in Pakistani environment. The MAE for mixes (GC1-GC3), with variation in molarity of NaOH, was 2.49 MPa. While for GC3-GC4 (having variation in the ratio between sodium silicate solution to sodium hydroxide solution) the MAE was 0.274 MPa. For both type of variation, the error is less than 10 %. The experimental analysis also confirms the robustness of the model and can be confidently used in the pre-design of FGPC.

Furthermore, before adding fly-ash as a geopolymer binder, it is suggested to perform a leachate analysis. The projected models can provide a detailed and practical foundation for increasing the use of toxic fly-ash for construction practices, instead of disposal in landfill sites. This would lead to effective and sustainable construction as green concrete is made by the incorporation of waste fly-ash that reduces the consumption of energy, emissions of greenhouse gases, disposal, and construction costs.

5.2. Recommendation for Future Study

Fly-ash (FA)- based geopolymer concrete (GPC) has a great potential to be used in the construction industry, as a replacement of ordinary Portland cement (OPC) concrete. The data set used in this paper is limited to 298 samples. In fact, proper testing must be carried out by varying maximum explanatory variables for a more efficient predictive model. Although, this paper considers a wide range comprehensive data base consisting of ten explanatory parameters for modelling the compressive strength of geopolymer concrete made with wasted fly-ash.

Moreover, study of other mechanical characteristics of fly-ash based GPC like tensile strength, elastic modulus, poison ratio, and flexural strength, is highly necessary; at normal temperature as well as at elevated temperature. A new data base is also needed for the durability study of fly-ash-based GPC. Furthermore, it is recommended to predict the stated mechanical properties of fly-ash-based GPC via different artificial intelligence (AI) techniques, such as fuzzy logic, adaptive fuzzy interface system (ANFIS), response surface methodology (RSM), support vector machine (SVM) analysis, random forest regression (RFR), decision tree (DT), artificial neural network (ANN), recurrent neural network (RNN), convolutional neural network (CNN), M5P tree and restricted Boltzmann machine (RBM), et cetera. Furthermore, an extensive study related to the interaction of geopolymer concrete and reinforcing steel is needed. It would also be worthwhile formalizing the different mechanical properties of fiber reinforced geopolymer concrete.

Normally it is considered that the production cost of GPC is greater than OPC concrete. It can be reduced by the use of different types of waste materials such as sand replacement that are rich in alumina silicates; like the use of locally available waste foundry sand, glass waste, and marble wastes, et cetera. The authors replaced fine aggregates with waste foundry sand in GPC. They reported that the initial production cost of M50 grade GPC is 11% lower than OPC concrete [108]. However, the M30 grades of GPC and OPC concrete have almost similar of production costs [108]. Environmental

safety delivered by GPC production from waste materials is worthwhile as it reduces the carbon-dioxide emission from the manufacture of cement and adds a carbon credit to the economy of the country as well. Comparing the overall cost, including the maintenance and durability, the cost of GPC is similar to OPC concrete as the geopolymer concrete is much more durable and resistive to chemical attacks than OPC concrete [109]. The authors immersed GPC and OPC concrete in a magnesium sulfate solution for 45 days and reported that the reduction of compressive strength of GPC is 13% lower than OPC concrete [109]. Additionally, the immersion for the same duration in a sulfuric acid solution resulted in 8% lower reduction of compressive strength of GPC as compared to OPC concrete [109].

REFERENCES

1. Aprianti, E. A huge number of artificial waste material can be supplementary cementitious material (SCM) for concrete production—A review part II. J. Clean. Prod. **2017**, 142, 4178–4194.

2. Akbar, A.; Farooq, F.; Shafique, M.; Aslam, F.; Alyousef, R.; Alabduljabbar, H. Sugarcane bagasse ash-based engineered geopolymer mortar incorporating propylene fibers. J. Build. Eng. **2021**, 33, 101492, doi:10.1016/j.jobe.2020.101492.

3. Dwivedi, A.; Jain, M.K. Fly ash—waste management and overview : A Review. Recent Res. Sci. Technol. **2014**, 6, 30–35.

4. Rafieizonooz, M.; Mirza, J.; Salim, M.R.; Hussin, M.W.; Khankhaje, E. Investigation of coal bottom ash and fly ash in concrete as replacement for sand and cement. Constr. Build. Mater. **2016**, 116, 15–24, doi:10.1016/j.conbuildmat.2016.04.080.

5. Abdulkareem, O.A.; Mustafa Al Bakri, A.M.; Kamarudin, H.; Khairul Nizar, I.; Saif, A.A. Effects of elevated temperatures on the thermal behavior and mechanical performance of fly ash geopolymer paste, mortar and lightweight concrete. Constr. Build. Mater. **2014**, 50, 377–387, doi:10.1016/j.conbuildmat.2013.09.047.

6. Nadesan, M.S.; Dinakar, P. Mix design and properties of fly ash waste lightweight aggregates in structural lightweight concrete. Case Stud. Constr. Mater. **2017**, 7, 336–347, doi:10.1016/j.cscm.2017.09.005.

7. Ghazali, N.; Muthusamy, K.; Wan Ahmad, S. Utilization of Fly Ash in Construction. In Proceedings of the IOP Conference Series: Materials Science and Engineering; Institute of Physics Publishing, Kazimierz Dolny, Poland, 21–23 November 2019; Volume 601.

8. Nordin, N.; Abdullah, M.M.A.B.; Tahir, M.F.M.; Sandu, A.V.; Hussin, K. Utilization of fly ash waste as construction material. Int. J. Conserv. Sci. **2016**, 7, 161–166.

9. Farooq, F.; Akbar, A.; Khushnood, R.A.; Muhammad, W.L.B.; Rehman, S.K.U.; Javed, M.F. Experimental investigation of hybrid carbon nanotubes and graphite nanoplatelets on rheology, shrinkage, mechanical, and microstructure of SCCM. Materials (Basel) **2020**, 13, 230, doi:10.3390/ma13010230.

10. Liew, K.M.; Akbar, A. The recent progress of recycled steel fiber reinforced concrete. Constr. Build. Mater. **2020**, 232, 117232.

11. Watts, J. Concrete: The most destructive material on Earth. Guardian. **2019**, 25, 1–9.

12. Mehta, P.K. Greening of the Concrete Industry for Sustainable Development. Concr. Int. **2002**, 24, 23–28.

13. Wongsa, A.; Siriwattanakarn, A.; Nuaklong, P.; Sata, V.; Sukontasukkul, P.; Chindaprasirt, P. Use of recycled aggregates in pressed fly ash geopolymer concrete. Environ. Prog. Sustain. Energy **2020**, 39, doi:10.1002/ep.13327.

14. Sumanth Kumar, B.; Sen, A.; Rama Seshu, D. Shear Strength of Fly Ash and GGBS Based Geopolymer Concrete. In Lecture Notes in Civil Engineering; Springer: Berlin/Heidelberg, Germany, 2020; Volume 68, pp. 105–117.

15. Farooq, F.; Rahman, S.K.U.; Akbar, A.; Khushnood, R.A.; Javed, M.F.; alyousef, R.; Alabduljabbar, H.; Aslam, F. A comparative study on performance evaluation of hybrid GNPs/CNTs in conventional and self-compacting mortar. Alex. Eng. J. **2020**, 59, 369–379, doi:10.1016/j.aej.2019.12.048.

16. Li, H.; Deng, Q.; Zhang, J.; Xia, B.; Skitmore, M. Assessing the life cycle CO2 emissions of reinforced concrete structures: Four cases from China. J. Clean. Prod. **2019**, 210, 1496–1506, doi:10.1016/j.jclepro.2018.11.102.

17. Akbar, A.; Liew, K.M. Influence of elevated temperature on the microstructure and mechanical performance of cement composites reinforced with recycled carbon fibers. Compos. Part B Eng. **2020**, 108245, doi:10.1016/j.compositesb.2020.108245.

18. Ok, Y.S.; Yang, J.E.; Zhang, Y.S.; Kim, S.J.; Chung, D.Y. Heavy metal adsorption by a formulated zeolite-Portland cement mixture. J. Hazard. Mater. **2007**, 147, 91–96, doi:10.1016/j.jhazmat.2006.12.046.

19. Wang, Q.; Wang, D.; Chen, H. The role of fly ash microsphere in the microstructure and macroscopic properties of high-strength concrete. Cem. Concr. Compos. **2017**, 83, 125–137, doi:10.1016/j.cemconcomp.2017.07.021.

20. Wang, L.; Chen, L.; Cho, D.W.; Tsang, D.C.W.; Yang, J.; Hou, D.; Baek, K.; Kua, H.W.; Poon, C.S. Novel synergy of Si-rich minerals and reactive MgO for stabilisation/solidification of contaminated sediment. J. Hazard. Mater. **2019**, 365, 695–706, doi:10.1016/j.jhazmat.2018.11.067.

21. Chen, L.; Wang, L.; Cho, D.W.; Tsang, D.C.W.; Tong, L.; Zhou, Y.; Yang, J.; Hu, Q.; Poon, C.S. Sustainable stabilization/solidification of municipal solid waste incinerator fly ash by incorporation of green materials. J. Clean. Prod. **2019**, 222, 335–343, doi:10.1016/j.jclepro.2019.03.057.

22. Noushini, A.; Castel, A.; Aldred, J.; Rawal, A. Chloride diffusion resistance and chloride binding capacity of fly ash-based geopolymer concrete. Cem. Concr. Compos. **2020**, 105, doi:10.1016/j.cemconcomp.2019.04.006.

23. Zhang, H.Y.; Qiu, G.H.; Kodur, V.; Yuan, Z.S. Spalling behavior of metakaolin-fly ash based geopolymer concrete under elevated temperature exposure. Cem. Concr. Compos. **2020**, 106, 103483, doi:10.1016/j.cemconcomp.2019.103483.

24. Xie, J.; Wang, J.; Rao, R.; Wang, C.; Fang, C. Effects of combined usage of GGBS and fly ash on workability and mechanical properties of alkali activated geopolymer concrete with recycled aggregate. Compos. Part B Eng. **2019**, 164, 179–190, doi:10.1016/j.compositesb.2018.11.067.

25. Nuaklong, P.; Jongvivatsakul, P.; Pothisiri, T.; Sata, V.; Chindaprasirt, P. Influence of rice husk ash on mechanical properties and fire resistance of recycled aggregate high-calcium fly ash geopolymer concrete. J. Clean. Prod. **2020**, 252, doi:10.1016/j.jclepro.2019.119797.

26. Bajpai, R.; Choudhary, K.; Srivastava, A.; Sangwan, K.S.; Singh, M. Environmental impact assessment of fly ash and silica fume based geopolymer concrete. J. Clean. Prod. **2020**, 254, doi:10.1016/j.jclepro.2020.120147.

27. Sandanayake, M.; Gunasekara, C.; Law, D.; Zhang, G.; Setunge, S.; Wanijuru, D. Sustainable criterion selection framework for green building materials—An optimisation based study of fly-ash Geopolymer concrete. Sustain. Mater. Technol. **2020**, 25, doi:10.1016/j.susmat.2020.e00178.

28. Li, N.; Shi, C.; Zhang, Z.; Wang, H.; Liu, Y. A review on mixture design methods for geopolymer concrete. Compos. Part B Eng. **2019**, 178, 107490.

29. Tran, T.T.; Pham, T.M.; Hao, H. Rectangular Stress-block Parameters for Fly-ash and Slag Based Geopolymer Concrete. Structures **2019**, 19, 143–155, doi:10.1016/j.istruc.2019.01.006.

30. Zhang, P.; Gao, Z.; Wang, J.; Guo, J.; Hu, S.; Ling, Y. Properties of fresh and hardened fly ash/slag based geopolymer concrete: A review. J. Clean. Prod. **2020**, 270, 122389.

31. Prachasaree, W.; Limkatanyu, S.; Hawa, A.; Sukontasukkul, P.; Chindaprasirt, P. Manuscript title: Development of strength prediction models for fly ash based geopolymer concrete. J. Build. Eng. **2020**, 101704, doi:10.1016/j.jobe.2020.101704.

32. Zhang, H.; Li, L.; Sarker, P.K.; Long, T.; Shi, X.; Wang, Q.; Cai, G. Investigating Various Factors Affecting the Long-Term Compressive Strength of Heat-Cured Fly Ash Geopolymer Concrete and the Use of Orthogonal Experimental Design Method. Int. J. Concr. Struct. Mater. **2019**, 13, doi:10.1186/s40069-019-0375-7.

33. Van Dao, D.; Ly, H.B.; Trinh, S.H.; Le, T.T.; Pham, B.T. Artificial intelligence approaches for prediction of compressive strength of geopolymer concrete. Materials (Basel) **2019**, 12, 983, doi:10.3390/ma12060983.

34. Luhar, S.; Chaudhary, S.; Luhar, I. Development of rubberized geopolymer concrete: Strength and durability studies. Constr. Build. Mater. **2019**, 204, 740–753, doi:10.1016/j.conbuildmat.2019.01.185.

35. Wang, Y.; Hu, S.; He, Z. Mechanical and fracture properties of fly ash geopolymer concrete addictive with calcium aluminate cement. Materials (Basel) **2019**, 12, 2982, doi:10.3390/ma12182982.

36. Javed, M.F.; Amin, M.N.; Shah, M.I.; Khan, K.; Iftikhar, B.; Farooq, F.; Aslam, F.; Alyousef, R.; Alabduljabbar, H. Applications of gene expression programming and regression techniques for estimating compressive strength of bagasse ash based concrete. Crystals **2020**, 10, 1–17, doi:10.3390/cryst10090737.

37. Javed, M.F.; Farooq, F.; Memon, S.A.; Akbar, A.; Khan, M.A.; Aslam, F.; Alyousef, R.; Alabduljabbar, H.; Rehman, S.K.U.; Ur Rehman, S.K.; et al. New Prediction Model for the

Ultimate Axial Capacity of Concrete-Filled Steel Tubes: An Evolutionary Approach. Crystals **2020**, 10, 741, doi:10.3390/cryst10090741.

38. Özcan, F. Gene expression programming based formulations for splitting tensile strength of concrete. Constr. Build. Mater. **2012**, 26, 404–410, doi:10.1016/j.conbuildmat.2011.06.039.

39. Tanyildizi, H.; Çevik, A. Modeling mechanical performance of lightweight concrete containing silica fume exposed to high temperature using genetic programming. Constr. Build. Mater. **2010**, 24, 2612–2618, doi:10.1016/j.conbuildmat.2010.05.001.

40. Nour, A.I.; Güneyisi, E.M. Prediction model on compressive strength of recycled aggregate concrete filled steel tube columns. Compos. Part B Eng. **2019**, 173, doi:10.1016/j.compositesb.2019.106938.

41. Iqbal, M.F.; Liu, Q. feng; Azim, I.; Zhu, X.; Yang, J.; Javed, M.F.; Rauf, M. Prediction of mechanical properties of green concrete incorporating waste foundry sand based on gene expression programming. J. Hazard. Mater. **2020**, 384, 121322, doi:10.1016/j.jhazmat.2019.121322.

42. Jalal, M.; Grasley, Z.; Gurganus, C.; Bullard, J.W. Experimental investigation and comparative machine-learning prediction of strength behavior of optimized recycled rubber concrete. Constr. Build. Mater. **2020**, 256, doi:10.1016/j.conbuildmat.2020.119478.

43. Chou, J.S.; Pham, A.D. Enhanced artificial intelligence for ensemble approach to predicting high performance concrete compressive strength. Constr. Build. Mater. **2013**, 49, 554–563, doi:10.1016/j.conbuildmat.2013.08.078.

44. Getahun, M.A.; Shitote, S.M.; Abiero Gariy, Z.C. Artificial neural network based modelling approach for strength prediction of concrete incorporating agricultural and construction wastes. Constr. Build. Mater. **2018**, 190, 517–525, doi:10.1016/j.conbuildmat.2018.09.097.

45. Mashhadban, H.; Kutanaei, S.S.; Sayarinejad, M.A. Prediction and modeling of mechanical properties in fiber reinforced self-compacting concrete using particle swarm optimization algorithm and artificial neural network. Constr. Build. Mater. **2016**, 119, 277–287, doi:10.1016/j.conbuildmat.2016.05.034.

46. Sebaaly, H.; Varma, S.; Maina, J.W. Optimizing asphalt mix design process using artificial neural network and genetic algorithm. Constr. Build. Mater. **2018**, 168, 660–670, doi:10.1016/j.conbuildmat.2018.02.118.

47. Sudin, R.; Swamy, N. Bamboo and wood fibre cement composites for sustainable infrastructure regeneration. Proc. J. Mater. Sci. **2006**, 41, 6917–6924.

48. Behnood, A.; Golafshani, E.M. Predicting the compressive strength of silica fume concrete using hybrid artificial neural network with multi-objective grey wolves. J. Clean. Prod. **2018**, 202, 54–64, doi:10.1016/j.jclepro.2018.08.065.

49. Gandomi, A.H.; Babanajad, S.K.; Alavi, A.H.; Farnam, Y. Novel approach to strength modeling of concrete under triaxial compression. J. Mater. Civ. Eng. **2012**, 24, 1132–1143, doi:10.1061/(ASCE)MT.1943-5533.0000494.

50. Gandomi, A.H.; Yun, G.J.; Alavi, A.H. An evolutionary approach for modeling of shear strength of RC deep beams. Mater. Struct. Constr. **2013**, 46, 2109–2119, doi:10.1617/s11527-013-0039-z.

51. Ferreira, C. Gene Expression Programming Mathematical Modeling by an Artificial Intelligence. Springer, 21, Berlin, Germany, **2006**; ISBN 3-540-32796-7.

52. Chen, L.; Kou, C.H.; Ma, S.W. Prediction of slump flow of high-performance concrete via parallel hyper-cubic gene-expression programming. Eng. Appl. Artif. Intell. **2014**, 34, 66–74, doi:10.1016/j.engappai.2014.05.005.

53. Beheshti Aval, S.B.; Ketabdari, H.; Asil Gharebaghi, S. Estimating Shear Strength of Short Rectangular Reinforced Concrete Columns Using Nonlinear Regression and Gene Expression Programming. Structures **2017**, 12, 13–23, doi:10.1016/j.istruc.2017.07.002.

54. Kara, I.F. Empirical modeling of shear strength of steel fiber reinforced concrete beams by gene expression programming. Neural Comput. Appl. **2013**, 23, 823–834, doi:10.1007/s00521-012-0999-x.

55. Sadrossadat, E.; Ghorbani, B.; Hamooni, M.; Moradpoor Sheikhkanloo, M.H. Numerical formulation of confined compressive strength and strain of circular reinforced concrete columns using gene expression programming approach. Struct. Concr. **2018**, 19, 783–794, doi:10.1002/suco.201700131.

56. Nazari, A.; Riahi, S., Computer-aided design of the effects of Fe2O3 nanoparticles on split tensile strength and water permeability of high strength concrete. Compos. Part B Eng. **2011**, 32(7), 3966-3979, doi:10.1016/j.compositesb.2010.12.004.

57. Gholampour, A.; Gandomi, A.H.; Ozbakkaloglu, T. New formulations for mechanical properties of recycled aggregate concrete using gene expression programming. Constr. Build. Mater. **2017**, 130, 122–145, doi:10.1016/j.conbuildmat.2016.10.114.

58. Behnia, D.; Ahangari, K.; Noorzad, A.; Moeinossadat, S.R. Predicting crest settlement in concrete face rockfill dams using adaptive neuro-fuzzy inference system and gene expression programming intelligent methods. J. Zhejiang Univ. Sci. A **2013**, 14, 589–602, doi:10.1631/jzus.A1200301.

59. Akbar, A.; Liew, K.M.; Farooq, F.; Khushnood, R.A. Exploring mechanical performance of hybrid MWCNT and GNMP reinforced cementitious composites. Constr. Build. Mater. **2020**, 120721, doi:https://doi.org/10.1016/j.conbuildmat.2020.120721.

60. Ishak, S.; Lee, H.S.; Singh, J.K.; Ariffin, M.A.M.; Lim, N.H.A.S.; Yang, H.M. Performance of fly ash geopolymer concrete incorporating bamboo ash at elevated temperature. Materials (Basel) **2019**, 12, 3404, doi:10.3390/ma12203404.

61. Albitar, M.; Visintin, P.; Ali, M.; Drechsler, M. Assessing Behaviour of Fresh and Hardened Geopolymer Concrete Mixed with Class-F Fly Ash. KSCE J. Civ. Eng. **2015**, 19, 1445–1455, doi:10.1007/s12205-014-1254-z.

62. Alkroosh, I.S.; Sarker, P.K. Prediction of the compressive strength of fly ash geopolymer concrete using gene expression programming. Comput. Concr. **2019**, 24, 295–302, doi:10.12989/cac.2019.24.4.295.

63. Hardjito, D.; Rangan, B.V. Development and Properties of Low-Calcium Fly Ash-Based Geopolymer Concrete. 2005. Available online: https://www.researchgate.net/publication/228794879_Development_and_Properties_of_Low-calcium_Fly_Ash_Based_Geopolymer_Concrete (accessed on 15 November 2020).

64. Joseph, B.; Mathew, G. Influence of aggregate content on the behavior of fly ash based geopolymer concrete. Sci. Iran. **2012**, 19, 1188–1194, doi:10.1016/j.scient.2012.07.006.

65. Koza, J.R.; Poli, R. Genetic Programming. In Search Methodologies: Introductory Tutorials in Optimization and Decision Support Techniques; Springer US: New York, NY, USA, 2005; pp. 127–164 ISBN 0387234608.

66. Saridemir, M. Genetic programming approach for prediction of compressive strength of concretes containing rice husk ash. Constr. Build. Mater. **2010**, 24, 1911–1919, doi:10.1016/j.conbuildmat.2010.04.011.

67. Nath, P.; Sarker, P.K. Flexural strength and elastic modulus of ambient-cured blended low-calcium fly ash geopolymer concrete. Constr. Build. Mater. **2017**, 130, 22–31, doi:10.1016/j.conbuildmat.2016.11.034.

68. Olivia, M.; Nikraz, H. Properties of fly ash geopolymer concrete designed by Taguchi method. Mater. Des. **2012**, 36, 191–198, doi:10.1016/j.matdes.2011.10.036.

69. Sarker, P.K.; Haque, R.; Ramgolam, K. V. Fracture behaviour of heat cured fly ash based geopolymer concrete. Mater. Des. **2013**, 44, 580–586, doi:10.1016/j.matdes.2012.08.005.

70. Long, T.; Shi, X.S.; Wang, Q.Y.; Li, L. Mechanical properties and microstructure of fly ash based geopolymeric polymer recycled concrete. J. Sichuan Univ. **2013**, 45, 43–47.

71. Sujatha, T.; Kannapiran, K.; Nagan, S. Strength assessment of heat cured geopolymer concrete slender column. Asian J. Civ. Eng. **2012**, 13, 635–646.

72. Vora, P.R.; Dave, U. V. Parametric studies on compressive strength of geopolymer concrete. Proc. Procedia Eng. **2013**, 51, 210–219.

73. Wardhono, A.; Gunasekara, C.; Law, D.W.; Setunge, S. Comparison of long term performance between alkali activated slag and fly ash geopolymer concretes. Constr. Build. Mater. **2017**, 143, 272–279, doi:10.1016/j.conbuildmat.2017.03.153.

74. Lokuge, W.; Wilson, A.; Gunasekara, C.; Law, D.W.; Setunge, S. Design of fly ash geopolymer concrete mix proportions using Multivariate Adaptive Regression Spline model. Constr. Build. Mater. **2018**, 166, 472–481, doi:10.1016/j.conbuildmat.2018.01.175.

75. Mehta, A.; Siddique, R. Properties of low-calcium fly ash based geopolymer concrete incorporating OPC as partial replacement of fly ash. Constr. Build. Mater. **2017**, 150, 792–807, doi:10.1016/j.conbuildmat.2017.06.067.

76. Ramujee, K.; Potharaju, M. Mechanical Properties of Geopolymer Concrete Composites. In Proceedings of the Materials Today: Proceedings; Elsevier Ltd.: Amsterdam, The Netherlands, 2017; Volume 4, pp. 2937–2945.

77. Sathanandam, T.; Awoyera, P.O.; Vijayan, V.; Sathishkumar, K. Low carbon building: Experimental insight on the use of fly ash and glass fibre for making geopolymer concrete. Sustain. Environ. Res. **2017**, 27, 146–153, doi:10.1016/j.serj.2017.03.005.

78. Nuaklong, P.; Sata, V.; Chindaprasirt, P. Influence of recycled aggregate on fly ash geopolymer concrete properties. J. Clean. Prod. **2016**, 112, 2300–2307, doi:10.1016/j.jclepro.2015.10.109.

79. Wongsa, A.; Zaetang, Y.; Sata, V.; Chindaprasirt, P. Properties of lightweight fly ash geopolymer concrete containing bottom ash as aggregates. Constr. Build. Mater. **2016**, 111, 637–643, doi:10.1016/j.conbuildmat.2016.02.135.

80. Shaikh, F.U.A. Mechanical and durability properties of fly ash geopolymer concrete containing recycled coarse aggregates. Int. J. Sustain. Built Environ. **2016**, 5, 277–287, doi:10.1016/j.ijsbe.2016.05.009.

81. Shehab, H.K.; Eisa, A.S.; Wahba, A.M. Mechanical properties of fly ash based geopolymer concrete with full and partial cement replacement. Constr. Build. Mater. **2016**, 126, 560–565, doi:10.1016/j.conbuildmat.2016.09.059.

82. Aliabdo, A.A.; Abd Elmoaty, A.E.M.; Salem, H.A. Effect of cement addition, solution resting time and curing characteristics on fly ash based geopolymer concrete performance. Constr. Build. Mater. **2016**, 123, 581–593, doi:10.1016/j.conbuildmat.2016.07.043.

83. Okoye, F.N.; Durgaprasad, J.; Singh, N.B. Mechanical properties of alkali activated flyash/Kaolin based geopolymer concrete. Constr. Build. Mater. **2015**, 98, 685–691, doi:10.1016/j.conbuildmat.2015.08.009.

84. Ganesan, N.; Abraham, R.; Deepa Raj, S. Durability characteristics of steel fibre reinforced geopolymer concrete. Constr. Build. Mater. **2015**, 93, 471–476, doi:10.1016/j.conbuildmat.2015.06.014.

85. Assi, L.N.; Deaver, E.; Elbatanouny, M.K.; Ziehl, P. Investigation of early compressive strength of fly ash-based geopolymer concrete. Constr. Build. Mater. **2016**, 112, 807–815, doi:10.1016/j.conbuildmat.2016.03.008.

86. Shaikh, F.U.A.; Vimonsatit, V. Compressive strength of fly-ash-based geopolymer concrete at elevated temperatures. Fire Mater. **2015**, 39, 174–188, doi:10.1002/fam.2240.

87. Joseph, B.; Mathew, G. Behaviour of Geopolymer Concrete Exposed To Elevated Temperatures School of Engineering. Ph.D Dissertation, Cochin University of Science and Technology, Kochi, India, **2015**.

88. Satpute, S.; Shirasath, M.; Hake, S. Investigation of alkaline activators for fly ash-based geopolymer concrete. Available online:

http://ijariie.com/AdminUploadPdf/INVESTIGATION_OF_ALKALINE_ACTIVATORS_FOR_FLY_ASH_BASED_GEO_POLYMER_CONCRETE_ijariie3062.pdf (accessed on 15 November 2020).

89. Lavanya, G.; Jegan, J. Evaluation of relationship between split tensile strength and compressive strength for geopolymer concrete of varying grades and molarity. Int. J. Appl. Eng. Res. **2015**, 10, 35523–35529.

90. Nuruddin, M.F.; Demie, S.; Shafiq, N. Effect of mix composition on workability and compressive strength of self-compacting geopolymer concrete. Can. J. Civ. Eng. **2011**, 38, 1196–1203, doi:10.1139/l11-077.

91. Patankar, S. V.; Ghugal, Y.M.; Jamkar, S.S. Mix Design of Fly Ash Based Geopolymer Concrete. In Advances in Structural Engineering: Materials, Volume Three; Springer India: New Delhi, India, 2015; pp. 1619–1634 ISBN 9788132221876.

92. Patankar, S. V.; Jamkar, S.S.; Ghugal, Y.M. Effect of Water-To-Geopolymer Binder Ratio on the Production of Fly Ash Based Geopolymer Concrete. Int. J. Adv. Technol. Civ. Eng. **2013**, 79–83, doi:10.13140/2.1.4792.1284.

93. Sumajouw, M.D.J; Rangan, B.V. Low-calcium fly ash-based geopolymer concrete: Reinforced beams and columns. Research report GC 3, Curtin Research Publications, Curtin University of Technology, Perth, Austrailia, **2006**, 1–120.

94. Fareed Ahmed, M.; Fadhil Nuruddin, M.; Shafiq, N. Compressive strength and workability characteristics of low-calcium fly ash-based self-compacting geopolymer concrete. World Acad. Sci. Eng. Technol. **2011**, 74, 8–14.

95. Deb, P.S.; Nath, P.; Sarker, P.K. Properties of fly ash and slag blended geopolymer concrete cured at ambient temperature. In Proceedings of the ISEC 2013 7th International Structural Engineering and Construction Conference: New Developments in Structural Engineering and Construction, Honolulu, HI, USA, 18–23 June 2013; pp. 571–576.

96. Deb, P.S.; Sarker, P.K.; Nath, P. Sulphate resistance of slag blended fly ash based geopolymer concrete Sulphate Resistance of Slag Blended Fly Ash Based Geopolymer Concrete. In Proceedings of the 26th Biennial National Conference of the Concrete Institute of Australia. Concrete Institute of Australia, Gold Coast, Australia, 16–18 October 2013.

97. Galvin, B.; Lloyd, N.; Lecturer, S. Fly Ash Based Geopolymer Concrete with Recycled Concrete Aggregate. Carbon N. Y. 1978. Available online: http://hdl.handle.net/20.500.11937/15785 (accessed on 15 November 2020).

98. Kusbiantoro, A.; Nuruddin, M.F.; Shafiq, N.; Qazi, S.A. The effect of microwave incinerated rice husk ash on the compressive and bond strength of fly ash based geopolymer concrete. Constr. Build. Mater. **2012**, 36, 695–703, doi:10.1016/j.conbuildmat.2012.06.064.

99. Nuruddin, M.F.; Qazi, S.A.; Kusbiantoro, A.; Shafiq, N. Utilisation of waste material in geopolymeric concrete. Proc. Inst. Civ. Eng. Constr. Mater. **2011**, 164, 315–327, doi:10.1680/coma.2011.164.6.315.

100. Hamad, A.J. Size and shape effect of specimen on the compressive strength of HPLWFC reinforced with glass fibres. J. King Saud Univ. Eng. Sci. **2017**, 29, 373–380, doi:10.1016/j.jksues.2015.09.003.

101. del Viso, J.R.; Carmona, J.R.; Ruiz, G. Shape and size effects on the compressive strength of high-strength concrete. Cem. Concr. Res. **2008**, 38, 386–395, doi:10.1016/j.cemconres.2007.09.020.

102. Van Jaarsveld, J.G.S.; Van Deventer, J.S.J.; Lukey, G.C. The effect of composition and temperature on the properties of fly ash- and kaolinite-based geopolymers. Chem. Eng. J. **2002**, 89, 63–73, doi:10.1016/S1385-8947(02)00025-6.

103. Gandomi, A.H.; Roke, D.A. Assessment of artificial neural network and genetic programming as predictive tools. Adv. Eng. Softw. **2015**, 88, 63–72, doi:10.1016/j.advengsoft.2015.05.007.

104. Babanajad, S.K.; Gandomi, A.H.; Alavi, A.H. New prediction models for concrete ultimate strength under true-triaxial stress states: An evolutionary approach. Adv. Eng. Softw. **2017**, 110, 55–68, doi:10.1016/j.advengsoft.2017.03.011.

105. Gandomi, A.H.; Alavi, A.H.; Mirzahosseini, M.R.; Nejad, F.M. Nonlinear Genetic-Based Models for Prediction of Flow Number of Asphalt Mixtures. J. Mater. Civ. Eng. **2011**, 23, 248–263, doi:10.1061/(ASCE)MT.1943-5533.0000154.

106. Aslam, F.; Farooq, F.; Amin, M.N.; Khan, K.; Waheed, A.; Akbar, A.; Javed, M.F.; Alyousef, R.; Alabdulijabbar, H. Applications of Gene Expression Programming for Estimating Compressive Strength of High-Strength Concrete. Adv. Civ. Eng. **2020**, 2020, 1–23, doi:10.1155/2020/8850535.

107. Alavi, A.H.; Ameri, M.; Gandomi, A.H.; Mirzahosseini, M.R. Formulation of flow number of asphalt mixes using a hybrid computational method. Constr. Build. Mater. **2011**, 25, 1338–1355, doi:10.1016/j.conbuildmat.2010.09.010.

108. Janardhanan, T.; Thaarrini, J.; Dhivya, S. Comparative Study on the Production Cost of Geopolymer and Conventional Concretes. Int. J. Civ. Eng. Res. **2016**, 7, 117–124.

109. Lavanya, G.; Jegan, J. Durability Study on High Calcium Fly Ash Based Geopolymer Concrete. Adv. Mater. Sci. Eng. **2015**, 2015, doi:10.1155/2015/731056.

APPENDIX A

Table A1. Experimental database for compressive strength of fly-ash based geopolymer concrete (FGPC).

Source	Sample description	Heat Curing		age of specimen (days)	Alkali-to-fly ash ratio	Na_2SiO_3-to-NaOH ratio	Molarity of NaOH solution	Total aggregate (% volume of concrete)	Fine-to-total aggregate ratio	Plasticizer (%)	sodium silicate solution				Extra water added (Kg/m3)	Extra water added as percent fly ash (% FA)	Compressive Strength (MPa)
		Curing temperature (^{0}C)	Curing time (hours)								SiO_2 solid (%)	Na_2O solid (%)	Water (%)	SiO_2-to-water (%)			
Joseph and Matthew	M1A60R20	100	24	7	0.55	2.5	10	60	0.2	2	34.64	16.27	49.09	70.564	0	0	38.0
	M1A60R25	100	24	7	0.55	2.5	10	60	0.25	2	34.64	16.27	49.09	70.564	0	0	39.0
	M1A60R30	100	24	7	0.55	2.5	10	60	0.3	2	34.64	16.27	49.09	70.564	0	0	40.0
	M1A60R35	100	24	7	0.55	2.5	10	60	0.35	2	34.64	16.27	49.09	70.564	0	0	42.0
	M1A60R40	100	24	7	0.55	2.5	10	60	0.4	2	34.64	16.27	49.09	70.564	0	0	39.0
	M1A65R20	100	24	7	0.55	2.5	10	65	0.2	2	34.64	16.27	49.09	70.564	0	0	40.0
	M1A65R25	100	24	7	0.55	2.5	10	65	0.25	2	34.64	16.27	49.09	70.564	0	0	41.0
	M1A65R30	100	24	7	0.55	2.5	10	65	0.3	2	34.64	16.27	49.09	70.564	0	0	42.0
	M1A65R35	100	24	7	0.55	2.5	10	65	0.35	2	34.64	16.27	49.09	70.564	0	0	44.0
	M1A65R40	100	24	7	0.55	2.5	10	65	0.4	2	34.64	16.27	49.09	70.564	0	0	42.0
	M1A70R20	100	24	7	0.55	2.5	10	70	0.2	2	34.64	16.27	49.09	70.564	0	0	43.0
	M1A70R25	100	24	7	0.55	2.5	10	70	0.25	2	34.64	16.27	49.09	70.564	0	0	45.0
	M1A70R30	100	24	7	0.55	2.5	10	70	0.3	2	34.64	16.27	49.09	70.564	0	0	47.0
	M1A70R35	100	24	7	0.55	2.5	10	70	0.35	2	34.64	16.27	49.09	70.564	0	0	52.0
	M1A70R40	100	24	7	0.55	2.5	10	70	0.4	2	34.64	16.27	49.09	70.564	0	0	46.0
	M1A75R20	100	24	7	0.55	2.5	10	75	0.2	2	34.64	16.27	49.09	70.564	0	0	33.0
	M1A75R25	100	24	7	0.55	2.5	10	75	0.25	2	34.64	16.27	49.09	70.564	0	0	35.0
	M1A75R30	100	24	7	0.55	2.5	10	75	0.3	2	34.64	16.27	49.09	70.564	0	0	41.0
	M1A75R35	100	24	7	0.55	2.5	10	75	0.35	2	34.64	16.27	49.09	70.564	0	0	45.0
	M1A75R40	100	24	7	0.55	2.5	10	75	0.4	2	34.64	16.27	49.09	70.564	0	0	40.0
	M1A60R35	100	24	28	0.55	2.5	10	60	0.35	2	34.64	16.27	49.09	70.564	0	0	45.0
	M1A65R35	100	24	28	0.55	2.5	10	65	0.35	2	34.64	16.27	49.09	70.564	0	0	47.0
	M1A70R35	100	24	28	0.55	2.5	10	70	0.35	2	34.64	16.27	49.09	70.564	0	0	56.0
	M1A75R35	100	24	28	0.55	2.5	10	75	0.35	2	34.64	16.27	49.09	70.564	0	0	49.0
	M1A60R35	100	24	3	0.55	2.5	10	60	0.35	2	34.64	16.27	49.09	70.564	0	0	42.0
	M1A65R35	100	24	3	0.55	2.5	10	65	0.35	2	34.64	16.27	49.09	70.564	0	0	45.0

M1A70R35	100	24	3	0.55	2.5	10	70	0.35	2	34.64	16.27	49.09	70.564	0	0	52.0
M1A75R35	100	24	3	0.55	2.5	10	75	0.35	2	34.64	16.27	49.09	70.564	0	0	45.0
M2AL35S1	100	24	7	0.35	1.5	10	70	0.35	2	34.64	16.27	49.09	70.564	0	0	31.0
M2AL35S2	100	24	7	0.35	2	10	70	0.35	2	34.64	16.27	49.09	70.564	0	0	34.0
M2AL35S3	100	24	7	0.35	2.5	10	70	0.35	2	34.64	16.27	49.09	70.564	0	0	39.0
M2AL35S4	100	24	7	0.35	3	10	70	0.35	2	34.64	16.27	49.09	70.564	0	0	36.0
M2AL35S5	100	24	7	0.35	3.5	10	70	0.35	2	34.64	16.27	49.09	70.564	0	0	34.0
M2AL45S1	100	24	7	0.45	1.5	10	70	0.35	2	34.64	16.27	49.09	70.564	0	0	34.0
M2AL45S2	100	24	7	0.45	2	10	70	0.35	2	34.64	16.27	49.09	70.564	0	0	40.0
M2AL45S3	100	24	7	0.45	2.5	10	70	0.35	2	34.64	16.27	49.09	70.564	0	0	47.0
M2AL45S4	100	24	7	0.45	3	10	70	0.35	2	34.64	16.27	49.09	70.564	0	0	43.0
M2AL45S5	100	24	7	0.45	3.5	10	70	0.35	2	34.64	16.27	49.09	70.564	0	0	38.0
M2AL55S1	100	24	7	0.55	1.5	10	70	0.35	2	34.64	16.27	49.09	70.564	0	0	47.0
M2AL55S2	100	24	7	0.55	2	10	70	0.35	2	34.64	16.27	49.09	70.564	0	0	54.0
M2AL55S3	100	24	7	0.55	2.5	10	70	0.35	2	34.64	16.27	49.09	70.564	0	0	58.0
M2AL55S4	100	24	7	0.55	3	10	70	0.35	2	34.64	16.27	49.09	70.564	0	0	52.0
M2AL55S5	100	24	7	0.55	3.5	10	70	0.35	2	34.64	16.27	49.09	70.564	0	0	43.0
M2AL65S1	100	24	7	0.65	1.5	10	70	0.35	2	34.64	16.27	49.09	70.564	0	0	41.0
M2AL65S2	100	24	7	0.65	2	10	70	0.35	2	34.64	16.27	49.09	70.564	0	0	43.0
M2AL65S3	100	24	7	0.65	2.5	10	70	0.35	2	34.64	16.27	49.09	70.564	0	0	44.0
M2AL65S4	100	24	7	0.65	3	10	70	0.35	2	34.64	16.27	49.09	70.564	0	0	42.0
M2AL65S5	100	24	7	0.65	3.5	10	70	0.35	2	34.64	16.27	49.09	70.564	0	0	41.0
M3AL35W1	100	24	7	0.35	1.5	10	70	0.35	2	34.64	16.27	49.09	70.564	0	0	40.0
M3AL35W2	100	24	7	0.35	2	10	70	0.35	2	34.64	16.27	49.09	70.564	0	0	38.0
M3AL35W3	100	24	7	0.35	2.5	10	70	0.35	2	34.64	16.27	49.09	70.564	0	0	35.0
M3AL35W4	100	24	7	0.35	3	10	70	0.35	2	34.64	16.27	49.09	70.564	0	0	31.0
M3AL35W5	100	24	7	0.35	3.5	10	70	0.35	2	34.64	16.27	49.09	70.564	0	0	30.0
M3AL45W1	100	24	7	0.45	2.5	10	70	0.35	2	34.64	16.27	49.09	70.564	0	0	49.0
M3AL45W2	100	24	7	0.45	2.5	10	70	0.35	2	34.64	16.27	49.09	70.564	0	0	45.0
M3AL45W3	100	24	7	0.45	2.5	10	70	0.35	2	34.64	16.27	49.09	70.564	0	0	42.0
M3AL45W4	100	24	7	0.45	2.5	10	70	0.35	2	34.64	16.27	49.09	70.564	0	0	39.0
M3AL45W5	100	24	7	0.45	2.5	10	70	0.35	2	34.64	16.27	49.09	70.564	0	0	35.0
M3AL55W1	100	24	7	0.55	2.5	10	70	0.35	2	34.64	16.27	49.09	70.564	0	0	60.0
M3AL55W2	100	24	7	0.55	2.5	10	70	0.35	2	34.64	16.27	49.09	70.564	0	0	56.0
M3AL55W3	100	24	7	0.55	2.5	10	70	0.35	2	34.64	16.27	49.09	70.564	0	0	52.0
M3AL55W4	100	24	7	0.55	2.5	10	70	0.35	2	34.64	16.27	49.09	70.564	0	0	49.0
M3AL55W5	100	24	7	0.55	2.5	10	70	0.35	2	34.64	16.27	49.09	70.564	0	0	46.0

M3AL65W1	100	24	7	0.65	2.5	10	70	0.35	2	34.64	16.27	49.09	70.564	0	0	47.0
M3AL65W2	100	24	7	0.65	2.5	10	70	0.35	2	34.64	16.27	49.09	70.564	0	0	44.0
M3AL65W3	100	24	7	0.65	2.5	10	70	0.35	2	34.64	16.27	49.09	70.564	0	0	40.0
M3AL65W4	100	24	7	0.65	2.5	10	70	0.35	2	34.64	16.27	49.09	70.564	0	0	37.0
M3AL65W5	100	24	7	0.65	2.5	10	70	0.35	2	34.64	16.27	49.09	70.564	0	0	32.0
M2AL35S3	28	24	7	0.35	2.5	10	70	0.35	2	34.64	16.27	49.09	70.564	0	0	14.0
M2AL35S3	60	24	7	0.35	2.5	10	70	0.35	2	34.64	16.27	49.09	70.564	0	0	28.0
M2AL35S3	70	24	7	0.35	2.5	10	70	0.35	2	34.64	16.27	49.09	70.564	0	0	30.0
M2AL35S3	80	24	7	0.35	2.5	10	70	0.35	2	34.64	16.27	49.09	70.564	0	0	32.0
M2AL35S3	90	24	7	0.35	2.5	10	70	0.35	2	34.64	16.27	49.09	70.564	0	0	36.0
M2AL35S3	100	24	7	0.35	2.5	10	70	0.35	2	34.64	16.27	49.09	70.564	0	0	39.0
M2AL35S3	110	24	7	0.35	2.5	10	70	0.35	2	34.64	16.27	49.09	70.564	0	0	32.0
M2AL35S3	120	24	7	0.35	2.5	10	70	0.35	2	34.64	16.27	49.09	70.564	0	0	30.0
M2AL45S3	28	24	7	0.45	2.5	10	70	0.35	2	34.64	16.27	49.09	70.564	0	0	14.0
M2AL45S3	60	24	7	0.45	2.5	10	70	0.35	2	34.64	16.27	49.09	70.564	0	0	32.0
M2AL45S3	70	24	7	0.45	2.5	10	70	0.35	2	34.64	16.27	49.09	70.564	0	0	34.0
M2AL45S3	80	24	7	0.45	2.5	10	70	0.35	2	34.64	16.27	49.09	70.564	0	0	35.0
M2AL45S3	90	24	7	0.45	2.5	10	70	0.35	2	34.64	16.27	49.09	70.564	0	0	38.0
M2AL45S3	100	24	7	0.45	2.5	10	70	0.35	2	34.64	16.27	49.09	70.564	0	0	44.0
M2AL45S3	110	24	7	0.45	2.5	10	70	0.35	2	34.64	16.27	49.09	70.564	0	0	39.0
M2AL45S3	120	24	7	0.45	2.5	10	70	0.35	2	34.64	16.27	49.09	70.564	0	0	35.0
M2AL55S3	28	24	7	0.55	2.5	10	70	0.35	2	34.64	16.27	49.09	70.564	0	0	16.0
M2AL55S3	60	24	7	0.55	2.5	10	70	0.35	2	34.64	16.27	49.09	70.564	0	0	37.0
M2AL55S3	70	24	7	0.55	2.5	10	70	0.35	2	34.64	16.27	49.09	70.564	0	0	41.0
M2AL55S3	80	24	7	0.55	2.5	10	70	0.35	2	34.64	16.27	49.09	70.564	0	0	44.0
M2AL55S3	90	24	7	0.55	2.5	10	70	0.35	2	34.64	16.27	49.09	70.564	0	0	49.0
M2AL55S3	100	24	7	0.55	2.5	10	70	0.35	2	34.64	16.27	49.09	70.564	0	0	55.0
M2AL55S3	110	24	7	0.55	2.5	10	70	0.35	2	34.64	16.27	49.09	70.564	0	0	48.0
M2AL55S3	120	24	7	0.55	2.5	10	70	0.35	2	34.64	16.27	49.09	70.564	0	0	44.0
M2AL65S3	28	24	7	0.65	2.5	10	70	0.35	2	34.64	16.27	49.09	70.564	0	0	15.0
M2AL65S3	60	24	7	0.65	2.5	10	70	0.35	2	34.64	16.27	49.09	70.564	0	0	34.0
M2AL65S3	70	24	7	0.65	2.5	10	70	0.35	2	34.64	16.27	49.09	70.564	0	0	38.0
M2AL65S3	80	24	7	0.65	2.5	10	70	0.35	2	34.64	16.27	49.09	70.564	0	0	40.0
M2AL65S3	90	24	7	0.65	2.5	10	70	0.35	2	34.64	16.27	49.09	70.564	0	0	42.0
M2AL65S3	100	24	7	0.65	2.5	10	70	0.35	2	34.64	16.27	49.09	70.564	0	0	45.0
M2AL65S3	110	24	7	0.65	2.5	10	70	0.35	2	34.64	16.27	49.09	70.564	0	0	40.0
M2AL65S3	120	24	7	0.65	2.5	10	70	0.35	2	34.64	16.27	49.09	70.564	0	0	36.0

	M2AL55S3	100	6	7	0.55	2.5	10	70	0.35	2	34.64	16.27	49.09	70.564	0	0	25.0
	M2AL55S4	100	12	7	0.55	2.5	10	70	0.35	2	34.64	16.27	49.09	70.564	0	0	36.0
	M2AL55S5	100	24	7	0.55	2.5	10	70	0.35	2	34.64	16.27	49.09	70.564	0	0	54.0
	M2AL55S6	100	48	7	0.55	2.5	10	70	0.35	2	34.64	16.27	49.09	70.564	0	0	56.0
	M2AL55S7	100	72	7	0.55	2.5	10	70	0.35	2	34.64	16.27	49.09	70.564	0	0	57.0
		100	24	7	0.55	2.5	8	70	0.35	2	34.64	16.27	49.09	70.564	0	0	45.0
		100	24	7	0.55	2.5	10	70	0.35	2	34.64	16.27	49.09	70.564	0	0	54.0
		100	24	7	0.55	2.5	12	70	0.35	2	34.64	16.27	49.09	70.564	0	0	47.0
		100	24	7	0.55	2.5	14	70	0.35	2	34.64	16.27	49.09	70.564	0	0	43.0
		100	24	7	0.55	2.5	16	70	0.35	2	34.64	16.27	49.09	70.564	0	0	51.0
	M_1	70	24	1	0.5	2.5	12	65	0.47	7	29.43	14.26	56.31	52.264	40	10	53.5
	M_2	70	24	1	0.5	2.5	12	65	0.47	7	29.43	14.26	56.31	52.264	48	12	45.0
	M_3	70	24	1	0.5	2.5	12	65	0.47	7	29.43	14.26	56.31	52.264	60	15	37.3
	M_4	70	24	1	0.5	2.5	12	65	0.47	7	29.43	14.26	56.31	52.264	80	20	22.6
M.Fareed Ahmad et.al	M_5	70	48	2	0.5	2.5	12	65	0.47	7	29.43	14.26	56.31	52.264	48	12	51.0
	M_6	70	72	3	0.5	2.5	12	65	0.47	7	29.43	14.26	56.31	52.264	48	12	51.4
	M_7	70	96	4	0.5	2.5	12	65	0.47	7	29.43	14.26	56.31	52.264	48	12	51.7
	M_8	60	48	2	0.5	2.5	12	65	0.47	7	29.43	14.26	56.31	52.264	48	12	44.8
	M_9	80	48	2	0.5	2.5	12	65	0.47	7	29.43	14.26	56.31	52.264	48	12	48.6
	M_{10}	90	48	2	0.5	2.5	12	65	0.47	7	29.43	14.26	56.31	52.264	48	12	48.0
	GPC 5	20	72	7	0.35	2.5	14	70	0.35	1.5	30.1	11.4	58.5	51.453	0	0	11.0
	GPC 5	20	72	28	0.35	2.5	14	70	0.35	1.5	30.1	11.4	58.5	51.453	0	0	25.0
	GPC 5	20	72	56	0.35	2.5	14	70	0.35	1.5	30.1	11.4	58.5	51.453	0	0	30.0
	GPC 5	20	72	90	0.35	2.5	14	70	0.35	1.5	30.1	11.4	58.5	51.453	0	0	33.0
	GPC 5	20	72	180	0.35	2.5	14	70	0.35	1.5	30.1	11.4	58.5	51.453	0	0	35.0
Deb et al.	GPC 8	20	72	7	0.35	1.5	14	70	0.35	1.5	30.1	11.4	58.5	51.453	0	0	8.0
	GPC 8	20	72	28	0.35	1.5	14	70	0.35	1.5	30.1	11.4	58.5	51.453	0	0	27.0
	GPC 8	20	72	56	0.35	1.5	14	70	0.35	1.5	30.1	11.4	58.5	51.453	0	0	32.0
	GPC 8	20	72	90	0.35	1.5	14	70	0.35	1.5	30.1	11.4	58.5	51.453	0	0	34.0
	GPC 8	20	72	180	0.35	1.5	14	70	0.35	1.5	30.1	11.4	58.5	51.453	0	0	37.0
	1	60	24	7	0.35	0.4	8	77.5	0.4	0	29.4	14.7	55.9	52.594	0	0	17.0
	2	30	4	7	0.35	2.5	8	77.5	0.4	0	29.4	14.7	55.9	52.594	0	0	8.0
	2	60	4	7	0.35	2.5	8	77.5	0.4	0	29.4	14.7	55.9	52.594	0	0	24.0
Hardjito and Rangan	2	60	8	7	0.35	2.5	8	77.5	0.4	0	29.4	14.7	55.9	52.594	0	0	31.0
	2	60	12	7	0.35	2.5	8	77.5	0.4	0	29.4	14.7	55.9	52.594	0	0	41.0
	2	60	48	7	0.35	2.5	8	77.5	0.4	0	29.4	14.7	55.9	52.594	0	0	72.0
	2	60	72	7	0.35	2.5	8	77.5	0.4	0	29.4	14.7	55.9	52.594	0	0	77.0

2	60	96	7	0.35	2.5	8	77.5	0.4	0	29.4	14.7	55.9	52.594	0	0	82.0
2	90	4	7	0.35	2.5	8	77.5	0.4	0	29.4	14.7	55.9	52.594	0	0	37.0
2	30	24	7	0.35	2.5	8	77.5	0.4	0	29.4	14.7	55.9	52.594	0	0	20.0
2	60	24	7	0.35	2.5	8	77.5	0.4	0	29.4	14.7	55.9	52.594	0	0	57.0
2	30	24	7	0.35	2.5	8	77.5	0.4	1.3	29.4	14.7	55.9	52.594	0	0	35.0
2	45	24	7	0.35	2.5	8	77.5	0.4	1.3	29.4	14.7	55.9	52.594	0	0	41.0
2	60	24	7	0.35	2.5	8	77.5	0.4	1.3	29.4	14.7	55.9	52.594	0	0	63.0
2	75	24	7	0.35	2.5	8	77.5	0.4	1.3	29.4	14.7	55.9	52.594	0	0	64.0
2	90	24	7	0.35	2.5	8	77.5	0.4	1.3	29.4	14.7	55.9	52.594	0	0	63.0
2	45	6	7	0.35	2.5	8	77.5	0.4	1.3	29.4	14.7	55.9	52.594	0	0	33.0
2	60	6	7	0.35	2.5	8	77.5	0.4	1.3	29.4	14.7	55.9	52.594	0	0	42.0
2	75	6	7	0.35	2.5	8	77.5	0.4	1.3	29.4	14.7	55.9	52.594	0	0	48.0
2	90	6	7	0.35	2.5	8	77.5	0.4	1.3	29.4	14.7	55.9	52.594	0	0	51.0
2	60	24	7	0.35	2.5	8	77.5	0.4	1	29.4	14.7	55.9	52.594	0	0	56.0
2	60	24	7	0.35	2.5	8	77.5	0.4	1.5	29.4	14.7	55.9	52.594	0	0	58.0
2	60	24	7	0.35	2.5	8	77.5	0.4	2	29.4	14.7	55.9	52.594	0	0	57.0
2	60	24	7	0.35	2.5	8	77.5	0.4	2.5	29.4	14.7	55.9	52.594	0	0	50.0
2	60	24	7	0.35	2.5	8	77.5	0.4	3	29.4	14.7	55.9	52.594	0	0	50.0
2	60	24	7	0.35	2.5	8	77.5	0.4	3.5	29.4	14.7	55.9	52.594	0	0	46.0
2	60	24	3	0.35	2.5	8	77.5	0.4	0	29.4	14.7	55.9	52.594	0	0	61.0
2	60	24	14	0.35	2.5	8	77.5	0.4	0	29.4	14.7	55.9	52.594	0	0	64.0
2	60	24	28	0.35	2.5	8	77.5	0.4	0	29.4	14.7	55.9	52.594	0	0	60.0
2	60	24	56	0.35	2.5	8	77.5	0.4	0	29.4	14.7	55.9	52.594	0	0	61.0
2	60	24	91	0.35	2.5	8	77.5	0.4	0	29.4	14.7	55.9	52.594	0	0	63.0
2	90	24	7	0.35	2.5	8	77.5	0.4	0	29.4	14.7	55.9	52.594	0	0	66.0
3	60	24	7	0.35	0.4	14	77.5	0.4	0	29.4	14.7	55.9	52.594	0	0	48.0
4	30	48	7	0.35	2.5	14	77.5	0.4	0	29.4	14.7	55.9	52.594	0	0	49.0
4	60	4	7	0.35	2.5	14	77.5	0.4	0	29.4	14.7	55.9	52.594	0	0	25.0
4	90	4	7	0.35	2.5	14	77.5	0.4	0	29.4	14.7	55.9	52.594	0	0	30.0
4	30	24	7	0.35	2.5	14	77.5	0.4	0	29.4	14.7	55.9	52.594	0	0	29.0
4	60	24	7	0.35	2.5	14	77.5	0.4	0	29.4	14.7	55.9	52.594	0	0	68.0
4	90	24	7	0.35	2.5	14	77.5	0.4	0	29.4	14.7	55.9	52.594	0	0	70.0
5	60	24	3	0.38	2	14	77.5	0.3	0	29.4	14.7	55.9	52.594	16.5	4	42.0
6	60	24	3	0.38	2	14	77.5	0.3	1	29.4	14.7	55.9	52.594	16.5	4	41.0
7	60	24	3	0.38	2	14	77.5	0.3	2	29.4	14.7	55.9	52.594	16.5	4	41.0
8	60	24	3	0.38	2	14	77.5	0.3	4	29.4	14.7	55.9	52.594	16.5	4	36.0
9	60	24	7	0.35	2.5	12	77.5	0.35	1.5	29.4	14.7	55.9	52.594	14.3	3.5	40.0

	10	60	24	7	0.35	2.5	14	77.5	0.35	1.5	29.4	14.7	55.9	52.594	17.6	4.3	43.0
	11	60	24	7	0.35	2.5	12	77.5	0.35	1.5	29.4	14.7	55.9	52.594	14.3	3.5	38.0
	12	60	24	7	0.35	2.5	8	77.5	0.35	1.5	29.4	14.7	55.9	52.594	0	0	63.0
	13	30	24	7	0.35	2.5	14	77.5	0.35	2	29.4	14.7	55.9	52.594	0	0	44.0
	13	45	24	7	0.35	2.5	14	77.5	0.3	2	29.4	14.7	55.9	52.594	0	0	55.0
	13	60	24	7	0.35	2.5	14	77.5	0.3	2	29.4	14.7	55.9	52.594	0	0	59.0
	13	75	24	7	0.35	2.5	14	77.5	0.3	2	29.4	14.7	55.9	52.594	0	0	65.0
	13	90	24	7	0.35	2.5	14	77.5	0.3	2	29.4	14.7	55.9	52.594	0	0	71.0
	14	30	24	7	0.35	2.5	14	77.5	0.3	2	29.4	14.7	55.9	52.594	10.7	2.62	35.0
	14	45	24	7	0.35	2.5	14	77.5	0.3	2	29.4	14.7	55.9	52.594	10.7	2.62	42.0
	14	75	24	7	0.35	2.5	14	77.5	0.3	2	29.4	14.7	55.9	52.594	10.7	2.62	60.0
	14	90	24	7	0.35	2.5	14	77.5	0.3	2	29.4	14.7	55.9	52.594	10.7	2.62	59.0
	15	30	24	7	0.35	2.5	14	77.5	0.3	2	29.4	14.7	55.9	52.594	21.3	5.22	32.0
	15	45	24	7	0.35	2.5	14	77.5	0.3	2	29.4	14.7	55.9	52.594	21.3	5.22	37.0
	15	60	24	7	0.35	2.5	14	77.5	0.3	2	29.4	14.7	55.9	52.594	21.3	5.22	44.0
	15	75	24	7	0.35	2.5	14	77.5	0.3	2	29.4	14.7	55.9	52.594	21.3	5.22	44.0
	15	90	24	7	0.35	2.5	14	77.5	0.3	2	29.4	14.7	55.9	52.594	21.3	5.22	44.0
	16	60	24	7	0.35	2.5	8	77.5	0.35	1.5	29.4	14.7	55.9	52.594	0	0	47.0
	17	60	24	7	0.35	2.5	10	77.5	0.35	1.5	29.4	14.7	55.9	52.594	7.5	1.84	45.0
	18	60	24	7	0.35	2.5	12	77.5	0.35	1.5	29.4	14.7	55.9	52.594	14.4	3.53	42.0
	19	60	24	7	0.35	2.5	14	77.5	0.35	1.5	29.4	14.7	55.9	52.594	20.7	5.1	40.0
	20	60	24	7	0.35	2.5	16	77.5	0.35	1.5	29.4	14.7	55.9	52.594	26.5	6.5	40.0
	21	60	24	21	0.35	2.5	14	77.5	0.35	1.5	29.4	14.7	55.9	52.594	20.7	5.1	40.0
	22	90	4	3	0.35	2.5	14	77.5	0.3	1.5	29.4	14.7	55.9	52.594	16.5	4	40.0
	23	90	24	90	0.35	2.5	14	77.5	0.35	2	29.4	14.7	55.9	52.594	0	0	89.0
	24	90	24	90	0.35	2.5	8	77.5	0.35	1.5	29.4	14.7	55.9	52.594	0	0	68.0
	25	60	24	90	0.4	2	8	77.5	0.35	1.5	29.4	14.7	55.9	52.594	0	0	55.0
	26	60	24	90	0.4	2	8	77.5	0.35	1.5	29.4	14.7	55.9	52.594	0	0	44.0
	R0	60	18	1	0.35	2.5	8	75	0.31	0	29.4	14.7	55.9	52.594	20	5	23.0
Galvin and Llyod	R0	60	18	7	0.35	2.5	8	75	0.31	0	29.4	14.7	55.9	52.594	20	5	26.0
	R0	60	18	28	0.35	2.5	8	75	0.31	0	29.4	14.7	55.9	52.594	20	5	33.0
	R0	60	18	91	0.35	2.5	8	75	0.31	0	29.4	14.7	55.9	52.594	20	5	36.0
	C1	65	24	3	0.4	2.5	8	78	0.54	0	29.75	14.73	55.52	53.584	35	10	43.2
Kubiantoro et al.	C1	65	24	7	0.4	2.5	8	78	0.54	0	29.75	14.73	55.52	53.584	35	10	44.0
	C1	65	24	28	0.4	2.5	8	78	0.54	0	29.75	14.73	55.52	53.584	35	10	50.0
	C1	65	24	56	0.4	2.5	8	78	0.54	0	29.75	14.73	55.52	53.584	35	10	54.0

Lloyd and Rangan	Mixture-1	60	24	7	0.35	2.5	8	77	0.3	1.5	29.4	14.7	55.9	52.594	0	0	56.0
	FA	30	24	3	0.4	2.5	8	78	0.35	3	29.43	14.26	56.31	52.264	35	10	34.5
	FA	30	24	7	0.4	2.5	8	78	0.35	3	29.43	14.26	56.31	52.264	35	10	42.3
Nuruddin et al.	FA	30	24	28	0.4	2.5	8	78	0.35	3	29.43	14.26	56.31	52.264	35	10	48.7
	FA	30	24	56	0.4	2.5	8	78	0.35	3	29.43	14.26	56.31	52.264	35	10	50.6
	FA	30	24	90	0.4	2.5	8	78	0.35	3	29.43	14.26	56.31	52.264	35	10	51.4
	A40 S00	23	24	3	0.4	2.5	14	78	0.35	0	30	11.5	58.5	51.282	0	0	5.0
	A40 S00	23	24	7	0.4	2.5	14	78	0.35	0	30	11.5	58.5	51.282	0	0	16.0
	A40 S00	23	24	28	0.4	2.5	14	78	0.35	0	30	11.5	58.5	51.282	0	0	25.6
Nath and Sarker	A40 S00	23	24	56	0.4	2.5	14	78	0.35	0	30	11.5	58.5	51.282	0	0	30.0
	A40 S00	23	24	90	0.4	2.5	14	78	0.35	0	30	11.5	58.5	51.282	0	0	33.4
	A35 S00	23	24	28	0.35	2.5	14	78	0.35	1.5	30	11.5	58.5	51.282	0	0	32.2
	A35 S00	23	24	90	0.35	2.5	14	78	0.35	1.5	30	11.5	58.5	51.282	0	0	41.1
	T1	60	24	1	0.3	1.5	14	72	0.35	1.22	29.4	14.7	55.9	52.594	26.47	5.3	37.8
	T1	60	24	7	0.3	1.5	14	72	0.35	1.22	29.4	14.7	55.9	52.594	26.47	5.3	39.5
	T1	60	24	28	0.3	1.5	14	72	0.35	1.22	29.4	14.7	55.9	52.594	26.47	5.3	39.9
	T2	70	12	1	0.35	2	14	72	0.35	1.27	29.4	14.7	55.9	52.594	23.65	5	34.6
	T2	70	12	7	0.35	2	14	72	0.35	1.27	29.4	14.7	55.9	52.594	23.65	5	35.3
	T2	70	12	28	0.35	2	14	72	0.35	1.27	29.4	14.7	55.9	52.594	23.65	5	37.1
	T3	75	24	1	0.4	2.5	14	72	0.35	1.32	29.4	14.7	55.9	52.594	21.23	4.6	49.7
	T3	75	24	7	0.4	2.5	14	72	0.35	1.32	29.4	14.7	55.9	52.594	21.23	4.6	49.9
	T3	75	24	28	0.4	2.5	14	72	0.35	1.32	29.4	14.7	55.9	52.594	21.23	4.6	49.6
	T4	75	24	1	0.3	2	14	74	0.35	1.32	29.4	14.7	55.9	52.594	18.61	4	41.9
	T4	75	24	7	0.3	2	14	74	0.35	1.32	29.4	14.7	55.9	52.594	18.61	4	40.9
Olivia and Nikraz	T4	75	24	28	0.3	2	14	74	0.35	1.32	29.4	14.7	55.9	52.594	18.61	4	42.5
	T4	75	24	91	0.3	2	14	74	0.35	1.5	29.4	14.7	55.9	52.594	18.6	4	58.9
	T5	60	24	1	0.35	2.5	14	74	0.35	1.37	29.4	14.7	55.9	52.594	18.55	4.2	32.5
	T5	60	24	7	0.35	2.5	14	74	0.35	1.37	29.4	14.7	55.9	52.594	18.55	4.2	37.6
	T5	60	24	28	0.35	2.5	14	74	0.35	1.37	29.4	14.7	55.9	52.594	18.55	4.2	38.7
	T6	70	12	1	0.4	1.5	14	74	0.35	1.42	29.4	14.7	55.9	52.594	28.51	6.65	25.2
	T6	70	12	7	0.4	1.5	14	74	0.35	1.42	29.4	14.7	55.9	52.594	28.51	6.65	27.2
	T6	70	12	28	0.4	1.5	14	74	0.35	1.42	29.4	14.7	55.9	52.594	28.51	6.65	28.6
	T7	70	12	1	0.3	2.5	14	76	0.35	1.44	29.4	14.7	55.9	52.594	15.97	3.76	54.1
	T7	70	12	7	0.3	2.5	14	76	0.35	1.44	29.4	14.7	55.9	52.594	15.97	3.76	52.3
	T7	70	12	28	0.3	2.5	14	76	0.35	1.44	29.4	14.7	55.9	52.594	15.97	3.76	54.9
	T7	70	12	91	0.3	2.5	14	76	0.35	1.51	29.4	14.7	55.9	52.594	17.9	4.21	56.5

	T8	75	24	1	0.35	1.5	14	76	0.35	1.5	29.4	14.7	55.9	52.594	24.46	6	32.4
	T8	75	24	7	0.35	1.5	14	76	0.35	1.5	29.4	14.7	55.9	52.594	24.46	6	34.5
	T8	75	24	28	0.35	1.5	14	76	0.35	1.5	29.4	14.7	55.9	52.594	24.46	6	35.7
	T9	60	24	1	0.4	2	14	76	0.35	1.55	29.4	14.7	55.9	52.594	21.47	5.4	25.9
	T9	60	24	7	0.4	2	14	76	0.35	1.55	29.4	14.7	55.9	52.594	21.47	5.4	29.3
	T9	60	24	28	0.4	2	14	76	0.35	1.55	29.4	14.7	55.9	52.594	21.47	5.4	29.7
	T10	75	24	7	0.3	2.5	14	72	0.35	1.5	29.4	14.7	55.9	52.594	18.8	3.77	59.1
	T10	75	24	28	0.3	2.5	14	72	0.35	1.5	29.4	14.7	55.9	52.594	18.8	3.77	60.2
	T10	75	24	91	0.3	2.5	14	72	0.35	1.5	29.4	14.7	55.9	52.594	18.8	3.77	63.3
	GPC 1	60	24	28	0.38	1.5	14	76	0.35	0	28.9	9.1	62	46.613	4	1	32
Sarker et al.	GPC 2	60	24	28	0.38	1.5	14	76	0.35	0	28.9	9.1	62	46.613	0	0	36
	GPC 3	60	24	28	0.42	1.5	14	76	0.35	0	28.9	9.1	62	46.613	0	0	48
	GRC0	80	24	3	0.5	2.5	8	77	0.3	0	29.4	14.7	55.9	52.594	0	0	74.37
	GRC0	80	24	7	0.5	2.5	8	77	0.3	0	29.4	14.7	55.9	52.594	0	0	80.58
Shi et al.	GRC0	80	24	28	0.5	2.5	8	77	0.3	0	29.4	14.7	55.9	52.594	0	0	85.66
	GRC0	80	24	60	0.5	2.5	8	77	0.3	0	29.4	14.7	55.9	52.594	0	0	86.15
	GRC0	80	24	90	0.5	2.5	8	77	0.3	0	29.4	14.7	55.9	52.594	0	0	88.22
Sujatha et al.	G30	70	24	28	0.46	2.5	12	75	0.3	2	29.4	14.7	55.9	52.594	0	0	35.48
	G50	70	24	28	0.5	2.5	12	75	0.35	2	29.4	14.7	55.9	52.594	0	0	53.5
	Mix-1	75	24	3	0.4	2.5	14	76	0.35	2	35.01	16.84	48.15	72.710	43	10	30
	Mix-2	75	24	3	0.35	2.5	14	76	0.35	2	35.01	16.84	48.15	72.710	43	10	30
	Mix-3	75	24	3	0.4	2	14	76	0.35	2	35.01	16.84	48.15	72.710	43	10	40
	Mix-4B	75	48	3	0.4	2.5	14	76	0.35	2	35.01	16.84	48.15	72.710	43	10	32
	Mix-5B	75	48	3	0.4	2.5	14	76	0.35	3	35.01	16.84	48.15	72.710	43	10	30
	Mix-5C	75	48	3	0.4	2.5	14	76	0.35	4	35.01	16.84	48.15	72.710	43	10	29
	Mix-7A	75	24	3	0.4	2	14	76	0.35	1	35.01	16.84	48.15	72.710	43	10	30
	Mix-7B	75	24	3	0.4	2	14	76	0.35	1	35.01	16.84	48.15	72.710	64	15	24
Vora and Dave	Mix-7C	75	24	3	0.4	2	14	76	0.35	1	35.01	16.84	48.15	72.710	86	20	20
	Mix-8A	75	24	7	0.4	2	8	76	0.35	1	35.01	16.84	48.15	72.710	43	10	32
	Mix-8B	75	24	7	0.4	2	10	76	0.35	1	35.01	16.84	48.15	72.710	43	10	35
	Mix-8C	75	24	7	0.4	2	12	76	0.35	1	35.01	16.84	48.15	72.710	43	10	43
	Mix-8D	75	24	7	0.4	2	14	76	0.35	1	35.01	16.84	48.15	72.710	43	10	46
	Mix-9A	60	24	7	0.4	2	14	76	0.35	1	35.01	16.84	48.15	72.710	43	10	38
	Mix-9B	75	24	7	0.4	2	14	76	0.35	1	35.01	16.84	48.15	72.710	43	10	46
	Mix-9C	90	24	7	0.4	2	14	76	0.35	1	35.01	16.84	48.15	72.710	43	10	49
Wardhono.A. et al.	FAGP	80	24	28	0.82	1.6	15	64	0.43	0	29.4	14.7	55.9	52.594	10	2.14	22.37
	FAGP	80	24	56	0.82	1.6	15	64	0.43	0	29.4	14.7	55.9	52.594	10	2.14	25.13

	FAGP	80	24	90	0.82	1.6	15	64	0.43	0	29.4	14.7	55.9	52.594	10	2.14	27.01
	FAGP	80	24	180	0.82	1.6	15	64	0.43	0	29.4	14.7	55.9	52.594	10	2.14	31.09
	FAGP	80	24	360	0.82	1.6	15	64	0.43	0	29.4	14.7	55.9	52.594	10	2.14	33.23
	FAGP	80	24	540	0.82	1.6	15	64	0.43	0	29.4	14.7	55.9	52.594	10	2.14	33.09
	M30	80	24	7	0.45	1.75	10	62	0.34	0	29.4	14.7	55.9	52.594	79.2	19.3	26.6
	M30	80	24	28	0.45	1.75	10	62	0.34	0	29.4	14.7	55.9	52.594	79.2	19.3	28.3
	M40	80	24	7	0.5	3	10	74	0.34	0	29.4	14.7	55.9	52.594	0.75	0.2	39.5
Weena Lokuge	M40	80	24	28	0.5	3	10	74	0.34	0	29.4	14.7	55.9	52.594	0.75	0.2	42.1
	M50	80	24	7	0.45	3.5	10	74	0.34	0	29.4	14.7	55.9	52.594	11.9	3	45.4
	M50	80	24	28	0.45	3.5	10	74	0.34	0	29.4	14.7	55.9	52.594	11.9	3	49
	M55	80	24	7	0.5	4	10	74	0.34	0	29.4	14.7	55.9	52.594	2.6	0.6	50.6
	M55	80	24	28	0.5	4	10	74	0.34	0	29.4	14.7	55.9	52.594	2.6	0.6	55.5
	G100C0	80	24	28	0.55	2.5	10	80	0.35	2	34.72	16.2	49.08	70.742	0	0	44.3
A.Mehta and R.Siddique	G100C0	80	24	90	0.55	2.5	10	80	0.35	2	34.72	16.2	49.08	70.742	0	0	46.9
	G100C0	80	24	365	0.55	2.5	10	80	0.35	2	34.72	16.2	49.08	70.742	0	0	47.3
	G20	60	24	28	0.5	2	8	77.5	0.35	0	29.4	14.7	55.9	52.594	22	6.7	31.33
K.Ramujeea and M.P.Raju	G40	60	24	28	0.4	2.5	16	77.5	0.35	1.5	29.4	14.7	55.9	52.594	0	0	50.66
	G60	60	24	28	0.345	2.5	16	77.5	0.3	1.5	29.4	14.7	55.9	52.594	0	0	71.1
	0%GF-Natural Curing	27	24	7	0.43	1	12	70	0.456	0	29.4	14.7	55.9	52.594	60.6	17.3	15.3
	0%GF-Natural Curing	27	24	14	0.43	1	12	70	0.456	0	29.4	14.7	55.9	52.594	60.6	17.3	18.6
	0%GF-Natural Curing	27	24	28	0.43	1	12	70	0.456	0	29.4	14.7	55.9	52.594	60.6	17.3	21.2
	0%GF-Thermal Curing	100	24	7	0.43	1	12	70	0.456	0	29.4	14.7	55.9	52.594	60.6	17.3	19.3
T.Sathanandam et al.	0%GF-Thermal Curing	100	24	14	0.43	1	12	70	0.456	0	29.4	14.7	55.9	52.594	60.6	17.3	20.4
	0%GF-Thermal Curing	100	24	28	0.43	1	12	70	0.456	0	29.4	14.7	55.9	52.594	60.6	17.3	22.4
	0%GF-Natural Curing	27	24	7	0.43	1	16	70	0.456	0	29.4	14.7	55.9	52.594	60.6	17.3	9.5
	0%GF-Natural Curing	27	24	14	0.43	1	16	70	0.456	0	29.4	14.7	55.9	52.594	60.6	17.3	12.7
	0%GF-Natural Curing	27	24	28	0.43	1	16	70	0.456	0	29.4	14.7	55.9	52.594	60.6	17.3	17.1
	0%GF-Thermal Curing	100	24	7	0.43	1	16	70	0.456	0	29.4	14.7	55.9	52.594	60.6	17.3	18.5

	0%GF-Thermal Curing	100	24	14	0.43	1	16	70	0.456	0	29.4	14.7	55.9	52.594	60.6	17.3	19.3
	0%GF-Thermal Curing	100	24	28	0.43	1	16	70	0.456	0	29.4	14.7	55.9	52.594	60.6	17.3	22.1
	0%GF-Natural Curing	27	24	7	0.43	1	20	70	0.456	0	29.4	14.7	55.9	52.594	60.6	17.3	10.1
	0%GF-Natural Curing	27	24	14	0.43	1	20	70	0.456	0	29.4	14.7	55.9	52.594	60.6	17.3	17.1
	0%GF-Natural Curing	27	24	28	0.43	1	20	70	0.456	0	29.4	14.7	55.9	52.594	60.6	17.3	21.6
	0%GF-Thermal Curing	100	24	7	0.43	1	20	70	0.456	0	29.4	14.7	55.9	52.594	60.6	17.3	20
	0%GF-Thermal Curing	100	24	14	0.43	1	20	70	0.456	0	29.4	14.7	55.9	52.594	60.6	17.3	22.4
	0%GF-Thermal Curing	100	24	28	0.43	1	20	70	0.456	0	29.4	14.7	55.9	52.594	60.6	17.3	24.5
	G100C0	80	24	3	0.55	2.5	10	80	0.35	2	34.72	16.2	49.08	70.742	0	0	41.5
	G100C0	80	24	7	0.55	2.5	10	80	0.35	2	34.72	16.2	49.08	70.742	0	0	43.4
A.Mehta and R.Siddique	G100C0	80	24	28	0.55	2.5	10	80	0.35	2	34.72	16.2	49.08	70.742	0	0	45
	G100C0	80	24	90	0.55	2.5	10	80	0.35	2	34.72	16.2	49.08	70.742	0	0	46
	G100C0	80	24	365	0.55	2.5	10	80	0.35	2	34.72	16.2	49.08	70.742	0	0	47.6
K.Pasupathy et al.	GPC	60	24	90	0.35	2.5	8	75	0.32	1.47	29.4	14.7	55.9	52.594	22.5	5.5	39
	GL8	60	48	7	0.6	1.5	8	70	0.3	0	30.2	12.5	57.3	52.705	0	0	40
P.Nuaklong et al.	GL12	60	48	7	0.6	1.5	12	70	0.3	0	30.2	12.5	57.3	52.705	0	0	41.4
	GL16	60	48	7	0.6	1.5	16	70	0.3	0	30.2	12.5	57.3	52.705	0	0	38.4
	0.70CLRS0.5	60	48	7	0.7	0.5	10	75	0.22	0	30.24	12.53	57.23	52.839	0	0	38.2
A.Wongsa et al.	0.70CLRS1.0	60	48	7	0.7	1	10	75	0.22	0	30.24	12.53	57.23	52.839	0	0	36
	0.70CLRS1.5	60	48	7	0.7	1.5	10	75	0.22	0	30.24	12.53	57.23	52.839	0	0	34.1
Faiz Uddin A.S	GPC0	60	24	7	0.4	2.5	8	75	0.31	0	29.4	14.7	55.9	52.594	0	0	41.1
	GPC0	60	24	28	0.4	2.5	8	75	0.31	0	29.4	14.7	55.9	52.594	0	0	45.3
	G1100	100	24	7	0.55	2.5	10	80	0.4	0	34.64	16.27	49.09	70.564	50.76	16.92	28.44
	G1100	100	24	28	0.55	2.5	10	80	0.4	0	34.64	16.27	49.09	70.564	50.76	16.92	31.38
	G2100	100	24	7	0.45	2.5	10	80	0.4	0	34.64	16.27	49.09	70.564	68.81	22.94	23.92
Hamdy K. Shehab	G2100	100	24	28	0.45	2.5	10	80	0.4	0	34.64	16.27	49.09	70.564	68.81	22.94	26.38
	G3100	100	24	7	0.55	2.5	10	75	0.4	0	34.64	16.27	49.09	70.564	59.23	16.92	32.36
	G3100	100	24	28	0.55	2.5	10	75	0.4	0	34.64	16.27	49.09	70.564	59.23	16.92	35.5
	G4100	100	24	7	0.45	2.5	10	75	0.4	0	34.64	16.27	49.09	70.564	80.28	22.94	27.16
	G4100	100	24	28	0.45	2.5	10	75	0.4	0	34.64	16.27	49.09	70.564	80.28	22.94	29.81

	Mix-4	50	48	7	0.35	2.5	16	75	0.5	3	29.4	14.7	55.9	52.594	35	10	18.3
	Mix-4	50	48	28	0.35	2.5	16	75	0.5	3	29.4	14.7	55.9	52.594	35	10	22.2
	Mix-5	50	48	7	0.35	2.5	16	75	0.5	2.625	29.4	14.7	55.9	52.594	35	8.75	25.5
	Mix-5	50	48	28	0.35	2.5	16	75	0.5	2.625	29.4	14.7	55.9	52.594	35	8.75	27.5
	Mix-6	50	48	7	0.35	2.5	16	75	0.5	2.33	29.4	14.7	55.9	52.594	35	7.77	33.3
	Mix-6	50	48	28	0.35	2.5	16	75	0.5	2.33	29.4	14.7	55.9	52.594	35	7.77	38.5
	Mix-10	28	48	7	0.35	2.5	16	75	0.5	2.625	29.4	14.7	55.9	52.594	35	8.75	10
Ali A. Aliabdo et al.	Mix-10	28	48	28	0.35	2.5	16	75	0.5	2.625	29.4	14.7	55.9	52.594	35	8.75	13.2
	Mix-11	70	48	7	0.35	2.5	16	75	0.5	2.625	29.4	14.7	55.9	52.594	35	8.75	35.6
	Mix-11	70	48	28	0.35	2.5	16	75	0.5	2.625	29.4	14.7	55.9	52.594	35	8.75	37.5
	Mix-12	90	48	7	0.35	2.5	16	75	0.5	2.625	29.4	14.7	55.9	52.594	35	8.75	30
	Mix-12	90	48	28	0.35	2.5	16	75	0.5	2.625	29.4	14.7	55.9	52.594	35	8.75	32.5
	Mix-13	50	24	7	0.35	2.5	16	75	0.5	2.625	29.4	14.7	55.9	52.594	35	8.75	22.8
	Mix-13	50	24	28	0.35	2.5	16	75	0.5	2.625	29.4	14.7	55.9	52.594	35	8.75	25.1
	Mix-14	50	72	7	0.35	2.5	16	75	0.5	2.625	29.4	14.7	55.9	52.594	35	8.75	28.8
	Mix-14	50	72	28	0.35	2.5	16	75	0.5	2.625	29.4	14.7	55.9	52.594	35	8.75	31
	Mix-1	100	72	3	0.4	2.5	14	77	0.3	1	29.4	14.7	55.9	52.594	0	0	29.2
	Mix-1	100	72	7	0.4	2.5	14	77	0.3	1	29.4	14.7	55.9	52.594	0	0	30
F.N. Okoye et al.	Mix-1	100	72	14	0.4	2.5	14	77	0.3	1	29.4	14.7	55.9	52.594	0	0	30.2
	Mix-1	100	72	21	0.4	2.5	14	77	0.3	1	29.4	14.7	55.9	52.594	0	0	32
	Mix-1	100	72	28	0.4	2.5	14	77	0.3	1	29.4	14.7	55.9	52.594	0	0	36.8
N.Ganesan et al.	GPC	60	24	28	0.35	2.5	10	75	0.32	2.5	29.4	14.7	55.9	52.594	14.5	3.55	37
Lateef N. Assi et al.	SS-W-OM-2	75	48	7	0.35	2.5	14	77	0.4	1.5	29.4	14.7	55.9	52.594	0	0	59.5
	SS-W-OM-3	75	48	7	0.35	2.5	14	77	0.5	1.5	29.4	14.7	55.9	52.594	22.5	5.5	56.7
	Mix-2	60	24	28	0.35	2.5	10	75	0.36	0	29.4	14.7	55.9	52.594	0	0	36.5
	Mix-3	60	24	28	0.35	2.5	13	75	0.36	0	29.4	14.7	55.9	52.594	0	0	64.3
F. U. A. Shaikh and V. Vimonsatit	Mix-4	60	24	28	0.35	2.5	16	75	0.36	0	29.4	14.7	55.9	52.594	0	0	72.1
	Mix-7	60	24	28	0.35	2.5	10	75	0.4	0	29.4	14.7	55.9	52.594	143	35	25
	Mix-8	60	24	28	0.35	2.5	16	75	0.4	0	29.4	14.7	55.9	52.594	143	35	27.5
	Mix-9	60	40	28	0.35	2.5	10	75	0.36	0	29.4	14.7	55.9	52.594	143	35	33
	$NaOH+Na_2SiO_3$	80	24	3	0.35	1	8	77	0.35	0	29.4	14.7	55.9	52.594	0.9	19.1	23.33
	$NaOH+Na_2SiO_3$	80	24	7	0.35	1	8	77	0.35	0	29.4	14.7	55.9	52.594	0.9	19.1	31.47
	$NaOH+Na_2SiO_3$	80	24	28	0.35	1	8	77	0.35	0	29.4	14.7	55.9	52.594	0.9	19.1	32.66
Sharayu Satpute et al.	$NaOH+Na_2SiO_3$	90	24	7	0.35	1	10	77	0.35	0	29.4	14.7	55.9	52.594	0.9	19.1	31.02
	$NaOH+Na_2SiO_3$	90	24	28	0.35	1	10	77	0.35	0	29.4	14.7	55.9	52.594	0.9	19.1	41.76
	$NaOH+Na_2SiO_3$	90	24	7	0.35	1	12	77	0.35	0	29.4	14.7	55.9	52.594	0.9	19.1	28.31

	$NaOH+Na_2SiO_3$	90	24	28	0.35	1	12	77	0.35	0	29.4	14.7	55.9	52.594	0.9	19.1	35.95
	$NaOH+Na_2SiO_3$	90	24	7	0.35	1	14	77	0.35	0	29.4	14.7	55.9	52.594	0.9	19.1	26.08
	$NaOH+Na_2SiO_3$	90	24	28	0.35	1	14	77	0.35	0	29.4	14.7	55.9	52.594	0.9	19.1	39.48
M.D.J. Sumajouw and B. V. Rangan	GBI	60	24	28	0.35	2.5	14	76	0.35	1.5	29.4	14.7	55.9	52.594	25.5	6.31	37
	GBII	60	24	28	0.35	2.5	14	76	0.35	1.5	29.4	14.7	55.9	52.594	17	4.21	46
S. Srinivasan et al.	GPC	70	24	28	0.45	2.5	8	75	0.3	2	29.4	14.7	55.9	52.594		14.65	32.74
	FGC-M1	70	24	28	1	2.5	16	74	0.44	1	31.35	14.74	53.91	58.152	0	0	17.48
	FGC-M2	70	24	28	0.886	2.5	16	72.03	0.44	1	31.35	14.74	53.91	58.152	0	0	19.92
	FGC-M3	70	24	28	0.793	2.5	16	70.3	0.44	1	31.35	14.74	53.91	58.152	0	0	26.59
	FGC-M4	70	24	28	0.717	2.5	16	68.5	0.44	1	31.35	14.74	53.91	58.152	0	0	28.44
Kumar S et al.	FGC-M5	70	24	28	0.650	2.5	16	66.8	0.44	1	31.35	14.74	53.91	58.152	0	0	31.55
	FGC-M6	70	24	28	0.603	2.5	16	65	0.44	1	31.35	14.74	53.91	58.152	0	0	35.25
	FGC-M7	70	24	28	0.558	2.5	16	63.3	0.44	1	31.35	14.74	53.91	58.152	0	0	37.11
	FGC-M8	70	24	28	0.520	2.5	16	61.5	0.44	1	31.35	14.74	53.91	58.152	0	0	33.55
	FGC-M9	70	24	28	0.486	2.5	16	59.79	0.44	1	31.35	14.74	53.91	58.152	0	0	28.07
Subhash V. Patankar		60	24	7	0.35	1	13	73	0.35	0	34.35	16.37	49.28	69.704	29.46	7.3	37.22
	1	70	24	3	0.37	1.5	14	75	0.33	2.034	29.4	14.7	55.9	52.594	0	0	53.8
	2	70	24	3	0.37	1.5	14	75	0.33	3.28	29.4	14.7	55.9	52.594	0	0	34.8
	3	70	24	3	0.37	1.5	14	75	0.33	11.3	29.4	14.7	55.9	52.594	0	0	29.4
	4	70	24	3	0.37	1.5	14	75	0.33	11.3	29.4	14.7	55.9	52.594	22.32	5.25	36.3
	5	70	24	3	0.37	1.5	14	75	0.33	5.65	29.4	14.7	55.9	52.594	3.36	0.79	74.5
	6	70	24	3	0.37	1.5	14	75	0.33	5.65	29.4	14.7	55.9	52.594	7.2	1.69	67.6
	7	70	24	3	0.37	1.5	14	75	0.33	5.65	29.4	14.7	55.9	52.594	9.6	2.25	64.4
	8	70	24	3	0.37	1.5	14	75	0.33	0	29.4	14.7	55.9	52.594	40.8	9.6	55.6
	9	70	24	3	0.37	1.5	14	75	0.33	0.2	29.4	14.7	55.9	52.594	35.28	8.87	44.4
M. Albitar et al. (2014)	10	70	24	3	0.37	1.5	14	75	0.33	7.45	29.4	14.7	55.9	52.594	9.6	2.25	66.9
	11	70	24	3	0.37	1.5	14	75	0.33	8.6	29.4	14.7	55.9	52.594	9.6	2.25	62.4
	12	70	24	3	0.37	1.5	14	75	0.33	9.72	29.4	14.7	55.9	52.594	9.6	2.25	57.1
	13	70	24	3	0.37	1.5	14	75	0.33	11.3	29.4	14.7	55.9	52.594	9.6	2.25	40.9
	13	70	24	7	0.37	1.5	14	75	0.33	11.3	29.4	14.7	55.9	52.594	9.6	2.25	49.3
	13	70	24	14	0.37	1.5	14	75	0.33	11.3	29.4	14.7	55.9	52.594	9.6	2.25	48.1
	13	70	24	28	0.37	1.5	14	75	0.33	11.3	29.4	14.7	55.9	52.594	9.6	2.25	50.2
	13	70	24	56	0.37	1.5	14	75	0.33	11.3	29.4	14.7	55.9	52.594	9.6	2.25	52.3
	13	70	24	90	0.37	1.5	14	75	0.33	11.3	29.4	14.7	55.9	52.594	9.6	2.25	50.6
	13	70	24	240	0.37	1.5	14	75	0.33	11.3	29.4	14.7	55.9	52.594	9.6	2.25	58.3

	13	23	24	3	0.37	1.5	14	75	0.33	11.3	29.4	14.7	55.9	52.594	9.6	2.25	1.52
	13	23	24	7	0.37	1.5	14	75	0.33	11.3	29.4	14.7	55.9	52.594	9.6	2.25	7.11
	13	23	24	14	0.37	1.5	14	75	0.33	11.3	29.4	14.7	55.9	52.594	9.6	2.25	17.1
	13	23	24	21	0.37	1.5	14	75	0.33	11.3	29.4	14.7	55.9	52.594	9.6	2.25	32.7
	13	23	24	28	0.37	1.5	14	75	0.33	11.3	29.4	14.7	55.9	52.594	9.6	2.25	40.7
	13	23	24	56	0.37	1.5	14	75	0.33	11.3	29.4	14.7	55.9	52.594	9.6	2.25	49.6
	13	23	24	90	0.37	1.5	14	75	0.33	11.3	29.4	14.7	55.9	52.594	9.6	2.25	49.3
	13	23	24	240	0.37	1.5	14	75	0.33	11.3	29.4	14.7	55.9	52.594	9.6	2.25	55.3
	14	70	24	3	0.37	1.5	14	75	0.33	0	29.4	14.7	55.9	52.594	45.6	10.73	46.2
	14	23	24	3	0.37	1.5	14	75	0.33	0	29.4	14.7	55.9	52.594	45.6	10.73	8.02
	14	23	24	7	0.37	1.5	14	75	0.33	0	29.4	14.7	55.9	52.594	45.6	10.73	14.3
	14	23	24	14	0.37	1.5	14	75	0.33	0	29.4	14.7	55.9	52.594	45.6	10.73	28.3
	14	23	24	21	0.37	1.5	14	75	0.33	0	29.4	14.7	55.9	52.594	45.6	10.73	36.8
	14	23	24	28	0.37	1.5	14	75	0.33	0	29.4	14.7	55.9	52.594	45.6	10.73	46
	14	23	24	56	0.37	1.5	14	75	0.33	0	29.4	14.7	55.9	52.594	45.6	10.73	58
	15	70	24	3	0.37	1.5	14	75	0.33	0	29.4	14.7	55.9	52.594	60	14.12	27.2
	100FA	27	24	7	0.4	2.5	10	70	0.5	3	27.8	8.2	64	43.438	63.18	5.2	16.15
Shafiq Ishaq et al.	100FA	27	24	14	0.45	2.5	10	70	0.5	3	27.8	8.2	64	43.438	63.18	5.2	33.39
	100FA	27	24	28	0.5	2.5	10	70	0.5	3	27.8	8.2	64	43.438	63.18	5.2	42.13
	S1	70	24	1	0.5	2.5	12	70	0.47	7	29.75	14.73	55.52	53.584	40	10	53.5
	S2	70	24	1	0.5	2.5	12	70	0.47	7	29.75	14.73	55.52	53.584	48	12	45
	S3	70	24	1	0.5	2.5	12	70	0.47	7	29.75	14.73	55.52	53.584	60	15	37.3
	S4	70	24	1	0.5	2.5	12	70	0.47	7	29.75	14.73	55.52	53.584	80	20	22.6
Muhd Fadhil Nuruddin et al.	S5	70	48	1	0.5	2.5	12	70	0.47	7	29.75	14.73	55.52	53.584	48	12	51
	S6	70	72	1	0.5	2.5	12	70	0.47	7	29.75	14.73	55.52	53.584	48	12	51.4
	S7	70	96	1	0.5	2.5	12	70	0.47	7	29.75	14.73	55.52	53.584	48	12	51.7
	S8	60	48	1	0.5	2.5	12	70	0.47	7	29.75	14.73	55.52	53.584	48	12	44.8
	S9	80	48	1	0.5	2.5	12	70	0.47	7	29.75	14.73	55.52	53.584	48	12	48.6
	S10	90	48	1	0.5	2.5	12	70	0.47	7	29.75	14.73	55.52	53.584	48	12	48
	M20	27	24	28	0.5	2.5	8	75	0.322	0	29.4	14.7	55.9	52.594	0	0	11.45
	M20	27	24	28	0.5	2.5	10	75	0.322	0	29.4	14.7	55.9	52.594	0	0	18.33
	M20	27	24	28	0.5	2.5	12	75	0.322	0	29.4	14.7	55.9	52.594	0	0	29.33
G Lavanya and J Jegan	M20	27	24	28	0.5	2.5	14	75	0.322	0	29.4	14.7	55.9	52.594	0	0	20
	M20	27	24	28	0.5	2.5	16	75	0.322	0	29.4	14.7	55.9	52.594	0	0	18.71
	M25	27	24	28	0.45	2.5	8	75	0.31	0	29.4	14.7	55.9	52.594	0	0	12.65
	M25	27	24	28	0.45	2.5	10	75	0.31	0	29.4	14.7	55.9	52.594	0	0	19.45
	M25	27	24	28	0.45	2.5	12	75	0.31	0	29.4	14.7	55.9	52.594	0	0	31.25

	M25	27	24	28	0.45	2.5	14	75	0.31	0	29.4	14.7	55.9	52.594	0	0	19.78
	M25	27	24	28	0.45	2.5	16	75	0.31	0	29.4	14.7	55.9	52.594	0	0	17.7
	M30	27	24	28	0.4	2.5	8	75	0.3	0	29.4	14.7	55.9	52.594	0	0	13.7
	M30	27	24	28	0.4	2.5	10	75	0.3	0	29.4	14.7	55.9	52.594	0	0	20.65
	M30	27	24	28	0.4	2.5	12	75	0.3	0	29.4	14.7	55.9	52.594	0	0	33
	M30	27	24	28	0.4	2.5	14	75	0.3	0	29.4	14.7	55.9	52.594	0	0	19.94
	M30	27	24	28	0.4	2.5	16	75	0.3	0	29.4	14.7	55.9	52.594	0	0	18.53
	M35	27	24	28	0.35	2.5	8	75	0.3	0	29.4	14.7	55.9	52.594	0	0	15
	M35	27	24	28	0.35	2.5	10	75	0.3	0	29.4	14.7	55.9	52.594	0	0	22.33
	M35	27	24	28	0.35	2.5	12	75	0.3	0	29.4	14.7	55.9	52.594	0	0	35
	M35	27	24	28	0.35	2.5	14	75	0.3	0	29.4	14.7	55.9	52.594	0	0	20.21
	M35	27	24	28	0.35	2.5	16	75	0.3	0	29.4	14.7	55.9	52.594	0	0	19.55
	1	60	24	1	0.35	2.5	8	75	0.312	2	36.7	18.2	45.1	81.375	0	0	16.42
	1	60	24	7	0.35	2.5	8	75	0.312	2	36.7	18.2	45.1	81.375	0	0	28.33
	1	60	24	14	0.35	2.5	8	75	0.312	2	36.7	18.2	45.1	81.375	0	0	34.22
	1	60	24	28	0.35	2.5	8	75	0.312	2	36.7	18.2	45.1	81.375	0	0	37.36
	2	60	24	1	0.35	2.5	10	75	0.312	2	36.7	18.2	45.1	81.375	0	0	20.18
	2	60	24	7	0.35	2.5	10	75	0.312	2	36.7	18.2	45.1	81.375	0	0	30.14
	2	60	24	14	0.35	2.5	10	75	0.312	2	36.7	18.2	45.1	81.375	0	0	35.24
	2	60	24	28	0.35	2.5	10	75	0.312	2	36.7	18.2	45.1	81.375	0	0	40.29
	3	60	24	1	0.35	2.5	12	75	0.312	2	36.7	18.2	45.1	81.375	0	0	23.1
Raijiwala and Patil	3	60	24	7	0.35	2.5	12	75	0.312	2	36.7	18.2	45.1	81.375	0	0	33.16
	3	60	24	14	0.35	2.5	12	75	0.312	2	36.7	18.2	45.1	81.375	0	0	39.12
	3	60	24	28	0.35	2.5	12	75	0.312	2	36.7	18.2	45.1	81.375	0	0	42.44
	4	60	24	1	0.35	2.5	14	75	0.312	2	36.7	18.2	45.1	81.375	0	0	24.12
	4	60	24	7	0.35	2.5	14	75	0.312	2	36.7	18.2	45.1	81.375	0	0	34.28
	4	60	24	14	0.35	2.5	14	75	0.312	2	36.7	18.2	45.1	81.375	0	0	40.18
	4	60	24	28	0.35	2.5	14	75	0.312	2	36.7	18.2	45.1	81.375	0	0	43
	5	60	24	1	0.35	2.5	16	75	0.312	2	36.7	18.2	45.1	81.375	0	0	25.02
	5	60	24	7	0.35	2.5	16	75	0.312	2	36.7	18.2	45.1	81.375	0	0	35.1
	5	60	24	14	0.35	2.5	16	75	0.312	2	36.7	18.2	45.1	81.375	0	0	41.18
	5	60	24	28	0.35	2.5	16	75	0.312	2	36.7	18.2	45.1	81.375	0	0	44.14